ANDRE VATARESCU

THE PHYSICAL REALITY OF APPLIED QUANTUM OPTICS

Physics *versus* Mathematics

The Physical Reality of Applied Quantum Optics

The Physical Reality of Applied Quantum Optics:

Physics versus Mathematics

By

Andre Vatarescu

Cambridge
Scholars
Publishing

The Physical Reality of Applied Quantum Optics:
Physics versus Mathematics

By Andre Vatarescu

This book first published 2021

Cambridge Scholars Publishing

Lady Stephenson Library, Newcastle upon Tyne, NE6 2PA, UK

British Library Cataloguing in Publication Data
A catalogue record for this book is available from the British Library

ISBN (10): 1-5275-6753-2
ISBN (13): 978-1-5275-6753-5

CONTENTS

Chapter One 1
Introduction
1.1 A Historical Perspective
1.2 An Outline of This Book
1.3 Remarks
References

Chapter Two 14
The Quantum Rayleigh Coupling of Optical Waves
2.1 Coupled-Wave Interactions in a Homogeneous Dielectric Medium
2.1.1 Inter-quadrature Coupling through Optically Linear Parametric Interactions
2.1.2 The operation of optical waveguide directional couplers
2.2 Phase-Sensitive Amplification of Optical Power
2.2.1 Equations of motion for interacting optical waves in a dielectric medium
2.2.2 Applications of the optically linear parametric interactions
2.3 Physical Aspects of Optically Linear Parametric Interactions
2.4 Quantum Aspects of Quantum Rayleigh Coupling of Photons
2.4.1 Evaluation of the spontaneously emitted power
2.4.2 Equations of motion of field operators
2.5 Conclusions
References

Chapter Three 34
The Intrinsic Optical Field of Photons
3.1 Instantaneous Measurements of Photonic Beam Fronts
3.2 Pure and Mixed Quantum States
3.3 Field Quantisation without Quantum Harmonic Oscillators
3.3.1 Optical fields of dynamic and coherent number states
3.3.2 The equations of motion of the optically linear parametric interactions
3.4 The Spatial Field Profile of Photons
3.4.1 The longitudinal distribution of photonic fields
3.4.2 The lateral distribution of photonic fields

3.5 Coherence of Dynamic Number States
3.6 Sub-Poissonian Distribution of Photons
3.7 Conclusions
Appendix - Alternative derivation of the dynamic and coherent number states
References

Chapter Four 58
Photonic Quantum Noise Reduction
4.1 Parametric Processes for Quantum Noise Reduction
4.2 Quantum Optic Second-Order Parametric Equations of Motion
4.3 Phase-dependent Gain Coefficients and Phase-pulling Effects
4.4 Simultaneous Amplification of a Signal and Sub-Poissonian Distributions of Photons
4.4.1 Optically linear parametric directional couplers
4.4.2 Electro-optic converters
4.5 Physical aspects of phase-sensitive gain coefficients
4.6 Conclusions
Appendix A - The deficiencies of the Bogoliubov-type solutions
Appendix B – The Quantum Regime of Electro-optic Modulation
References

Chapter Five 80
The Quantum Regime Operation of Dielectric Devices
5.1 The Role of the Rayleigh Quantum Scattering
5.1.1. The pure quantum state of individual measurements
5.1.2 The HOM experiments
5.2 Interference Patterns between Dynamic and Coherent Number States
5.3 The Beam Splitter
5.3.1 The glass plate beam splitters and the HOM dip
5.3.2 The cubic prism beam splitter
5.3.3 The fibre-optic beam splitter
5.4 The Interference Filter
5.5 The Distorted Outputs of Single-Photon Sources
5.6 Conclusions
References

Chapter Six 103
Photonic Coincidences and Correlations
6.1 Deficiencies of the Ensemble Quantum State
6.2 The Pure State of Single Measurements
6.2.1 The second-order interference
6.2.2 The fourth-order interference
6.3 The Probability Amplitude as a Consequence of Optical Field Detection

6.4 Correlations of the Balanced Homodyne Detection
6.4.1 Continuous-variable optical quantum states
6.4.2 The “miracle” of quantum imaging
6.5 Conclusions
References

Chapter Seven 127
Quantum Rayleigh Annihilation of Entangled Photons
7.1 Spontaneous Emission and Polarisation Rotation
7.2 Quantum Correlation Functions
7.2.1 Pure states of polarization
7.2.2 The Heisenberg uncertainty of predicted values
7.2.3 Mixed states of polarisation
7.3 Physical Aspects of Simultaneous Measurements of Independent Photons
7.4 Quantum Local Realism
7.5 The Deficiencies of the Concept of Quantum Nonlocality
7.6 Conclusions
References

Chapter Eight 149
The Physical Reality of Quantum Optics
8.1 Processes for Physical Quantum Interference
8.2 The Question of Single Photon Sources
8.2.1 The spontaneous parametric down-conversion of photons
8.2.2 The quantum dot sources of photons
8.3 The Case for a Paradigm Shift
8.4 Conclusions
References

Index 162

CHAPTER ONE

INTRODUCTION

Over the past 60 years, the field of Quantum Optics has seen technological developments in various attempts to develop sources emitting a single-photon per radiation mode, as well as corresponding photodetectors for resolving very low numbers of photons (e.g., Hepp *et al*. [1]; Lodahl *et al*. [2]).

Quantum Optics (e.g., Garrison and Chiao [3]) is predicated on the superposition and entanglement of apparently single-photon number states. The processing of such quantum states by means of beam splitters is supposed to enhance the performance and sensitivity of various information assessing operations. The theoretical model is based on the mixed quantum states of an ensemble of measurements, which provides time-independent distributions for the numerical evaluation of probability amplitudes associated with alternative propagation pathways of one single-photon.

The detection and measurement of correlated photons and their degrees of freedom constitute the experimental demonstration of concepts in Quantum Optics. The three stages of generation, propagation, and detection impact, in various ways, on the properties of measured outcomes.

An early application of Quantum Optics occurred in the experiments intended to prove quantum nonlocality by generating a pair of polarised, highly correlated (or entangled) photons, with an optically nonlinear crystal (e.g., Garrison and Chiao [3]). One photon is sent in one direction and the other in the opposite direction. Remote and independent measurements would appear to be correlated, leading to the concept of quantum nonlocality. Surprisingly, though, the same correlation function can be derived without entanglement, by using single and independent quantum polarisation states, or qubits (Vatarescu [4-5]).

In an article published in August 2014 by Tipler [6] and titled "The quantum nonlocality does not exist", the author detailed physical arguments for the statistical nature of the experimental results contradicting the concept of quantum nonlocality. While initiating the analysis with ensemble entangled states, Tipler points out that quantum wave functions need not collapse into a specific state upon measurement. Rather, the overall wave

function continues to evolve and branches out into one of four possible options, thereby generating an ensemble distribution of measured values.

A recent article in the Physical Review A authored by R. B. Griffiths [7], appears to be the first editorial exception to the uncompromising protection of the concept of quantum nonlocality. Additional analyses disproving the physical validity of the concept of quantum nonlocality have been published recently in other journals, e.g. (Boughn [8]; Khrennikov [9]; Kupczynski [10]).

It is noteworthy that a large body of analytic rebuttals of the concept of quantum nonlocality has been continually ignored in tens of articles which are published every year on this subject. These continual omissions, in the legacy journals of professional literature, of challenging and physically meaningful interpretations of the experimental results can only be an indication of the resistance organised by vested interests. As yet, not one single article has reported any evidence – at the level of pure quantum states of a single measurement – of a correlated or entangled collapse of the quantum wave function at one location as a result of a measurement carried out at another remote location. The global, mixed quantum states which are claimed to generate those quantum correlations are distributions of ensemble measurement possessing no dependence of the time and location of the measured observables. Despite the physical impossibility of a photon to maintain its polarisation state or even survive propagation through a dielectric medium because of the quantum Rayleigh scattering (Louisell [11]; Marcuse [12]), the concept of quantum nonlocality is still believed to provide an untapped resource for some future applications.

Additionally, in 2015, experimental results presented by Qian *et al*. [13] in the classical regime of large numbers of photons, found strong correlations, known as concurrences, between variables of polarised light. These results broadened the concept of correlation between observable values of quantum variables, raising questions about the quantum signature of such correlations.

These analytic and experimental results prompted this author to scrutinise the physical processes and interactions involved in the experimental setups, and which have continually been ignored and overlooked in major professional journals. Although detrimental to scientific development, the editorial policy of many journals would aim to preserve the status quo of physical understanding.

Another application of Quantum Optics has to do with the combination of a single-photon source, a beam splitter and simultaneous detections with two separate photodetectors. This combination is commonly described by

means of a time-independent mixed state of correlation measurements (Garrison and Chiao [3]; Mandel [14]).

However, a few questions have been overlooked: 1) How can a single-single propagate in a straight line in a homogenous dielectric medium given the multitude of electric dipoles it encounters? 2) How can a probability amplitude, instead of an optical field associated with a photon throughout its propagation, trigger or activate a photodetector? 3) How can a single-photon state of an ensemble of measurements, at a given time, interfere with another state that is physically absent at the same time? 4) How can the physical duration of a monochromatic photon be described mathematically by a polychromatic Fourier wave packet of the ensemble of measurements, given that only one Fourier spectral line would be measured at any given time?

Technological advances in material fabrication for integrated photonic devices and circuits will need to be matched by improved physical understandings of light-matter interactions. These will facilitate the design and operations of functional devices such as phase-sensitive amplifications of photons, sub-Poissonian sources of photons, low-power phase-sensitive switches and modulators, etc. and will have the potential to open up new applications in optical communication relying on easy to control quantum interactions.

The tenets of Quantum Optics consist of single photons propagating in a straight line in a dielectric medium, the interference patterns of probability amplitudes based on ensemble-evaluated mixed states of photons, and the use of beam splitters as entangling devices. Nevertheless, any probability amplitude of a quantum event should be evaluated from wave functions that reflect the physical reality. Discarding temporal information – which becomes a lack of information – about the propagation pathway of a single photon does not create a physical effect; it can only mask or obscure the existence of physical interactions.

This book adopts a physical approach. As photons propagate through a dielectric medium, the quantum Rayleigh spontaneous emission replaces entangled photons with independent ones in homogeneous dielectric media where single photons cannot propagate in a straight line. Pure quantum states of wavefronts of independent groups of photons deliver the intrinsic field profile associated with a photonic wavefront and the correct expectation values for its number of photons, its complex optical field, and phase quadratures. The spatial distribution of a photon, both longitudinally and laterally, is found from the quantised Maxwell equations in the context of a Wigner-type monochromatic time-varying spectral component. These photonic properties enable a direct analysis of various beam splitters and

interferometric filters, leading to generalized expressions for the correlation functions characterizing counting of coincident numbers of photons for the fourth-order field interference.

1.1 A Historical Perspective

The need to detect and analyse very week optical signals from distant stars led in the 1950s to the method of intensity interferometry in a bid to overcome the sensitivities associated with optical fields' interference. The Hanbury Brown and Twiss experiment [15] of 1956 with a mercury arc lamp as the optical source of radiation, measured "correlation between photons in coherent light rays". In that experiment, the light was produced by many different atoms, and one spontaneously emitted photon would have been slightly amplified on its way out. Thus, some photons might arrive in pairs at the half-silvered mirror (or beam splitter), which may explain the results showing a correlation between pairs of photon counts in terms of statistical distributions of bosons (Purcell [16]).

In 1961, Fano developed a theory of two-photon interference involving two emitting atoms and two photo-detecting atoms [17]. Employing generic transition or interaction matrix elements, the theory leads to "… a cosine function of both space and time" of the joint one-photon absorption by each of the two detectors.

The next stage of the theoretical development in 1963, saw Glauber specify the probability amplitude of photon detection in terms of the annihilation operator and input quantum states [18-19]. Given that the photon creation operator and the annihilation operator are the adjoint of each other, the detection probability became identical to the expectation value of the number operator. This enabled the use of number states defined as the eigenstates of the free-space Hamiltonian operator of optical fields. An equivalence with classical optical fields was derived in the form of an ensemble eigenstate of the annihilation operator, and which became known as the coherent states of light. While the removal of one photon may not have any consequence for a very large number of photons as is the case in the classical regime, in the quantum regime of a few photons per radiation mode, ironically, the coherent state is impractical; additionally, the coherent states fail to deliver the eigenvalues of phase quadratures (Carruthers and Nieto [20]).

The Glauber theory of photon detection and correlation (or coherence) is based on ensemble distributions of photons However, the corresponding quantum states lack information about time-dependent, instantaneous measurements or interactions which require the use of pure quantum states

that are allowed to be time-dependent. This shortcoming of quantum evaluations was pointed out by Mandel and Wolf in 1965 [21, Section 7.3] where one finds the following statement:

> "We have already shown in Sec. 3.2 that a description of ordinary interference effects may readily be given in terms of the quantized field, and that it follows the classical treatment fairly closely. It might therefore be thought that the transient superposition effects discussed in the last two sections can also be described quantum mechanically, in a closely parallel manner. However, here we come up against the basic feature that quantum mechanics is always concerned with expectation values of observables, whereas the calculation of expectation values was deliberately avoided in the simple treatment leading to Eqs. (7.6) and (7.10)."

This shortcoming of the quantum approach was ignored in the developments of following decades. This book aims to rectify this deficiency, prompted by the very fact that experimental results are measured one value at a time, and the final resultant distribution of the ensemble of measurements is time-independent once the experiment is complete.

Equally, the Glauber theory would have properties of instantaneous photons determined by the ensemble distribution to which they belong. For the number states, the photons would have no optical field, while for the coherent states the optical field arises from the overall superposition of a very large, if not infinite, number of photons. Yet, photons interact with dipoles and are detected at a given location and a particular time.

Another branch of Quantum Optics was initiated in 1965 by Jaynes and Cummings with an article analysing the interactions between single photons and atoms placed in resonant cavities [22]. In this case the photonic state is time-dependent, consisting of two consecutive number states.

Over the next two decades, 1965 to 1985, laser sources were used to prove interference between independent radiation modes of various numbers of photons. A review of possible single-photon interference patterns was presented by Walls in 1977, and space and time overlaps were included [23]. As the photon is the lowest amount of indivisible energy carried by an electromagnetic field, it can only be detected at one of two photodetectors located in the two alternative pathways. By contrast, the ensemble distribution of measurements would attach a non-zero value to both possibilities of the transition matrix evaluated with a pathway-entangled state of one photon. It is this discrepancy between the single measurement and the overall distributions that gives rise to a mathematical single-photon interference pattern in the context of a large number of measurements. The corresponding experimental results seemingly supporting quantum interference of probability amplitudes, are interpreted

on the basis of there being only one photon emitted by the optical source for each measurement.

In a 1986 article (Grangier *et al*. [24]), an optical source based on Calcium atoms was reported to yield an anti-correlation parameter as low as 0.18 which the authors classified as practically a single-photon source. The apparent quantum interference patterns of probability amplitudes obtained with a Mach-Zehnder configuration containing two beam splitters are interpreted as a clear evidence of single-photon interference. However, as one single photon would be scattered randomly in a quantum Rayleigh interaction with electric dipoles in the dielectric medium of the beam splitter, the possibility does exist that the interference was, in fact, created by the 18% of the groups of photons emitted spontaneously and slightly amplified on their way out, and which split at the first beam splitter and recombined at the second one, on their way to the same photodetector.

Over the next 15 years, to the turn of the century, optically nonlinear parametric crystals occupied centre stage as the most practical source of allegedly single photons. Pairs of spontaneously emitted photons are generated simultaneously by the interaction of an optical pump with nonlinear crystals. The optical frequencies and wavevectors of the two emitted photons obey conservation laws resulting in a high degree of correlation between the same degrees of freedom, and known as entanglement of photon states. From a physical perspective, measuring one photon's characteristic values would indicate the pair photon's values of frequency, wavevector, and, given the anisotropic polarisation or birefringence of the crystal, the polarisation of the other photon.

Although the optical pump pulses exciting the nonlinear crystals have relatively low levels of power, parametric amplification cannot be prevented resulting in a few, rather than one, photons per temporally discrete group. Therefore, the experimental results presented in the 1999 review article by Mandel [14] can be explained without quantum interference of probability amplitudes, and, in so doing, taking the counterintuitive element out of the picture [25]. This is, particularly, the case for the Hong-Ou-Mandel dip associated with a reduced counting of photon coincidences between the output modes of a beam splitter mixing two input synchronised and identical streams of single photons.

Similarly, the claim of remotely collapsing a wave function is highly questionable (Fuwa *et al*. [26]). A single photon propagating through a beam splitter would be deflected from its planned pathway by quantum Rayleigh scattering. Furthermore, the maximum likelihood method of numerically reconstructing a quantum state from raw data "aims to find, among the variety of all possible density matrices, the one that maximizes

the probability of obtaining the given experimental data set and is physically plausible" (Lvovsky and Raymer [27]). From the experimental point of view, the observer B's "photoreceivers do not have to be efficient, and he can post-select on finding his system in a particular subspace" [26]. The maximum likelihood method of reconstruction requires a target state, and the sign parameter *s* is delivered from observer A for the reconstruction of the quantum state by observer B. Therefore, the reconstruction is not independent. Indeed, the quantum Rayleigh scattering would deflect any single-photon crossing the beam splitter, and bearing in mind the slight parametric amplification inside the source, the two observers share the same photon phase from the same group of photons split at the beam splitters. There was no direct link at the level of a pure quantum state of a single measurement between the two observers, if only, because with only one photon in the experimental setup at any given time, only one detector can be triggered, whether or not the photon is entangled. Additional experiments (Ringbauer *et al*. [28, p. 4]) attempting to identify a cause and effect for quantum nonlocality between remote photodetectors found that "a direct causal influence from one outcome to the other can therefore not explain quantum correlations ".

This century, the next stage in the quest for practical single-photon sources involved semiconductor quantum dots placed inside dielectric micro-cavities (e.g., Hepp *et al*. [1]; Lodahl *et al*. [2]); Senellart *et al*. [29]). It is pointed out in [30] that a quantum dot "emits a cascade of photons and a single photon is obtained only through *spectral filtering* of one emission line". High-finesse optical cavities incorporated in a measurement setup distort the temporally regular sequence of single photons because of multiple internal reflections. The emerging stream may contain groups of a few temporally overlapping photons, e.g. five, which may be unevenly split by a beam splitter and reduced in number through quantum Rayleigh spontaneous emission, so as to generate no coincidence for a zero delay-time, in a Hanbury Brown and Twiss measurement. Obviously, the beam splitter can precede the interference filter, in which case quantum Rayleigh stimulated emission can cause two photons from different radiation modes to interact with the same dipole so that one of the photons is coupled into the other radiation mode.

A quantum dot placed in a high finesse micro-cavity of a few-wavelengths long and excited with a picosecond pulse, can emit a photon spontaneously and be re-excited within the duration of the same pulse. If the photon was reflected towards the quantum dot, stimulated emission may occur due to the small dimensions of the micro-cavity. This will result in two, or more, photons leaving the emitter simultaneously, as well as a

reduced lifetime of the excited state of the quantum dot, manifesting itself as a higher decay rate overshadowing the Purcell effect.

The conventional description of a photon as an ensemble wave packet composed of Fourier components - which can only exist individually one at a time - leads to counterintuitive explanations. A physically meaningful description of a photon can be identified as a monochromatic Wigner-type spectral component which varies with time. Furthermore, any photon-dipole interactions occurring during the propagation is completely ignored in the professional literature, with the propagation phase being attached to the optical field operator, as the number states carry no optical field.

Equally, in the professional literature, an interference term for a single-photon is provided, mathematically, by creating a pathway-entangled quantum wave function for the photon's propagation (Garrison and Chiao [3]; Walls [23]). Thus, a mysterious quantum effect appears as a result of an ensemble distribution, even though each individual measurement described by a pure quantum state, i.e., only one component of the ensemble, fails to generate that particular effect. This contradiction leads to the question of whether or not the optical source emits only one photon. Additionally, rather puzzlingly, the operations of beam splitters and interference filters are modelled in terms of continuous waves, ignoring the temporally discrete nature of the stream of photons.

The probability amplitude approach to photonic quantum interference leads to physical contradictions and counterintuitive conclusions which are held up as evidence of non-classical features. These are, however eliminated and physically explained by identifying the intrinsic field of photonic wavefronts, as explained throughout this book.

1.2 An Outline of This Book

Four major elements underpin the purpose of this book. The first two elements are linked to the presence, in a homogeneous dielectric medium, of the quantum Rayleigh conversion of photons. As a result, one photon cannot propagate in a straight line and, initially, entangled photons are annihilated and replaced with independent photons. The other two elements arise from employing a time-dependent pure quantum state to deliver the measured values of photonic degrees of freedom. As a consequence, the quantization of the optical field is derived without any equivalence to quantum harmonic oscillators, and the photon is identified as an energy excitation characterised by a Wigner-type or mixed time-frequency representation of a monochromatic signal pulse.

With a view to identifying and probing a possible boundary between the quantum and classical regimes of optics, Chapter 2 of this book headlined "The Quantum Rayleigh Coupling of Optical Waves" describes the functional roles of the quantum Rayleigh emissions of photons and the resultant classical manifestations.

The conventional interpretation assigns no optical field to photon number states which are the number eigenstates of the electromagnetic field. Any propagation effect is attached to the field operators and the absorption of a particle-like photon requires a transition between two consecutive number states. An optical field, known as a coherent state, is generated by an infinite superposition of number states under the condition of an ensemble eigenstate of the annihilation operator. Nevertheless, a photonic wavefront interacts with electric dipoles instantaneously, and the need arises for an intrinsic and instantaneous optical field for any number of photons, regardless of the overall distribution of the optical beam. A physical solution to this problem is presented in Chapter 3 which identifies dynamic and coherent number states under the headline of "The Intrinsic Optical Field of Photons"

"Photonic quantum noise reduction" can be implemented by means of parametric processes. Their scrutiny reveals common features such as phase dependent gain coefficients accompanied by a phase pulling effect as described in Chapter 4. These physical mechanisms can generate sub-Poissonian distributions of photons through a saturation-like effect and using only integrated photonic circuits.

In Chapter 5, "The Quantum Regime Operation of Dielectric Devices" is analysed in the light of evidence that emerged from the previous chapters, leading to different physical processes for various types of beam splitters, and to the temporal role that interferometric filters play in altering the original time sequence of a beam of single photons. As a consequence, individual measurements reveal the physical processes involved in creating interference patterns and are represented by pure quantum states which are dependent on the position and time of the measurements. The ensemble statistical distribution ensues from repeated measurements.

"Photonic coincidences and correlations" is the headline of Chapter 6 which identifies temporal and spatial properties and aspects of an individual measurement, as well as photon-dipole interactions by means of the pure dynamic and coherent number states derived in Chapter 3. The use of pure, dynamic and coherent quantum states enables us to demystify the quantum nonlocality alleged to create coincidences between two separate photocurrents generated by mixing single photons across a beam splitter.

"Quantum Rayleigh Annihilation of Entangled Photons" of Chapter 7 specifies the Hamiltonian of interaction between the electric dipoles in a dielectric medium and the optical field of photons propagating through that medium. As a result, one single photon is absorbed and spontaneously emitted in a random direction with a random state of polarisation. Yet, the remote correlations between these individual photons lead to the same correlation functions producing the same Bell-type outcomes as the absorbed entangled photons. The statistical character of the "quantum nonlocality" outcomes is reinforced by the possibility of obtaining the same correlations with two separate sources placed in the vicinity of the respective photodetectors.

In Chapter 8, recent experimental and theoretical developments are explained in the context of this textbook's formalism, pointing to a blurred boundary between quantum and classical regimes, which is borne out by the analyses of the previous chapters. A paradigm shift in the interpretation of experimental outcomes of Quantum Optics is highly necessary, being based on the following physical processes and elements:

1. The quantum Rayleigh spontaneous and stimulated emissions;
2. The unavoidable parametric amplification of spontaneous emission, and the formation of groups of monochromatic photons in a high finesse cavity incorporating a quantum dot;
3. Self-contained quantisation of the optical field without any harmonic oscillators leading to the dynamic and coherent number states;
4. The intrinsic optical field of photons and their localised spatial distributions;
5. The description of instantaneous and localised photon-dipole interactions by means of pure, dynamic and coherent number states;
6. The quantum evolution and predictions being described by the Ehrenfest theorem, for any level of optical field excitation, to evaluate the expectation value of an operator in the context of a given set of pure wavefunctions.
7. Identifying quantum phenomena at the level of single events and measurements with a space- and time-dependence, leading to quantum locality and realism.

Overall, there are no quantum optic "miracles" once the physically present effects are correctly identified.

1.3 Remarks

The smooth transition from the quantum regime of one or a few photons to the classical one of a large number of photons is due to the adequate choice of a wavefunction in the form of the *pure*, *dynamic and coherent* number states derived in Chapter 3. These states deliver the correct number of photons carried by a radiation mode, its field amplitude and phase quadratures. The equations of motion for the evolution of these variables are derived in Chapter 3 and applied in the following Chapters for any levels of mode excitation and photon-dipole interactions.

Measurements of instantaneous wave fronts are described by dynamic and coherent number states which erase any quantum-classical boundary. While the intrinsic optical field of photons is critical for time-correlations at the level of one or a few photons, its importance could still be significant at high levels of photon numbers for a monochromatic group of photons as the optical field does not have a Fourier spectrum but is represented by a mixed time-frequency structure of the form $S(\omega, t)$. That is, the monochromatic spectral component exhibits a time-varying amplitude which is not related to an optical Fourier spectrum corresponding to time-independent spectral components.

Entangled photons are scattered by the quantum Rayleigh spontaneous emission but remote correlations of measured states of polarisations are still reproduced by single and independent photons.

The quantum Rayleigh photon-dipole interaction may involve two photons colliding at a dipole, with a possible outcome being the transfer of the excitation from one radiation mode to the other. This process may take place inside the dielectric medium of an interference filter or beam splitter, thereby creating groups of monochromatic photons from initially independent photons bouncing back and forth inside a resonant cavity. This quantum Rayleigh coupling of photons may explain the Hong-Ou-Mandel dip as one photon carried by one radiation mode may be captured by another photon associated with a second radiation mode inside a cavity.

Equally, a remote wavefunction state preparation through a detection of one of the entangled photons is practically impossible because the photodetector's excitation is triggered by an energy level of its structure rather than a quadrature state of a quantum harmonic oscillator.

References

1. S. Hepp, M. Jetter, S. L. Portalupi, and P. Michler, "Semiconductor Quantum Dots for Integrated Quantum Photonics", Adv. Quantum Technol., **2**, 1900020, (2019).
2. P. Lodahl, S. Mahmoodian, and S. Stobbe, "Interfacing single photons and single quantum dots with photonic nanostructures", Rev. Mod. Phys., **87**, 347– 400, (2015).
3. J. C. Garrison and R. Y. Chiao, *Quantum Optics*, Oxford University Press, 2008.
4. A. Vatarescu, "The Scattering and Disappearance of Entangled Photons in a Homogeneous Dielectric Medium", Rochester Conference on Coherence and Quantum Optics (CQO-11), doi.org/10.1364/CQO.2019.M5A.19, (2019).
5. A. Vatarescu, "Quantum Rayleigh Annihilation of Entangled Photons", www.preprints.org/manuscript/201807.0280/v2.
6. F. J. Tipler,"Quantum nonlocality does not exist", PNAS **111** (31), 11281–11286, (2014).
7. R. B. Griffiths, "Nonlocality claims are inconsistent with Hilbert-space quantum mechanics", Phys. Rev. A **101**, 022117, (2020).
8. S. Boughn, "Making Sense of Bell's Theorem and Quantum Nonlocality", Found. Phys., **47**, 640-657, (2017)
9. A. Khrennikov, "Get Rid of Nonlocality from Quantum Physics", Entropy, **21**, 806, (2019).
10. M. Kupczynski, "Closing the Door on Quantum Nonlocality ", Entropy **20**, 877, (2018).
11. W. H. Louisell, *Quantum Statistical Properties of Radiation*, John Wiley & Sons, 1973.
12. D. Marcuse, *Principles of Quantum Electronics*, Academic Press, 1980.
13. X.-F. Qian, B. Little, J. C. Howell, and J. H. Eberly, "Shifting the quantum-classical boundary: theory and experiment for statistically classical optical fields", Optica, **2**, 611–615, (2015).
14. L. Mandel, "Quantum effects in one-photon and two-photon interference", Rev. Mod. Phys., **71**, S274–S282, (1999).
15. R. Hanbury Brown, and R. Q. Twiss, "Correlation between photons in two coherent beams of light", Nature ,**177**, 27–29, (1956).
16. E. M. Purcell, "The question of correlation between photons in coherent light rays", Nature, **178**, 1449 (1956).
17. U. Fano, "Quantum theory of interference effects in the mixing of light from phase independent sources", Am. J. Phys., **29**, 539–545, (1961).

18. R. J. Glauber, “The quantum theory of optical coherence”, Phys. Rev., **130**, 2529–2539, (1963).
19. R. J. Glauber, “Coherent and incoherent states of radiation field”, Phys. Rev., **131**, 2766 –2788, (1963).
20. P. Carruthers and M. M. Nieto, “Phase and Angle Variables in Quantum Mechanics”, Rev. Mod. Phys., **40**, 411– 440, (1968).
21. L. Mandel and E. Wolf, “Coherence Properties of Optical Fields”, Rev. Mod. Phys., **37**, 231–287, (1965).
22. E.T. Jaynes and F.W. Cummings, "Comparison of quantum and semiclassical radiation theories with application to the beam maser". Proc. IEEE., **51**(1): 89–109, (1963)
23. D. F. Walls, “A simple field theoretic description of photon interference”, Am. J. Phys., **45**, 952 – 956, (1977).
24. P. Grangier, G. Roger and A. Aspect, “Experimental Evidence for a Photon Anticorrelation Effect on a Beam Splitter: A New Light on Single-Photon Interferences“, Europhys. Lett., **1** (4), 173–179, (1986).
25. A. Vatarescu, ”The Quantum Regime Operation of Beam Splitters and Interference Filters”, DOI: 10.20944/preprints201909.0191.v1.
26. M. Fuwa, S. Takeda, M. Zwierz, H. M. Wiseman, and A. Furusawa, “Experimental proof of nonlocal wavefunction collapse for a single particle using homodyne measurements”, Nat. Commun. **6**: 6665, (2015).
27. A. I. Lvovsky and M. G. Raymer,“Continuous-variable optical quantum-state tomography”, Rev. Mod. Phys. **81**, 299, (2009).
28. M. Ringbauer, C. Giarmatzi, R. Chaves, F. Costa, A. G. White and A. Fedrizzi”, Experimental test of nonlocal causality”, Sci. Adv. **2**, e1600162 (2016).
29. P. Senellart, G. Solomon, and A. White, “High-performance semiconductor quantum-dot single-photon sources”, Nature Nanotech., **12**, 1026- 1039 (2017).

CHAPTER TWO

THE QUANTUM RAYLEIGH COUPLING OF OPTICAL WAVES

Most activities in Quantum Optics aim to generate and manipulate one photon per radiation mode. It is assumed that once generated, a single photon will propagate unimpeded through a dielectric medium despite encountering a large number of electric dipoles. However, as a result of photon-dipole interactions, the process of quantum Rayleigh scatterings or emissions comes into play involving the absorption of one photon and the spontaneous emission of another photon of the same energy or frequency. At the photodetection stage, the temporally discrete electronic signals are assumed to be triggered by one single photon despite the possibility of a few photons arriving simultaneously and triggering a similar signal.

From a physical perspective, in dielectric devices such as optical fibres and integrated optic waveguides, beam splitters, interference filters, polarisation controllers, etc., a single photon cannot propagate in a straight line, thereby raising significant questions about the validity of the conventional model or interpretation of Quantum Optics experimental outcomes.

Despite having been well documented before the 1980s, the quantum Rayleigh spontaneous and stimulate emissions were totally ignored in any explanation of optical mode coupling devices such as directional waveguide couplers. Two optical beams of the same frequency but different wave vectors propagating through a homogeneous dielectric medium can exchange photons with each other and/or undergo mutually induced phase shifts as a result of stimulated Rayleigh emission underpinning the coupling term of the Poynting theorem. Quadrature fields of the same optical wave exchange power as they propagate through a homogeneous and linear dielectric medium. Consequently, coupling of photons between two optical waveguides takes place in the shared cladding region.

The widely used coupled-mode theory describing optical power coupling between two adjacent waveguides – introduced in the 1960s – relies on a perturbation of the cladding as a physical mechanism. However,

the gradient of the perturbed dielectric constant gives rise to a randomly scattering term in the comprehensive wave equation. This approach is inconsistent with directional coupling of photons and leads to physically impossible outcomes raising questions about the validity of its application as in recently published articles in the *IEEE J. Quantum Electron*., vol. 54, 2018 (no. 1, article 6300206, and no. 2, article 6800207).

A physically meaningful and correct identification of processes underpinning the description of propagation and coupling of photons in dielectric media is crucial in order to open up new practical ways of designing, fabricating, and operating integrated photonic devices. The quantum Rayleigh conversion of photons (QRCP), provides a meaningful explanation for the operation of the optical directional couplers, in contrast to the perturbation approach based on the fictional splitting of the dielectric constant $\varepsilon\,(x, y, z) = \varepsilon_b + \Delta\,\varepsilon$ into a uniform background ε_b and a perturbation $\Delta\,\varepsilon\,(x, y, z)$ which is supposed to generate a coupling polarisation $\Delta\,\boldsymbol{P} = \Delta\,\varepsilon\;\boldsymbol{E}$ induced by an overlapping optical field. No explanation has been provided, at least in this context, as to how the optical field can discriminate, physically, between the total local value of the optical susceptibility and the added perturbation to the refractive index, as opposed to the mathematical splitting of the permittivity.

2.1 Coupled-Wave Interactions in a Homogeneous Dielectric Medium

Optical parametric processes are well established for the second- and third- order susceptibilities (Shen [1]; Boyd [2]) and are characterized by conservation of the total energy of photons before and after the interactions. The parametric gain displays a strong dependence on the relative phase between the pump and signal waves. A quantum feature of a parametric process of photon conversion is the amplification of spontaneously emitted photons to generate another optical wave (Vatarescu [3]; Inoue and Mukai [4-5]). These interactions can take place in both homogeneous and inhomogeneous dielectric media.

Similarly, an optically linear parametric (OLP) interaction consists of an electric dipole absorbing one photon and emitting one photon of the same frequency or energy, e.g. the elastic or Rayleigh scatterings (Marcuse [6]; Louisell [7]). The corresponding Hamiltonian of interaction and the Heisenberg equation of motion for the photon annihilation and creation operators are presented below in this Chapter.

This quantum process is localized, can take place in both homogeneous and inhomogeneous dielectric media, and is described macroscopically, or

classically, by means of the interaction term included in the Poynting theorem of the flow of energy. The resultant combination of in-quadrature waves is similar to the quadrature states of light (Mandel and Wolf [8], Ch. 21) exchanging photons through parametric interactions.

The classical Rayleigh scattering which is attributed to local perturbations or fluctuations in the dielectric constant is linked to optical power losses in optical fibers.

Quantum electronically, an oscillating electric dipole polarisation can be the source of spontaneous and stimulated emissions of photons [6-7]. Consequently, coupling of photons between two arbitrary waves interacting simultaneously with the same dielectric medium can take place with one beam of photons exciting the electric dipole polarisation and the other beam de-exciting the dipoles and gaining power through stimulated emission. The direction of coupling will depend on the relative phase between the waves. These physical processes require that Maxwell's *curl* $\boldsymbol{H}$ equation of *each* wave be driven by the *total* electric dipole polarisation available in the medium.

A practical device based on optical power coupling is the two-waveguide optical directional coupler. The conventional electromagnetic coupled- mode theory, e.g., (Huang [9]; Yishen,*et al*. [10]; Huang and Mu [11]; Marcatili [12]) links the optical power coupling between two single-mode waveguides to the perturbation of the permittivity of the optical waveguide cladding and the unperturbed evanescent modal fields that existed in the absence of the second waveguide. But the tail end of these fields no longer exists physically, having been disturbed by the introduction of the other waveguide. In reference [12], two sets of wave equations are mixed up to generate an "interaction" between the guided modes of the individual waveguides. One set of equations involves the normal, even and odd, modes of the coupler and the other set involves the modes of the individual waveguides. But no physical effect underpins this mathematical technique. Equally, the incoming guided mode of one waveguide is *instantly* converted, at the input to the coupler, into a superposition of the normal modes. But no explanation is provided as to how the propagation constant of the incoming photons is converted into the propagation constants of the normal modes.

Additionally, the approach based on the normal modes [9], [12] of the two-waveguide structure fails to explain how the incoming guided wave is converted instantly, at the input, into the orthogonal even and odd modes or why the same converting process does not occur between the two single mode waveguides in the cladding region they share. Equally, a group of photons cannot simultaneously cross from one waveguide into the other

while propagating in the same normal mode *without converting* the propagation constant. Furthermore, the comprehensive wave equations incorporating the gradient of the dielectric constant would cause the tail end of the evanescent field of one waveguide to be scattered by the existence of the second waveguide.

It is the effect of stimulated emission which is capable of causing photons to propagate with the same wave vector as the stimulating field [6-7] instead of being spontaneously emitted or classically scattered. The gain providing stimulated emission is always the source of spontaneous emission. The spontaneous emission, which is a feature of the quantum wave-dipole interactions, is dependent on the optical susceptibility and the level of the optical pump and is distinct from the zero-point fluctuations of the electromagnetic field, as presented below in this Chapter.

The phase-dependent parametric gain in optical fibers for the third-order susceptibility involving four-photon mixing interactions was analyzed [3] and demonstrated experimentally [4-5]. Conceptually, the following analysis adapts reference [3] to an *optically linear* medium.

In this Chapter, a physically meaningful framework is developed – Section 2.1.1 – for the optically linear parametric (OLP) coupling of photons by making it consistent with the quantum effects of spontaneous and stimulated emissions associated with the linear parametric gain. The optical wave propagates forwards through stimulated emission as a result of the optimal phase-dependent gain. This propagation involves a cascade of photonic conversions between quadrature waves in dielectric media, emerging from the Poynting theorem of the flow of energy. The refractive index results from local exchanges of energy between the optical field and the electric dipole polarisation.

In the case of an optical directional coupler – Section 2.1.2 – composed of two waveguides, the extinction of the wave launched into one waveguide gives rise to in-quadrature waves, one in each waveguide. The related coupling coefficients are determined from the total value of the local susceptibility at every point in space where any two waves overlap. No approximations are made in the derivation of results and no assumptions are needed. Previous experimental results are reassessed and physical aspects of optically linear parametric interactions (OLP) are outlined.

2.1.1 Inter-quadrature Coupling through Optically Linear Parametric Interactions

An optical collimated beam, or a travelling radiation mode, characterized by a field amplitude E_o, an initial phase φ, an angular

frequency ω, a wave vector $\boldsymbol{k}$ and a field polarisation unit $\boldsymbol{u}$, is represented, at time t and distance $\boldsymbol{r}$ = (x, y, z) from origin, by the relations:

$$\boldsymbol{E}\,(\boldsymbol{k},\varphi) = E_o\,(z)\,f(\boldsymbol{r})e^{-i\varphi}\,e^{i(\,\omega\,t\,-\,\boldsymbol{k}\cdot\boldsymbol{r}\,)}\,\boldsymbol{u} \qquad (2.1a)$$

$$\iint f^2\,(x,y,z)dx\,dy = 1 \qquad (2.1b)$$

$$\mathrm{P}\,(z) = 0.5\,\varepsilon_o n\,c\,E_o^2\,(z) \qquad (2.1c)$$

The field distribution $\boldsymbol{E}$ is given in terms of the peak amplitude E_o and the spatial distribution $f(x, y, z)$ which has units of m^{-1} and is normalized across any (x, y)-plane in eq. (2.1b) so that P(z) represents the total average power crossing that surface. Additionally, ε_o is the permittivity of free space, n is the refractive index of the medium, and c is the speed of light in vacuum.

The dipole polarisations involved in the interaction are linear, i.e.

$$\boldsymbol{P} = \varepsilon_o\,\chi\,\boldsymbol{E}$$

where $\chi\,(x, y, z)$ is the susceptibility of the medium, and in terms of the photon frequency notation,

$$\boldsymbol{P}\,(\omega) = \varepsilon_o\,\chi\,(\omega\,;\,\omega)\;\;\boldsymbol{E}\,(\omega)$$

indicating a parametric dipole polarisation with one photon being absorbed and one photon being emitted, both having the same energy [1-2].

The conventional approach in electromagnetic theory is to insert the total field $\boldsymbol{E}_{\mathrm{tot}} = \boldsymbol{E}_1 + \boldsymbol{E}_2$ in the Maxwell equations and then select terms of identical indices on both sides. This approach, however, leads to two difficulties: 1) the need to single out one wave by using an orthogonality condition; and 2) it disregards the quantum process of two optical waves of the same frequency but different wave vectors interacting with each other in an optically linear dielectric medium (as described below). As any wave propagating through the dielectric medium will interact with every electric dipole polarisation $\boldsymbol{P}$ oscillating at the same frequency, the Maxwell *curl* $\boldsymbol{H}$ equation (Ampère's law) needs to be driven by the total electric dipole polarisation or the macroscopic dipole polarisation, leading to an additional term:

$$\nabla \times \boldsymbol{H}_1 = \frac{\partial}{\partial t}\,(\boldsymbol{E}_1 + \boldsymbol{P}_1) + \frac{\partial}{\partial t}\,(\boldsymbol{P}_2) \qquad (2.2)$$

And a similar equation applies, with the indices interchanged, for the magnetic field $\boldsymbol{H}_2$.

As the optical beam crosses an (x, y) - plane interface from free-space into a dielectric material, the wave equations for its electric $\boldsymbol{E}_1$ and magnetic

$\boldsymbol{H}_1$ fields describing its propagation are derived from the Maxwell equations (Orfanidis [13, Ch. 14]) as

$$\nabla^2 \boldsymbol{E_1} + (k_o n)^2 \boldsymbol{E_1} = \nabla\left(\boldsymbol{E_1} \cdot \frac{\nabla \varepsilon}{\varepsilon}\right) - \omega^2 \mu_0 \boldsymbol{P_2} \tag{2.3a}$$

$$\nabla^2 \boldsymbol{H_1} + (k_o n)^2 \boldsymbol{H_1} = -i\,\omega\,\nabla\,\varepsilon \times \boldsymbol{E_1} - i\,\omega\,\nabla \times \boldsymbol{P_2} \tag{2.3b}$$

where $k_o = \omega / c$, $\varepsilon / \varepsilon_o = n^2 = 1 + \chi$ is the dielectric constant, and the time derivative operator was replaced with $\partial\, \boldsymbol{E}$, (or $\boldsymbol{H}$) / $\partial\, t = i\,\omega\, \boldsymbol{E}$, (or $\boldsymbol{H}$). The polarisation density $\boldsymbol{P}_1$ was included on the left-hand side of eqs. (2.3) and a second source polarisation $\boldsymbol{P}_2$ was added in the *curl* $\boldsymbol{H}$ Maxwell equation in order to point out the various quantum operations that these polarisations carry out simultaneously. Equivalent equations apply to $\boldsymbol{E}_2$ with the indices interchanged.

The initial direction of propagation of the refracted wave from the boundary between the free-space and the medium is determined from Snell's law which is indicative of the conservation of wave momentum in the (*x, y*) - plane. The refracted wave is generated by a boundary layer of source terms incorporating the gradient $\nabla\varepsilon$ and $\boldsymbol{E}_1$ in eqs. (2.3). Inside the medium, for $\nabla\varepsilon \neq 0$, scattering of the optical wave takes place – see the right-hand side of eqs. (2.3) – unless the field propagates along an optical waveguide, satisfying the boundary conditions for a guided mode. The polarisation $\boldsymbol{P}_2$ can radiate into mode $\boldsymbol{k}_1$ and a mutual interaction emerges from the Poynting theorem.

The differential, local and temporal, Poynting theorem [13, Ch. 1] of the optical flow of energy has the following form, with the asterisk denoting the complex conjugate of the variable:

$$\nabla \cdot \boldsymbol{\mathcal{P}_1} = -i\,\omega\,\boldsymbol{D}_1 \cdot \boldsymbol{E}_1^* - i\,\omega\,\boldsymbol{B}_1 \cdot \boldsymbol{H}_1^* - i\,\omega\,\boldsymbol{P}_2 \cdot \boldsymbol{E}_1^* \tag{2.4}$$

where $\boldsymbol{\mathcal{P}}_1 = \boldsymbol{E}_1 \times \boldsymbol{H}_1^*$ is the Poynting vector parallel to the wave vector $\boldsymbol{k}_1$, and the vectors $\boldsymbol{k}$, $\boldsymbol{E}$ and $\boldsymbol{H}$ are perpendicular to each other for the same radiation mode. We align $\boldsymbol{k}_1$ to be parallel to the z-axis in a bulk medium. The constitutive relations are: $\boldsymbol{D} = \varepsilon\, \boldsymbol{E}$ and $\boldsymbol{B} = \mu\, \boldsymbol{H}$. Making use of the identity $1/c^2 = \varepsilon_o\, \mu_o$ and, for a radiation field $\varepsilon E^2 = \mu H^2$, we obtain from the real part of eq. (2.4) the longitudinal rate of change of the optical intensity E_j^2 at a point (*x, y, z*), and from the entire complex equation, the rate of change of the field $E(\boldsymbol{k}_j) = E_j \exp(-i\,\varphi)$ of eq.(2.1a) after setting $E_j = E_{oj}\, f_j(x, y, z)$, with j = 1 or 2 :

$$\frac{d\,E_1^2}{dz} = -2\,\gamma E_1\,E_2\,sin\,\theta_{21} \tag{2.5a}$$

$$\frac{d\,E\,(\boldsymbol{k}_1)}{dz} = -i\left(k_0\,n + \gamma\,\frac{E_2}{E_1}cos\,\theta_{21}\right)E_1 - \gamma E_2\,sin\,\theta_{21} \tag{2.5b}$$

$$\frac{d\,\theta_{21}}{dz} = (\,\boldsymbol{k}_2 - \boldsymbol{k}_1)\cdot\,\boldsymbol{u}_z + \gamma\left(\frac{E_1}{E_2} - \frac{E_2}{E_1}\right)cos\,\theta_{21} \tag{2.5c}$$

$$\frac{d}{dz}\varphi_1 = \gamma\frac{E_2}{E_1}\,cos\,\theta_{21} \tag{2.5d}$$

$$\theta_{21} = (\,\boldsymbol{k}_2 - \boldsymbol{k}_1)\cdot\,\boldsymbol{z} + \varphi_2 - \varphi_1 \tag{2.5e}$$

where $\gamma = k_o\,\chi\,\boldsymbol{u}_1\cdot\,\boldsymbol{u}_2\,/\,(2\,n)$ is the local coupling coefficient, $\boldsymbol{k}_1 = k_o\,n\,\boldsymbol{u}_z$ is the wavevector, with $\boldsymbol{u}_z$ being a unit vector in the z-direction, and θ_{21} is the phase difference between the two fields. Similar equations to (2.5) hold for E_2 with the indices interchanged.

The refractive index n in eq. (2.5*b*) arises from the first two terms on the right-hand side of eq. (2.4) and is the result of local and instantaneous exchanges of energy between the optical field and the dielectric medium. It corresponds to the self-coupling term with $\boldsymbol{P}_1$ from $\boldsymbol{D}_1 = \boldsymbol{E}_1 + \boldsymbol{P}_1$ replacing $\boldsymbol{P}_2$ in eq. (2.4) and setting $\theta = 0$ in eqs. (2.5). The second term on the right-hand side of eq. (2.5*b*) emerges from the last term of eq. (2.4), indicating a possible phase shift brought about by a mutual interaction between the optical waves E_2 and E_1.

As indicated by the last term of eq. (2.4) or by eq. (2.5*a*), for $E_1 \neq 0$, coupling of power can take place in a homogeneous medium, i.e. where $\nabla\varepsilon = 0$. This effect is not identified by the wave equations (2.3). For a real value χ, the coupling term in eq. (2.4) conserves the number and energy of the photons involved in the process of stimulated emission. A non-vanishing stimulating field of a particular radiation mode $\boldsymbol{k}_1$ is obtained from spontaneous emission or scattering of the incoming wave, e.g. elastic or Rayleigh scatterings. An expression evaluating the amount of spontaneous emission is outlined at the end of this Chapter.

The maximum parametric gain is found from eqs. (2.5) to occur in the same direction as that of the pump wave E_2, i.e. $\boldsymbol{k}_1 = \boldsymbol{k}_2$, and for $\theta = -\pi\,/\,2$. Groups of photons spontaneously emitted by $\boldsymbol{P}_2$ and identified as E_1 will have their arbitrary phase changed rapidly by the interaction as pointed out by eq. (2.5*c*), and the relative phase will become locked at $\theta = -\pi\,/\,2$. As a

result, an optical field E_1 will appear and the outgoing field will consist of an amplitude modulation, taking the form:

$$E_{out} = (E_2 + i E_1) e^{i(\omega t - \boldsymbol{k}\cdot\boldsymbol{r})} =$$

$$= E_o[cos(\gamma z) + i sin(\gamma z)] e^{i(\omega t - \boldsymbol{k}\cdot\boldsymbol{r})} \quad (2.6a)$$

$$Re E_{out} = E_o [cos(\gamma z) cos(\omega t - \boldsymbol{k}\cdot\boldsymbol{r}) -$$

$$- sin(\gamma z) sin(\omega t - \boldsymbol{k}\cdot\boldsymbol{r})] \quad (2.6b)$$

which has the appearance of a phase modulation. The real part of E_{out} reveals two quadrature waves [8] exchanging power as they propagate alongside each other in the z- direction, i.e. $\boldsymbol{k}\cdot\boldsymbol{r} = k_z \cdot z$. Each quadrature field rotates in the (*x, y*) plane with its amplitude varying periodically.

2.1.2 The operation of optical waveguide directional couplers

Bearing in mind the physical elements of the quantum Rayleigh emissions as outlined in Section 2.1.1 above, and relying on the quadrature states derived in the previous Section, we turn our attention to the case of an optical directional coupler composed of two single-mode waveguides. After identifying the waveguides by the letters *a* and *b*, we define the normalized fields $e = E / E_o$ (where E_o^2 corresponds to the normalizing input power) as

$$e_a = \left(p_a e^{-i\varphi_{pa}} + q_a e^{-i\varphi_{qa}}\right) f_a(\boldsymbol{r}) e^{i(\omega t - \boldsymbol{k}_a\cdot\boldsymbol{r})} \quad (2.7a)$$

$$e_b = \left(p_b e^{-i\varphi_{pb}} + q_b e^{-i\varphi_{qb}}\right) f_b(\boldsymbol{r}) e^{i(\omega t - \boldsymbol{k}_b\cdot\boldsymbol{r})} \quad (2.7b)$$

where the subscripts *p* and *q* correspond, respectively, to the initial quadrature phases of $\varphi = 0$ and $-\pi/2$, and amplitudes $p_{a(b)}$ and $q_{a(b)}$.

A mathematical solution to eqs. (2.5) can be derived by means of elliptic functions for the total field phasors of e_a and e_b as defined in eqs. (2.1) but its complexity obscures physical features of the optically linear parametric interactions. Such characteristics are outlined in the remainder of this Section.

As the waves propagate along a directional coupler – illustrated in cross-section in Fig. 2.1 – changes in the evanescent fields spread across the entire

modal field through the boundary conditions. For an input launched into one of the waveguides, the generated in-quadrature wave appears in both waveguides – see Fig. 2.2 – from amplified spontaneously emitted photons captured by each modal field. The evanescent fields of the two waveguides overlap in the cladding region they share – see Fig. 2.1 - bringing about coupling interactions between the two modal fields through the quantum Rayleigh field-dipole effects.

The tail of the evanescent field of either waveguide is scattered by the gradient of the local dielectric constant created by the core-cladding boundary of the other waveguide, as indicated by the source terms of the wave equations (2.3) containing $\nabla\varepsilon$. This scattering will lead to a loss factor being added to eqs. (2.4) and (2.5) and the scattered photons could become seed photons to be amplified in the other waveguide.

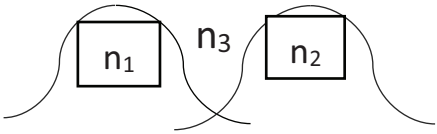

Fig. 2.1 The Rayleigh induced coupling of photons takes place in the cladding between the two waveguides with refractive index n_3

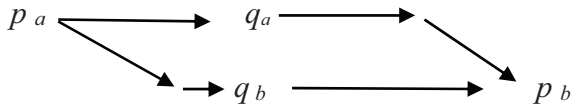

Fig. 2.2 A diagram of the longitudinal stages of the comprehensive coupling effects between the two waveguides of a directional coupler.

These effects are illustrated in (Marcatili *et al*. [14, Fig. 1(c)]; Syms and Peall [15]) where the measured optical power is coupled into the output waveguide through the cladding region, predominantly from the wave emerging from the terminated input waveguide. A small fraction of power associated with the evanescent tail of the input guided wave may directly excite the outgoing modal core field. These interactions are also present in Fig. 1(a) and (b) of [14] where two coupling stages can be identified: the conventional two-waveguide coupler and the coupling between the mode of the waveguide continuing to the output and the optical field propagating alongside the waveguide and originating from the terminated waveguide.

The exchange of power between any two modal fields is evaluated from eq. (2.4) integrated over the (*x, y*) - plane. Eqs. (2.5) are modified by substituting $P^{1/2}$ from eq. (2.1c) for the fields *E*, by replacing $\boldsymbol{k}$ with the propagation constant $\beta = \boldsymbol{k} \cdot \boldsymbol{u_z}$ and γ with this coupling coefficient:

$$\kappa_{12}(z) = \iint \gamma\,(x,y,z)\, f_1\,(x,y,z)\, f_2(x,y,z)dx\, dy \tag{2.8}$$

where $\kappa_{12}(z)$ is the total coupling coefficient across the (x, y) – plane, f_1 and f_2 being the modal field spatial distributions in the cladding. This coupling coefficient is similar to the butt-overlap coefficient measured in [14-15], it is always symmetric, i.e. $\kappa_{12}(z) = \kappa_{21}(z)$, and its numerical evaluation requires the normalization of eq. (1b). This is in contrast to the coefficients of [9] where the normalized modes carry an amplitude corresponding to one unit of power (1W) for the tail of the evanescent field which was physically scattered by the introduction of the other waveguide.

If a third wave is present, then each wave will interact with the other two, adding corresponding terms to the power and phase variations.

For $\beta_1 = \beta_2$, and $\theta = \pi/2$ or $(-\pi/2)$, the coupling of power from P_1 to P_2 or from P_2 to P_1, respectively, continues until complete depletion of the pump – see eqs. (2.5). For other values, θ shifts towards $-\pi/2$ for $P_1 < P_2$ and towards $\pi/2$ for $P_2 < P_1$. When $\Delta\beta = \beta_1 - \beta_2 \neq 0$ and initially $\theta = -\pi/2$, a substantial amplification of spontaneously emitted photons can occur as the relative phase θ is pulled back towards $-\pi/2$ by the strength of the optically linear parametric term $\Delta\varphi' = d\,(\varphi_2 - \varphi_1)/\,dz$ in eq. (2.5c) .

For initially $\theta = 0$, and with large values of $\Delta\beta$ dominating the rate of change of the relative phase shift, power is coupled from P_1 to P_2 for $\Delta\beta > 0$ and from P_2 to P_1 for $\Delta\beta < 0$. The condition of $\Delta\beta >> \Delta\varphi'$ will lead to the appearance of side lobes in the coupling profile when θ does not cover an entire $(0, 2\pi)$ interval, leaving in place residual coupled power – (see Fig. 2 of [14]). Starting with $\theta = 0$, $P_1 \neq P_2$ and $\Delta\beta \neq 0$, the rate of change of θ is asymmetric between $\Delta\beta > 0$ and $\Delta\beta < 0$, with the interaction term adding varying values.

With reference to eqs. (2.7), an optical pump p_a launched into waveguide a of the directional coupler will generate and amplify spontaneously emitted photons as they propagate in both waveguides a and b but with different coupling coefficients, giving rise to fields q_a and q_b in-quadrature with the pump p_a – see Fig. 2.2. Initially, power will flow from the input p_a into q_a and q_b, resulting in $P_a > P_b$. The next stage of longitudinal power coupling will have power from q_a transferred into p_b. This will lead to the appearance of a fourth wave in-quadrature with q_b and two quadratures phase shifted from the input pump p_a.

An instructive case of optical power being launched into both waveguides leads to couplings between in-quadrature waves ($\theta = -\pi/2$) and phase shifts resulting from interactions between in-phase waves ($\theta = 0$), e.g.:

$$\frac{d\, q_a^2}{dz} == -2\,(\,\kappa_{a\,a}\, p_a \sin\theta_{pa,\ qa} + \kappa_{a\,b}\, p_b \sin\theta_{pb,\ qa} + \\ + \kappa_{a\,b}\, q_b \sin\theta_{qb,\ qa}\,)\, q_a \qquad (2.9a)$$

$$\frac{d\,\varphi_{q\,a}}{dz} =$$

$$= \frac{\kappa_{a\,a}\, p_a \cos\theta_{pa,\ qa} + \kappa_{a\,b}\, p_b \cos\theta_{pb,\ qa} + \kappa_{a\,b}\, q_b \cos\theta_{qb,\ qa}}{q_a} \qquad (2.9b)$$

$$\frac{d\,\theta_{p\,b,\ q\,a}}{dz} = \beta_b - \beta_a + \frac{d\,(\varphi_{p\,b} - \varphi_{\,q\,a})}{dz} \qquad (2.9c)$$

where the subscripts *p* and *q* identify the two quadratures in each waveguide *a* and *b*. The other rate equations can be formulated by adjusting the subscripts. Despite the strong coupling coefficient, the net transfer of power is the difference between the simultaneous cross-coupling processes. Additionally, the intra-waveguide exchange of power between the quadrature waves may reduce the magnitude of the cross-coupling terms. This physically meaningful interpretation contrast with the mathematical techniques of references [16 -17].

2. 2 Phase-Sensitive Amplification of Optical Power

An optically linear parametric (OLP) interaction (Vatarescu [18]) consists of an electric dipole absorbing one photon and emitting one photon of the same frequency or energy, e.g. the elastic or Rayleigh scatterings associated with the Quantum Rayleigh conversion of photons (QRCP). This quantum process is localized, can take place in both homogeneous and inhomogeneous dielectric media, and is described classically, or macroscopically, by means of the interaction term included in the Poynting theorem of the flow of energy presented in equation (2.4) above. These physical processes require that Maxwell's *curl* $\boldsymbol{H}$ equation of *each* wave be driven by the *total* electric dipole polarisation available in the medium. The coupling term $\boldsymbol{P}_2 \cdot \boldsymbol{E}_1^*$ between one wave $\boldsymbol{E}_1^*$ and the dipole polarisation induced – through the linear susceptibility – by a second wave $\boldsymbol{P}_2 = \chi\, \boldsymbol{E}_2$, and included in the equation of motion of the complex Poynting vector equation, would correspond to stimulated emission initiated by the

spontaneous emission or another co-propagating wave of the same frequency [18].

The QRCP can couple photons between two optical waves propagating simultaneously through a homogeneous medium, i. e., for which $\Delta\,\varepsilon = 0$. Two optical waves of the same frequency, co-propagating through an optically linear and homogeneous dielectric medium, can exchange photons and undergo mutually induced phase-shifts providing the possibility for a variety of low-power integrated photonic devices such as phase-dependent amplification polarisation-dependent amplification, optical directional couplers, X-junctions, Y-junctions, polarisation rotation with spontaneous emission, etc.

2.2.1 Equations of motion for interacting optical waves in a dielectric medium

A physically meaningful coupled-wave formalism has been developed in the context of quantum Rayleigh coupling of photons for the operation of optical directional and counter-directional couplers, and other devices, in optically linear media as suggested in (Vatarescu [18-20]), for both homogeneous and inhomogeneous dielectric configurations. The resultant rate equations for the exchange of optical power $P_j = \hbar\,\omega\,N_j$ (j = 1 or 2) or the corresponding numbers of photons N_j between two interacting wavefronts and their corresponding phases φ_j, are derived from equations (2.5) above, and have the following forms [18-20]:

$$\frac{\partial}{\partial z}\,N_1 = g_1\,N_1 \qquad (2.10a)$$

$$g_1 = -\,\kappa\,\left(\frac{N_2}{N_1}\right)^{1/2}\sin\theta_{21} \qquad (2.10b)$$

$$\frac{\partial}{\partial z}\,\theta_{21} = \Delta\beta + \kappa\,\left[\left(\frac{N_1}{N_2}\right)^{1/2} - \left(\frac{N_2}{N_1}\right)^{1/2}\right]cos\,\theta_{21} \qquad (2.10c)$$

$$\frac{\partial}{\partial z}\,\varphi_1 = \kappa\,\left(\frac{N_2}{N_1}\right)^{1/2}cos\,\theta_{21} \qquad (2.10d)$$

$$\kappa = \frac{k_0}{2\,n}\iint dx\,dy\,\chi^{(1)}\,f_1\,f_2\,e_1\cdot\,\boldsymbol{e}_2 \qquad (2.10e)$$

$$\theta_{21} = (\,\beta_2 - \,\beta_1)\cdot z + \varphi_2 - \varphi_1 \qquad (2.10f)$$

where the gain coefficient g includes a phase dependence and the coupling coefficient κ is affected by the three-dimensional polarisation states of the two waves, that is, $\boldsymbol{e}_1$ and $\boldsymbol{e}_2$. The phase difference between the two waves is θ_{21}, β being the propagation constant and $z/t = \mathrm{v_p}$ is the phase velocity. In eq. (2.10 *e*), k_o and n specify the free-space wave vector and the effective refractive index, respectively. It should be noted that eqs. (2.10) describe the physically meaningful process of quantum Rayleigh conversion of photons [18-20]. The coupling coefficient of eq. (2.10*e*) indicates that the entire local value of the optically linear susceptibility $\chi^{(1)}$ is involved in the coupling process inside the dielectric medium at any point where the two spatial distributions f_1 and f_2 overlap, each having units of m^{-1}, and the field squared f^2 being normalized to a dimensionless unit over the cross-section area. This is in contrast to the physically impossible coupling between two optical waveguides apparently induced by a perturbation of the dielectric constant $\Delta\varepsilon$ in the cladding which leads, physically, to random, classical Rayleigh scattering [21]. Once again, it is worthwhile reiterating that a correct identification of physical processes will enable improved design and operation of photonic devices.

2.2.2 Applications of the optically linear parametric interactions

As an application the optical power coupling of eqs. (2.10) underpinned by the physical process of quantum Rayleigh conversion of photons, we consider the optical directional coupler depicted in Fig. 2.1 as a cross-section of two waveguides of core indices $\mathrm{n_1}$ and $\mathrm{n_2}$ separated by a cladding of refractive index $\mathrm{n_3}$. It is the overlap of modal fields in the cladding that brings about the exchange of optical power, with the coupling coefficient being proportional to the optically linear susceptibility $\chi^{(1)}$. The gain coefficient is phase- and polarisation- sensitive enabling selective amplification. Overall, it is possible to control the properties of a signal wave by adjusting the input values of a low-power pump wave because of the strong value of the optically linear susceptibility $\chi^{(1)}$. The relative phase (or phase-mismatch) can be controlled by adjusting the power ratio between the pump and the signal waves. Equations (2.10*c*-*d*) indicate the existence of a built-in mechanism for phase-matching between a strong pump and a weak signal through the parametrically induced phase shift. For converging or diverging Y-junctions, the coupling coefficient would have polarisation vectors projected onto each other.

By using the same optical frequency for an entire photonic circuit made up of dielectric waveguides, it should be possible to reduce the complexity associated with multiple waves and types of materials. Additionally,

electro-optic waveguides provide connections between the electrical signals and optical ones.

The case of a refractive index grating incorporated into a waveguide as depicted in Fig. 2.3, would be of particular interest in order to couple power between two waves of different propagation constants, either co – propagating or counter-propagating. The susceptibility (or the refractive index $n^2 = \varepsilon / \varepsilon_o = 1 + \chi$) becomes periodic

$$\chi^{(1)}(z) = \chi_o + \Delta\chi\,(z) \tag{2.11}$$

leading to a z-dependent coupling coefficient $\kappa\,(z)$. The local coupling gain is maximized in eq. (2.10*b*) above, for the longitudinal overlap between $\Delta\,\chi\,(z)$ and $sin\ \theta_{21}$. For a sinusoidal variation of amplitude ξ_o and period Λ, the perturbation of the susceptibility is

$$\Delta\chi\,(z) = \xi_o\, sin\left(\frac{2\,\pi\,z}{\Lambda}\right) \tag{2.12}$$

and the gain difference $\Delta\,g$ between the two halves of one periodic length Λ, and coupling direction over each half of Λ, i.e. $\pm\,g$, is proportional to

$$\Delta\,g\,(\,z,\theta) \propto \xi_0\, sin\left(\frac{2\,\pi z}{\Lambda}\right)\ sin\ (\,\Delta\beta\cdot z\ +\Delta\varphi\,) \tag{2.13}$$

resulting in the phase- matching condition

$$\frac{2\,\pi}{\Lambda} = \ \Delta\beta\ +\ \frac{d}{dz}\Delta\varphi \tag{2.14}$$

between the periodicity of χ and the relative phase $\theta = \Delta\,\beta\cdot z + \Delta\,\varphi$. A rectangular periodic perturbation of the susceptibility – see Fig. 2.3 – results in step-by-step amplification as the coupling in the first half of the period Λ, from one wave to the other is stronger than the opposite coupling over the second half of the period where $\Delta\,\chi = 0$. We point out that the coupling coefficient varies with distance and is not the Fourier transform of the refractive index modulation function as suggested in [22, 23].

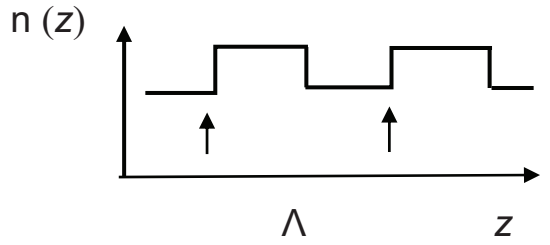

Fig. 2.3 The longitudinally varying coupling coefficient κ (z) for an index grating.

Another interesting application of equation (2.10) involves the optically linear parametric phase-pulling effect which shifts the phase of a weak signal towards a ($-\pi/2$) difference from that of strong pumps – see equations (2.10*c*-*d*). As a result, two optical waves co-propagating through a dielectric medium will have their photons transfer from one wave to the other depending on the relative phase between the two waves. This process, repeatedly, will eliminate optical waves whose phases diverge substantially from the phase of the surviving wave which will dominate the output and preserve the coherence of the optical beam despite light-matter interactions.

2.3 Physical Aspects of Optically Linear Parametric Interactions

If the optical coupler is capable of supporting two composite symmetric and anti-symmetric eigenmodes [9], [12] – which satisfy the necessary electromagnetic boundary conditions – their superposition cannot replace the incoming wave at the input because, physically, the photons have to undergo a change of wave vectors and momenta through the mediation of a radiating electric dipole polarisation. These eigenmodes could also take part in the coupling interactions. The coupled-mode theory [9–12] does not provide any explanation as to how a group of photons can, simultaneously, cross from one waveguide into the other as well as propagating in each of the eigenmodes of the composite two-waveguide structure, with different propagation constants.

A common analytical expression for optical field coupling between two modes can be seen in (Xu *et al*. [24, eqs. (1–3)]), where the analytical solution reveals a quadrature wave as a result of a phase-mismatch between the modes and which would persist even if the coupling coefficient vanishes. Furthermore, that set of equations disregards the power (or amplitude) – phase interplay which is evident in eqs. (2.10) above and

typical of parametric interactions [3-4], [25-26]. It is the phase shift $\Delta\varphi$ induced by the optically linear parametric interactions which enables the amplification of spontaneously emitted photons up to a certain level of power by countering the phase-mismatch effect of a large $\Delta\beta$. The optically linear parametric term of $\Delta\varphi$ can also modify the coupling length by adding to or subtracting from $\Delta\beta$.

The coupling coefficient of eq. (2.8) is symmetric and includes all three vectorial components of the optical modes existent in the common cladding, which is not the case in references [9–12]. In this Chapter, the coupled-wave equations have been derived without resorting to a mode orthogonality relation and they apply to any two optical waves, e.g., guided, unguided, or partially guided. The conservation of energy in eq. (2.4-5) leads to coupled wave equations with longitudinally varying coefficients multiplying the optical fields.

For backward stimulated Rayleigh scattering (Zhu *et al*. [27]), the approach presented in this analysis should be adjusted for counter-propagating waves [25-26], with the relative phase between the forward propagating pump and the photons spontaneously emitted at location l being $\theta = \beta\ z - \beta\ (l - z) + \Delta\varphi$. Up to a certain level of power, backward amplification can take place subject to the conditions of $d\ \theta / dz = 0$ and $-\pi < \theta < 0$.

In the following chapters, these properties of wave coupling mechanisms will be adopted for photon coupling processes.

2.4 Quantum Aspects of Quantum Rayleigh Coupling of Photons

This Section presents some preliminary aspects of the quantum Rayleigh processes that will be applied and further expanded upon in following Chapters.

2.4.1 Evaluation of the spontaneously emitted power

An estimate of the optical power of the parametric spontaneous emission P_{sp} is made from the product of the photon energy and the transition rate of pump photons being converted into spontaneous photons by the electric dipole polarisation. The derivation follows the analysis by Tang [28], adjusted for SI or MKSA units and linear dipole polarisations; the result, as expected, corresponds to the quantum Rayleigh emission rates, proportional to the fourth power of the frequency. It is based on the Fermi Golden Rule involving the transition matrix element between number states, and the

density of radiation modes in an infinite medium [6-7]. The resultant formula is

$$P_{sp} = \frac{\chi^2 \, h \, P_{pump} \Omega \triangle z}{\pi n \, \lambda^4} \tag{2.15}$$

where h is Planck's constant, λ is the wavelength, and Ω is the solid angle, centred on the fibre's axis into which photons are emitted and are likely to be captured by the guided mode. This solid angle has the geometrical shape of a cone and its apex half-angle is

$$\alpha = arccos\,(\beta / k_{\text{core}}) = arccos\,(n_{\text{eff}} / n_{\text{core}})$$

so that $\Omega = \pi \alpha^2$, k_{core} and n_{core} being, respectively, the wavenumber and the refractive index of the core, and n_{eff} being the effective index of the mode. For $\lambda = 1.55 \times 10^{-6}$ m, $\Omega = 2 \times 10^{-2}$ sr, and $\Delta z = 10^{-6}$ m, one calculates $P_{sp} = 2 \times 10^{-19} \; P_{pump}$.

While necessary as a source of photons to be amplified, the spontaneously emitted Rayleigh radiation may be difficult to isolate from other interactions which were measured in [27].

2.4.2 Equations of motion of field operators

Quantum mechanically [6-8], the Hamiltonian of interaction $\hat{H}_{int}$ for stimulated emission involving an electric dipole and two optical fields of the same frequency but different wave vectors takes the form:

$$\hat{H}_{int} = \hbar\chi \left(\hat{a}_2^{\dagger} \, \hat{a}_1 + \hat{a}_1^{\dagger} \, \hat{a}_2 \right) \tag{2.16}$$

where $\hat{a}$ and $\hat{a}^{\dagger}$ represent the annihilation and creation operators of the two fields. The reduced Planck constant and the linear susceptibility are, respectively, denoted by $\hbar$ and χ.

The Heisenberg equation of motion for $\hat{a}_1$ leads to

$$\frac{d}{dt} \, \hat{a}_1 = -\frac{i}{\hbar} \left[\hat{a}_1 \, , \hat{H}_{int} \right] = \; -i\chi \, \hat{a}_2 \tag{2.17}$$

This simple relation indicates that quantum mechanically (optically) coupling of photons can take place in a homogeneous dielectric medium, i.e. where the susceptibility χ is constant. This effect is easily linked to the quantum Rayleigh emission of spontaneous and stimulated photons [6-7]. The corresponding macroscopic density of the electric dipole polarisation

$\boldsymbol{P} = \varepsilon_o \chi (\boldsymbol{E}_1 + \boldsymbol{E}_2)$ will drive the *curl* $\boldsymbol{H}$ Maxwell equation for *each* optical wave. This effect cannot be derived classically and its quantum nature is emphasized in the Introduction to this Chapter.

2.5 Conclusions

This Chapter outlines a photonic beam conversion and coupling formalism based on the Poynting theorem of the flow of energy in a dielectric medium, in conjunction with the quantum Rayleigh effects of spontaneous and stimulated emissions from oscillating electric dipoles. The linear parametric gain couples photons from a pump wave into an in-quadrature wave by amplifying the initial spontaneously emitted photons or other available seed photons. Two optical waves of the same frequency interact with each other if they share the same linear dielectric medium. The coupling coefficient involves the total value of the local susceptibility where any two waves overlap in space and time, and all three vectorial components are treated equally.

Despite being presented in tens of textbooks and hundreds of published papers over half a century, the perturbation-based coupled-mode theory does not involve a physically meaningful process of stimulated emission which could be controlled in order to develop new photonic devices and applications. In contrast, the couple-wave analysis emerging from the quantum Rayleigh conversion of photons has the potential to operate with low levels of pump powers and delivers phase-sensitive and polarisation-sensitive gain coefficients.

References

1. Y. R. Shen, *The Principles of Nonlinear Optics*, John Wiley & Sons, 1984.
2. R. W. Boyd, *Nonlinear Optics*, Academic Press, 1992.
3. A. Vatarescu, "Light conversion in nonlinear monomode optical fibers", IEEE J. Lightwave Technol., **5**, 1652 - 1659, (1987).
4. K. Inoue and T. Mukai, “Signal wavelength dependence of gain saturation in a fiber optical parametric amplifier", Opt. Lett., **26**, 10 -12, (2001).
5. K. Inoue and T. Mukai, "Spectral hole in the amplified spontaneous emission spectrum of a fiber optical parametric amplifier", Opt. Lett., **26**, 869-871, (2001).
6. D. Marcuse, *Principles of Quantum Electronics*, Academic Press, 1980.

7. W. H. Louisell, *Quantum Statistical Properties of Radiation*, John Wiley & Sons, 1973.
8. L. Mandel and E. Wolf, *Optical Coherence and Quantum Optics*, Cambridge University Press, 1995.
9. W. P. Huang, "Coupled-mode theory for optical waveguides: an overview", J. Opt. Soc. Am. A, **11**, 963-683, (1994).
10. Q. Yishen, Li Denfeng, Li Gaoming, and Li Denfeng ," Rigorous vectorial coupled-mode theory for the isotropic waveguide with anisotropic disturbance ", J. Opt. Soc. Am. B, **23**,120-125, (2006).
11. W. P. Huang and J. Mu, "Complex coupled-mode theory for optical waveguides", Opt. Express, **17**, 19134 -19152, (2009).
12. E. Marcatili, "Improved Coupled-Mode Equations for Dielectric Guides", IEEE J. Quantum Electron., **22**, 988-993, (1986).
13. S. J. Orfanidis, *Electromagnetic Waves and Antennas*, Rutgers University.
14. E. A. J. Marcatili, L. L. Buhl and R. C. Alferness, "Experimental verification of the improved coupled-mode equations ', Appl. Phys. Lett., **49**, 1692-3, (1986).
15. R. R. A. Syms and R. G. Peall, "Mode confinement and modal overlap in electro-optic channel waveguide devices", Optics Comm., **74**, 46 -48, (1989.
16. B. Bai, L. Liu, and Z. Zhou, "Ultracompact, high extinction ratio polarisation beam splitter-rotator based on hybrid plasmonic-dielectric directional coupling", Opt. Lett., **42**, 4752 - 4755, (2017).
17. G. P. Agrawal, Optical Waveguides; w2.optics.rochester.edu/users/gpa/opt468a.pdf.
18. A. Vatarescu, "Photonic coupling between quadrature states of light in a homogeneous and optically linear dielectric medium", J. Opt. Soc. Am. B**, 31**, 1741–1745, (2014).
19. A. Vatarescu, "Photonic Quantum Noise Reduction with Low-Pump Parametric Amplifiers for Photonic Integrated Circuits", Photonic*s,* **3**, article 61, (2016).
20. A. Vatarescu, "Phase-Sensitive Amplification with Low Pump Power for Integrated Photonics, "*OSA Advanced Photonics Congress*, paper ID: IM3A.6., (2016).
21. Z. Wang, H. Wu, X. Hu, N. Zhao, Qi Mo and & G. Li, "Rayleigh scattering in few-mode optical fibers", Sci. Rep. **6**, 35844, (2016).
22. T. Erdogan, "Fiber Grating Spectra", J. Lightwave Technol., **15**, 1277 - 1294, (1997).

23. L. Jin, W. Jin, J. Ju, and Y. Wang, "Coupled Local-Mode Theory for Strongly Modulated Long Period Gratings ", J. Lightwave Technol., **28,** 1745-1751, (2010).
24. M. Xu, F. Li, T. Wang, J. Wu, L. Lu, L. Zhou, and Y. Su, "Design of an Electro-Optic Modulator Based on a Silicon-Plasmonic Hybrid Phase Shifter", IEEE J. Lightwave Technol., **31**, 1170-1177, (2013).
25. A. Vatarescu, "Intensity discrimination through nonlinear power coupling in birefringent fibers", Appl. Phys. Lett., vol. **49**, p. 61, (1986).
26. A. Vatarescu, "Nonperiodic power coupling in highly birefringent nonlinear optical fibers", Appl. Phys. Lett., vol. **49**, p. 1409, (1986).
27. T. Zhu, X. Bao, L. Chen, H. Liang, and Y. Dong, "Experimental study on stimulated Rayleigh scattering in optical fibers", Opt. Express, **18,** 22958-64, (2010).
28. C. L. Tang, Spontaneous and Stimulated Parametric Processes, in Quantum Electronics, eds. H. Rabin and C. L. Tang, vol. 1, p. 419, section C, Academic Press, 1975.

CHAPTER THREE

THE INTRINSIC OPTICAL FIELD OF PHOTONS

The quantum environment of very small levels of energy and spatial and temporal dimensions is described by means of operators and wavefunctions. These orthogonal and normalised wavefunctions solve the Schrödinger equation, being eigenfunctions of the unperturbed Hamiltonian representing a quantum system. They provide the probability of a quantum event appearing at a particular location and specific time, as well as delivering expectation values for observable operators. The mathematical construct is defined as a Hilbert space within which any combination of the eigenstates with arbitrary weighting coefficients will always lie. The eigenfunctions are normalised and orthogonal to each other as well as satisfying inner products. The operators correspond to physical variable, while the Hilbert space will provide numerical values for characteristic properties – also known as degrees of freedom of each operator – of the quantum objects or systems.

In the context of photonic systems involving properties of optical entities such as photonic beams propagating through and interacting with dielectric media, two types of quantum states can be identified. The first type consists of time-dependent pure states that deliver - upon a single measurement – one value out of a set of possible eigenvalues corresponding to the observable operator. Because of various perturbations such as intervening photon-dipole interactions, temperature fluctuations, surrounding electric field disturbances, etc., even for identical input conditions, an output distribution of values will arise. The second type of quantum states is known as mixed states which, additionally, describe classical distributions of ensemble of measurements taking place in different locations and/ or occurring at different times.

The amount of energy carried by a steady-stream radiation mode is given by an integer number of the smallest indivisible amount of energy labelled as a photon. The corresponding pure quantum state of a single measurement of energy is, accordingly, named a number state (or a Fock state). However, such number states always have a vanishing optical field, which is

physically impossible. To overcome this deficiency, the stream of photons needs to be represented by two consecutive number states.

For physically realistic, temporarily fluctuating number of photons, an ensemble of time-dependent single measurements will give rise to an overall output distribution of value probabilities. One such ensemble having a Poissonian distribution of probabilities over the number states is defined as a coherent state. However, by their mathematical definition, coherent states are not impacted by a loss of photons, while a process of amplification breaks down their structure, rendering them unsuitable for photon - dipole interactions.

An apparent isomorphism between quantum harmonic oscillators and optical fields would connect the position operator of the oscillator to a quadrature component of the field by means of a rather complicated transformation between bases of eigenstates. Yet, the optical field is not composed of oscillators.

This Chapter develops a physically meaningful formalism for the quantum description of optical fields and their interactions with matter. No equivalence or isomorphism with quantum harmonic oscillators is invoked in the derivation of dynamic and coherent number states.

3.1 Instantaneous Measurements of Photonic Beam Fronts

Optical sources of sub-Poissonian radiation (Davidovich [1]) would enhance the detection resolution of optical signals by virtue of reduced fluctuations in their number of photons and, possibly, better defined phases and states of polarization. A broad range of applications can be envisaged from optical sensing of environmental variables to improved signal-to-noise ratio in optical communications (Kikuchi [2]) provided controllable and highly-efficient sources could be developed.

It is commonly assumed that the sub-Poissonian distribution of photons is a quantum property of light because it requires a quasi-distribution for its description [1] in terms of coherent states of light (CSL). However, CSLs do not specify *instantaneous* properties of photonic wavefronts which are required for localized interactions between optical waves simultaneously propagating through the same dielectric medium. Yet, by identifying a physically meaningful quantum wavefunction (Vatarescu [3]), sub-Poissonian distributions can be generated with any number of photons for any overall distribution, by means of the optically linear parametric (OLP) amplification of photons in the “classical” regime (Vatarescu [4-6]).

In the context of parametric amplification of photons by a factor of G, for unsaturated gain, the expectation value $|\alpha|^2$ of the number of photons

corresponding to a coherent state of light $|\alpha\rangle$ will become $G\,|\alpha|^{2}$, but, physically, the photon distribution will develop gaps between any two consecutive number states as $G\,\mathrm{n} - G\,(\mathrm{n}-1) = G$. Thus, the coherent state is destroyed and replaced, *mathematically*, by a mixed state of quasi-distributions of coherent states [1]. As a result, rather complicated and roundabout procedures are needed to, apparently, specify the number of photons in terms of quasi-probabilities of coherent states which are, themselves, expressed as a superposition of number states.

A criterion for generating sub-Poissonian distributions of photons through differential amplification of photons was outlined in [4] involving the phase-dependent gain coefficient. However, in order to design and control such sources, a physical model for amplification of any photon distribution and level of number states needs to be developed beyond the identification of the phase-dependent gain coefficient (Vatarescu [4-7]) accompanied by a parametric phase-pulling effect which shifts the phase of a weak signal towards a $(-\pi)/2$ difference from that of strong pumps. Photon coupling processes involve the *instantaneous* values of the wavefronts interacting simultaneously at a point in space within a dielectric medium [4 -7].

A photonic wavefront carries a number of photons across a plane hosting dipoles and its duration will be determined by the response time of the photon-dipole interaction. A simple and practical photonic quantum state $|\Psi_{n}\rangle$ is needed which is capable of delivering the *instantaneous* number of photons of an optical, or photonic, wavefront, and the associated phase regardless of the overall photon distribution of the beam, so that $\langle \Psi_{n}|\,\hat{a}^{\dagger}\,(\text{or }\hat{a})\,|\Psi_{n}\rangle \neq 0$ for the annihilation and creation operators, $\hat{a}$ and $\hat{a}^{\dagger}$, respectively. Such a state vector is readily identifiable in the derivation below, from the two-component Hamiltonian of the optical field in free-space. The dynamic number states defined for a given number of photons as $|\Psi_{n}(t)\rangle = (|\,\mathrm{n}(t)\rangle + |\,\mathrm{n}(t)-1\rangle)/2^{1/2}$ can deliver a non-vanishing expectation value for the field operators. This will enable direct calculations of the wavefront number of photons and phase shifts stemming from interactions with dielectric media. This is in contrast to the quadrature eigenstates of $\langle x\,|\,\hat{a}^{\dagger}+\hat{a}\,|\,x\rangle \neq 0$ used in quantum tomography (Breitenbach *et al*.[8]; Lvovsky and Raymer [9]) which invoke, by analogy, the eigen-functions $|\,x\,\rangle$ of the coordinate, or position, operator of a mass particle harmonic oscillator. Nevertheless, the strength of the optical field is determined by the instantaneous number of photons (Glauber and Lewenstein [10]) without any connection to the position of a harmonically moving mass particle. The spatial field profile of a group of photons is also derived below.

A long series of intensity measurements [8-9] of the *instantaneous* number of photons carried by the wavefronts reaching the detection surface will provide a probability distribution for the ensemble of the number states of the wavefronts forming the optical beam. Upon detection [8], a photonic wavefront delivers (or collapses into) a particular number state whose values of number of photons, phase, wave vector, state of polarization, etc. would be stochastic. The sequence of optical wavefronts of the beam will form an ensemble of photonic systems composed of an ergodic distribution, i.e., within a long enough duration, the characteristics of the wavefronts are reproduced. These measured *instantaneous* values will build up probability distributions from which the ensemble expectation values and variances can be calculated. Nevertheless, it should be pointed out that the localized measurement method of quantum tomography [8 - 9] does not deal with photon couplings or interactions in a dielectric medium.

Similarly, the definition of the phase eigenstates (Pegg and Barnett [11]) leads to a rather problematic aspect as pointed out in [11]: "We note that a phase state is not a physical state because the expectation value of the photon number diverges as $s \rightarrow \infty$. " [11, Sec. IV, p. 1668].

Identifying photons with levels of energy of the electromagnetic field and without any analogy to the quantum harmonic oscillator, the longitudinal and lateral profiles of the intrinsic field of photons is obtained in this Chapter from the corresponding electromagnetic vector potential.

The optical field of a dynamic and coherent number state – derived below from its equation of motion – will enable direct prediction and control of the output distribution of photons, for further signal processing and interactions, of both magnitudes and phases of the instantaneous wavefront values for any overall distribution. Phase information will be obtained from the quadrature phase operators, and the physical spatial profile of the field of one single photon or a group of photons associated with a wave or beam front will be evaluated by combining the expectation value of the intrinsic field with the Maxwell equations. Additional properties of the dynamic and coherent number states of light are discussed in this Chapter. The advantages of the dynamic and coherent states in characterizing sub-Poissonian distributions of photons are outlined.

3.2 Pure and Mixed Quantum States

The field of Quantum Optics employs the postulates and notations of Quantum Mechanics but it also requires specific features resulting from the propagation of electromagnetic radiation and its interactions with various dynamic electrons and their environments of atoms and molecules. The

quantum optic operators are derived from the quantization of the electromagnetic field while the state vectors are conventionally formed by means of superpositions of the eigenstates of the Hamiltonian of the free field.

The measurements of optical waves would deliver various properties of the optical beam such as the instantaneous intensity, phase, polarisation, frequency, etc. Overall distributions will be obtained for a large number of repeated wavefront measurements. By contrast, it is a common approach to represent a quantum state by means of only an overall distribution of values (Garrison and Chiao [12]) such as the coherent state, even though each measurement provides an instantaneous eigenvalue of the observable operator being investigated.

A pure state delivers one single measurement (Breitenbach *et al*. [8]; Fano [13]) whereas a mixed state describes the statistical distribution of an ensemble of measurements (Fano [13]). A photonic beam front carries a number of photons across a plane hosting dipoles and its duration will be determined by the response time of the photon-dipole interaction.

With the energy eigenstates – in the Dirac notation – denoted by $| S_j \rangle$, a pure state $|\Psi (\boldsymbol{r}, t)\rangle$ takes the form of a coherent superposition and is a solution of the the Schrödinger equation driven by a space and time dependent Hamiltonian $\hat{H} (\boldsymbol{r}, t)$, with the common expressions (Garrison and Chiao [12]; Steck [14]):

$$|\Psi (\boldsymbol{r}, t)\rangle = \Sigma_j \, c_j (\boldsymbol{r}, t) \, | S_j \rangle \tag{3.1a}$$

$$i \hbar \frac{\partial}{\partial t} |\Psi (\boldsymbol{r}, t)\rangle = \hat{H} (\boldsymbol{r}, t) |\Psi (\boldsymbol{r}, t)\rangle \tag{3.1b}$$

where the coefficients of expansion $c_j (\boldsymbol{r}, t)$ are space $\boldsymbol{r}$ and time t dependent, satisfying the condition $\Sigma_j \, | c_j (\boldsymbol{r}, t) |^2 = 1$. The orthogonality and normalisation conditions are given by $\langle S_j \, | \, S_i \rangle = \delta_{ij}$. The pure state is associated with a maximum amount of information and, initially, identically prepared input sates. The overall distribution of measured values describing a mixed quantum state $| \Phi (\boldsymbol{r}, t)\rangle$ incorporates the statistical distribution of output measurements for specific input states, in the form (Garrison and Chiao [12]; Steck [14]):

$$| \Phi (\boldsymbol{r}, t)\rangle = \Sigma_k \sqrt{p}_k \, |\Psi (\boldsymbol{r}, t)\rangle_k = \Sigma_k \Sigma_j \sqrt{p}_k \, c_j^{(k)} \, | S_j \rangle \tag{3.2}$$

with the initial distribution p_k of the pure states $|\Psi(\boldsymbol{r},t)\rangle_k$, satisfying $\Sigma_k\ p_k = 1$.

A commonly used operator for various predictions is the state density operator defined as an outer product of quantum states (Garrison and Chiao [12]; Steck [14]):

$$\hat{\rho} \equiv |\Psi(\boldsymbol{r},t)\rangle\langle\Psi(\boldsymbol{r},t)| = \Sigma_j\ |c_j(\boldsymbol{r},t)|^2\ |S_i\rangle\langle S_i| + \\ + \Sigma_i\ \Sigma_{j\neq i}\ c_i(\boldsymbol{r},t)\ c_j^*(\boldsymbol{r},t)\ |S_i\rangle\langle S_j| \qquad (3.3)$$

where the last term indicates whether or not a coherent outcome is possible. When the interference term on the second line of eq. (3.3) vanishes, the density operator corresponds to a mixed state. The time-dependent expectation value $\lambda(t)$ of an observable operator $\widehat{\Lambda}$ is evaluated by calculating the inner product between the Hermitian conjugate state and the operator-modified state vector, i.e, these relations:

$$\lambda(t) = \left\langle \widehat{\Lambda} \right\rangle = \langle\Psi(\boldsymbol{r},t)|\widehat{\Lambda}|\Psi(\boldsymbol{r},t)\rangle = \\ = \int_{-\infty}^{\infty} dr\ \Psi^*(\boldsymbol{r},t)\ \widehat{\Lambda}\ \Psi(\boldsymbol{r},t) \qquad (3.4a)$$

$$\lambda(t) = \Sigma_j\ |c_j(\boldsymbol{r},t)|^2\ \langle S_j|\widehat{\Lambda}|S_j\rangle + \\ + \Sigma_i\ \Sigma_{j\neq i}\ c_i(\boldsymbol{r},t)\ c_j^*(\boldsymbol{r},t)\ \langle S_j|\widehat{\Lambda}|S_i\rangle \qquad (3.4b)$$

The detection process is represented by a projection operator $\widehat{\Pi} = |S_i\rangle\langle S_i|$ which leaves the quantum object in an output state $|\Psi(\boldsymbol{r},t)\rangle_{out}$ associated with the measuring apparatus, i.e.,

$$|\Psi(\boldsymbol{r},t)\rangle_{out} = \widehat{\Pi}(\boldsymbol{r},t)\,|\Psi(\boldsymbol{r},t)\rangle = c_i(\boldsymbol{r},t)\ |S_i\rangle \qquad (3.5)$$

By attaching position and time coordinates to the projection operator, we identify the location of the measuring apparatus and the time of a particular type of measurement taking place therein (R. B. Griffiths [15]).

A composite system of two quantum objects will be described in a Hilbert space $\mathcal{H}$ spanned by the tensor product of the individual Hilbert spaces, i.e., $\mathcal{H}_{AB} = \mathcal{H}_A \otimes \mathcal{H}_B$ leading to a composite quantum state (Garrison and Chiao [12]; Steck [14]):

$$|\Psi_{12}(\boldsymbol{r},t)\rangle = |\Psi_1(\boldsymbol{r},t)\rangle \otimes |\Psi_2(\boldsymbol{r},t)\rangle =$$

$$= \Sigma_i \Sigma_j \, c_i(\boldsymbol{r},t)\, c_j^*(\boldsymbol{r},t) \mid S_i \rangle \mid S_j \rangle \qquad (3.6)$$

where the subscripts *i* and *j* correspond to the Hilbert spaces *A* and *B*, respectively. The relations of (3.4) requires space and time overlaps between the two Hilbert spaces.

Another case of combined Hilbert spaces arises when one quantum object is characterised, for example, by two variables and corresponding operators leading to $\mathcal{H}_{12} = \mathcal{H}_1 \otimes \mathcal{H}_2$, where the subscripts indicate the two degrees of freedom. In this case, in eq. (3.6), the subscripts *i* and *j* correspond to the Hilbert spaces 1 and 2, respectively. It should be emphasized that spatial and temporal overlaps are required for the interference or cross term to make a contribution in the expressions of equations (3.3), (3.5), and (3.6). This is in contrast to the concept of global functions of a mixed state of an ensemble of distributions that carry neither space nor time dependence, and which are claimed to generate nonlocal quantum effects.

3.3 Field Quantisation without Quantum Harmonic Oscillators

A field quantisation should be derived without invoking an equivalence with quantum harmonic oscillators, if only because there are no oscillators carried by an optical wave.

As the number of photons and related field amplitude and phase carried by a photonic beam or wave front may change as a result of the quantum Rayleigh conversion of photons presented in Chapter 2, the equations of motions for the corresponding expectation values will be evaluated with the Ehrenfest theorem (Steck [14]; D. J. Griffiths [16]). To this end, a pure quantum state is needed, capable of delivering correct values for the instantaneous number of photons, the optical field amplitude and the phase quadratures.

Photons and their *instantaneous* properties are detected and measured as a sequence of wavefront energy number states | n ⟩ (Breitenbach *et al*. [8]) which make up a pure quantum state vector

$$|\Psi(\boldsymbol{r},t)\rangle = \Sigma_n \, c_n(\boldsymbol{r},t) \mid \mathrm{n} \rangle \qquad (3.7)$$

regardless of the overall distribution to which the photons belong [8-9]. The overall quantum probability of occupation of an eigenstate is given by the

normalized distribution of photons – crossing a surface at location $\boldsymbol{r}$ –with the time-varying coefficients $|c_n|^2$ satisfying the condition $\Sigma_n |c_n|^2 = 1$, and based on the orthogonality $\langle n \mid m \rangle = \delta_{nm}$. The detection of photons occurs as a result of their optical field exchanging energy with electrons of the atomic structure of the detector, similarly to the Jaynes - Cummings model ([12]; [14]) for the quantized dipole-photon exchange of energy. The detection, or any other interaction process, is meant to "collapse" the photonic quantum state into an instantaneous eigenvalue of a number operator regardless of the ensemble distribution to which it belongs, e.g., a coherent state or any arbitrary distribution.

3.3.1 Optical fields of dynamic and coherent number states

Based on the formalism presented by Glauber and Lewenstein [10] and Blow *et al*. [17], the magnitude of the Poynting vector, i.e. the flux of energy $\mathcal{E}$ (or number of photons /s) carried by an optical wavefront of frequency ω and crossing a plane surface at position z is given in terms of the electromagnetic field magnitudes E and B by the equalities:

$$\mathcal{E} = \omega \, \varepsilon E^2 + c^2 \omega B^2 = 0.5 \, \hbar \cdot \omega \, (a\, a^* + a^* a) \tag{3.8}$$

with $a = (\varepsilon / \hbar)^{1/2} \, (E + i\, c\, B)$ and its complex conjugate being a^*. From this relation, one defines the annihilation and creation operators as:

$$\hat{a} = \sqrt{\frac{\varepsilon}{\hbar}} \left(\hat{E} + i\, c\, \hat{B} \right) \tag{3.9a}$$

$$\hat{a}^\dagger = \sqrt{\frac{\varepsilon}{\hbar}} \left(\hat{E} - i\, c\, \hat{B} \right) \tag{3.9b}$$

with ε and $\hbar$ indicating the permittivity of the medium and the reduced Planck constant, respectively. The constant c is the speed of light in vacuum. The free-space Hamiltonian $\hat{H}_f$ is explicitly written as [10]:

$$\hat{H}_f = \hbar\omega \hat{N}_c \tag{3.10a}$$

$$\hat{N}_c = 0.5 \, (\hat{a}^\dagger \hat{a} + \hat{a}\, \hat{a}^\dagger) \tag{3.10b}$$

where $\hat{N}_c$ is the symmetric and complete number operator and its eigenstates are the number states $| n \rangle$. The two terms of eq. (3.10) would

have different eigenvalues. Based on experimental results indicating that one photon is an indivisible amount of energy, we seek a wave function $| \Psi_n \rangle$ which will deliver the number of photons n from the equalities:

$$\langle \Psi_n | \widehat{N}_c | \Psi_n \rangle = n \qquad (3.11a)$$

$$\langle \Psi_n | \hat{a}^\dagger \hat{a} | \Psi_n \rangle + \langle \Psi_n | \hat{a} \hat{a}^\dagger | \Psi_n \rangle = 2\,n \qquad (3.11b)$$

so that, from Eqs. (3.10) the number states $| n \rangle$ are eigenfunctions, with different eigenvalues, of both of the product operator terms:

$$\langle n | \hat{a}^\dagger \cdot \hat{a} | n \rangle = n \qquad (3.12a)$$

$$\langle n-1 | \hat{a} \cdot \hat{a}^\dagger | n-1 \rangle = n\,; \text{ or } \langle n | \hat{a} \cdot \hat{a}^\dagger | n \rangle = n+1 \qquad (3.12b)$$

Thus, in the basis of number states, the commutator $[\hat{a}, \hat{a}^\dagger] = 1$ is obtained as a result of the quantization rather than leading to it. This does not affect the choice of the superposition wave function $| \Psi_n \rangle$ and related expectation values:

$$| \Psi_n \rangle = (| n \rangle + | n-1 \rangle) / 2^{1/2} \qquad (3.13a)$$

$$\langle \Psi_n | \hat{a}^\dagger \hat{a} | \Psi_n \rangle = 0.5\,(n + n - 1) = n - 0.5 \qquad (3.13b)$$

$$\langle \Psi_n | \hat{a} \hat{a}^\dagger | \Psi_n \rangle = 0.5\,(n + n + 1) = n + 0.5 \qquad (3.13c)$$

$$\langle \Psi_n | \widehat{N}_c | \Psi_n \rangle = 0.5 \times 2\,n = n \qquad (3.13d)$$

which is the number of photons per time or the photonic flux of its beam front.

This relation satisfies the conditions of eqs. (3.11) and implies two opposite processes which can be interpreted as shifting a number state up or down by one photon which is the smallest indivisible amount of energy of an optical field. Their illustration can be seen in Fig. 3.1. Experimentally, from the photoelectric effect, the optical fields consist of an integer number of the lowest indivisible amount of energy, i.e. photons. However, for the lowest state of $n = 1$, the *expectation value* would be half a photon because the lower bound (Carruthers and Nieto [18]) leads to $(\langle 0 | \hat{a}^\dagger)(\hat{a} | 0\rangle) = 0$. For physical reasons, one photon will be ascribed to the first non-zero eigenvalue. Nevertheless, an alternative derivation presented in the

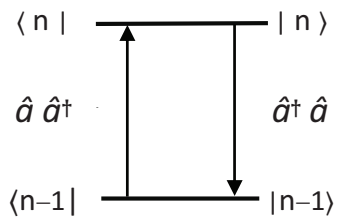

Fig. 3.1. An illustration of the dynamic and coherent two-component number states. Note that: $\langle n \mid \hat{a}^{\dagger} = n^{1/2} \langle n-1 \mid$ and $\langle n-1 \mid \hat{a} = n^{1/2} \langle n \mid$.

Appendix to this Chapter confirms the validity of this approach.

The field operators $\hat{a}$ and its adjoint $\hat{a}^{\dagger}$ connect two consecutive number states, and consequently, a superposition of $| n-1\rangle$ and $| n \rangle$ should give rise to a non-zero optical field for the following state vector:

$$| \Psi_n(t) \rangle = c_1(t) \, | n \rangle + c_2(t) \, | n-1 \rangle \tag{3.14a}$$

$$| \Psi_n \rangle = (| n \rangle + | n-1 \rangle) / 2^{1/2} \tag{3.14b}$$

with the normalization of $| c_1 |^2 + | c_2 |^2 = 1$. For reasons that will become clear below, these states of eqs. (3.14) will be identified as dynamic and coherent number states.

Analogously to the derivation [14] of coherent states of light $| \alpha \rangle$, the non-Hermiticity of the photon annihilation and creation operators allows for complex classical numbers (c –numbers) to be delivered when these operators act on number states. Applying $\hat{a}$ and $\hat{a}^{\dagger}$ to $| n \rangle$ returns a complex c – number

$$s_n = | s_n | \, exp(-i\varphi_n) \tag{3.15}$$

which will become the complex amplitude of the state, so that:

$$\hat{a} \, | n \rangle = s_n | n-1 \rangle \tag{3.16a}$$

$$\hat{a}^{\dagger} \, | n-1 \rangle = s_n^{*} \, | n \rangle \tag{3.16b}$$

Recalling that $\hat{a}$ and $\hat{a}^{\dagger}$ are adjoint operators of each other, they interchange roles when acting on the Hermitian conjugate (or bra) wave functions, so that:

$$\langle n-1|\ \hat{a}\ = s_n \langle\ n\ | \qquad (3.17a)$$

$$\langle\ n\ |\ \hat{a}^{\dagger}\ \ = s_n^{*}\ \langle\ n-1\ | \qquad (3.17b)$$

The condition of the number states being eigenstates of the number operator $\hat{N} = \hat{a}^{\dagger}\,\hat{a}$ requires that $|\,s_n|^{\,2} = n$. The symmetric Hamiltonian of (3.10) suggests the two-component state vector of eq. (3.14) as depicted in Fig. 3.1. This Hamiltonian carries out two simultaneous operations: one as a two-step number operator

$$\langle\ n\ |\ \hat{a}^{\dagger}\,\hat{a}\ |\ n\ \rangle = \langle\ n\ |\ \hat{a}^{\dagger}\ |\ n-1\ \rangle\ \ s_n = \langle\ n\ |\ n\ \rangle\ \ s_n\, s_n^{*} \qquad (3.18)$$

and the second operation as a one-step transition operator between two consecutive number states, each operator acting on the state vector next to it (or the left-hand operators acting on the Hermitian conjugate wave functions $\langle\ n\ |$, the result being:

$$\langle\ n\ |\ \hat{a}^{\dagger}\cdot\hat{a}\ |\ n\ \rangle\ =\ s_n^{*}\ \langle\ n-1\ |\ n-1\rangle\ \ s_n\ = |\,s_n|^{\,2} = n \qquad (3.19a)$$

$$\langle\ n-1|\ \hat{a}\cdot\hat{a}^{\dagger}\ |\ n-1\rangle\ =\ s_n^{*}\ \langle\ n\ |\ n\ \rangle\ \ s_n = |\,s_n|^{\,2}\ = n \qquad (3.19b)$$

In the Heisenberg picture or the interaction picture, and using the retarded phase $\varphi = \omega\, t - z\, n\,/c$, the propagating photon field operators take the form [10]:

$$\hat{a}\ (\omega, z, t) = \ \hat{a}\ (\omega)\ \ f(x, y, z)\ e^{-i(\,\omega\, t - \beta\, z)}\ \mathbf{e_p} \qquad (3.21a)$$

$$\hat{a}^{\,\dagger}(\omega, z, t) = \ \hat{a}^{\,\dagger}(\omega)\ f(x, y, z)\ e^{\,i(\,\omega\, t - \beta\, z)}\ \mathbf{e_p} \qquad (3.21b)$$

where the spatial distribution $f\,(x, y, z)$ is a solution of the Helmholtz wave equation [10], and $\mathbf{e_p}$ denotes the polarisation of the radiation mode. The observable quantity of the expectation value of the quadrature field operator $\hat{Q} = \hat{a} + \hat{a}^{\dagger}$ is found by combining eqs. (3.14 -21) to yield:

$$\langle\ \Psi_n\ (\ t\ )|\ \hat{a}\ |\Psi_n\ (\ t\ )\rangle = \\ =\ 0.5 e^{-i\,(\,\omega\, t\, -\, \beta\, z\, +\, \varphi\,(0))}\ n^{1/2}\ e^{-i\,\varphi_n} \qquad (3.22a)$$

$$\langle\ \Psi_n\ (\ t\ )\big|\ (\ \hat{a}\ +\ \hat{a}^{\dagger}\ )\big|\Psi_n\ (\ t\ )\rangle\ =\ n^{1/2}\ cos(\omega\, t - \beta\, z - \ \varphi_n) \qquad (3.22b)$$

reproducing the c - number $\langle\ \hat{Q}\ \rangle$ corresponding to the "classical" optical

field with a time-varying number of photons n (t) and related phase φ_n (t). An alternative derivation of the quadrature field is presented in the Appendix below.

The correct expectation values can also be found for the phase quadrature operators (Carruthers and Nieto [18]). These are defined in terms of the field operators and the conventional number operator $\widehat{N} = \hat{a}^{\dagger}\,\hat{a}$, having the form, for n > 0:

$$\hat{C} = \hat{a}\,\widehat{N}^{-1/2} + \widehat{N}^{-1/2}\,\hat{a}^{\dagger} \tag{3.23a}$$

$$\hat{S} = i\,(\hat{a}\,\widehat{N}^{-1/2} - \widehat{N}^{-1/2}\,\hat{a}^{\dagger}) \tag{3.23b}$$

which will provide information about the phase associated with the dynamic number states. With the photon number operator $\widehat{N}$ returning the number of photons in the basis of number states i.e., $\widehat{N} \mid \mathrm{n}\rangle = \mathrm{n} \mid \mathrm{n}\rangle$, any operator function $f(\widehat{N})$ can be expanded in a power series and replaced in terms of the number of photons, as follows (Garrison and Chiao [12]):

$$F\left(\widehat{N}\right) = \Sigma_p\, d_p\, \widehat{N}^p\,; \qquad F\left(\widehat{N}\right) \mid \mathrm{n}\rangle = \mathrm{F(n)} \mid \mathrm{n}\rangle; \qquad \text{and}$$

$$\widehat{N}^{-1/2} \mid \mathrm{n}\rangle = \mathrm{n}^{-1/2} \mid \mathrm{n}\rangle$$

where d_p are expansion coefficients. For the particular case of the zero-photon state $|0\rangle$, the product operator needs to be inverted [18] by substituting $\hat{a}\,\hat{a}^{\dagger} = \hat{a}^{\dagger}\,\hat{a} + 1$ into the power series expansion of $\hat{a}\,f(\widehat{N})$ to obtain $f(\widehat{N}+1)\,\hat{a}$. The corresponding expressions of the expectation values are:

$$\langle \Psi_{\mathrm{n}} \mid \hat{C}_j \mid \Psi_{\mathrm{n}} \rangle = cos\,(\omega\, t + \varphi_j) \tag{3.24a}$$

$$\langle \Psi_{\mathrm{n}} \mid \hat{S}_j \mid \Psi_{\mathrm{n}} \rangle = sin\,(\omega\, t + \varphi_j) \tag{3.24b}$$

These relations of the field and phase quadratures apply to any number of photons spanning the entire range from the quantum regime of a few photons to the large number of photons characteristic of classical optical waves. Consequently, the quantum state of eqs. (3.14) of dynamic and coherent number states make a smooth transition between the quantum and classical regimes. These variables will be measured by the method of balanced homodyne detection [9].

The dynamic and coherent number states identified in eqs. (3.14) possess an optical field which can be compared with the classical field. Consequences of these properties are discussed in the following Section.

3.3.2 The equations of motion of the optically linear parametric interactions

As an optical beam propagates through a dielectric medium, the magnitude and phase of the expectation value s_n may be modified by the simultaneous presence of another beam of photons of the same frequency. This effect is described by the Ehrenfest theorem [14]; [16]:

$$i\,\hbar\,\frac{\partial}{\partial t}\,\langle\,\Psi_n\,(t)|\,\hat{a}\,|\,\Psi_n\,(t)\rangle = \langle\,\Psi_n\,(t)|\,\big[\,\hat{a}\,,\widehat{H}_{int}\,\big]|\,\Psi_n\,(t)\rangle \qquad (3.25)$$

indicating that the expectation value of the optical field is modified by its commutator with the Hamiltonian of interaction $\widehat{H}_{int}$.

Having identified a quantum wave function capable of delivering the instantaneous magnitude and phase of an optical field, we can now apply the formalism of [4-5] to the propagation along an optical waveguide directional coupler by employing the following composite photonic quantum state function $|\Phi\rangle$ for two optical waves identified by their waveguide $|\Psi_{n,j}\rangle$ (j = 1 or 2), their Hamiltonian of interaction $\widehat{H}_{int}$, and the equation of motion derived from (3.25):

$$|\,\Phi\,\rangle\;=\;|\,\Psi_{n,1}\,\rangle\;\;|\,\Psi_{n,2}\,\rangle \qquad (3.26a)$$

$$\widehat{H}_{int}\;=\hbar\,\omega\,\chi_q^{(1)}\,(\hat{a}_2^{\dagger}\,\hat{a}_1+\;\hat{a}_2\,\hat{a}_1^{\dagger}\,) \qquad (3.26b)$$

$$\chi_q^{(1)}=\frac{\hbar}{\varepsilon}\,\chi^{(1)} \qquad (3.26c)$$

where the real part of the first-order susceptibility of the dielectric medium $\chi_q^{(1)}$ includes the coefficient square linking the photon annihilation or creation operators and the electric field operator in eqs. (3.9). The Hamiltonian $\widehat{H}_{int}$ is derived from the interaction term $\boldsymbol{P}_2\cdot\boldsymbol{E}_1^*$ of the Poynting vector in eq. (2.4).

The resultant equation of motion describing the mutual interaction is derived by substituting into eq. (3.25) the relations of (3.26), yielding:

$$\frac{\partial}{\partial t}\langle \Phi \mid \hat{a}_1 \mid \Phi\rangle = -i\,\omega\,\chi_q^{(1)}\,\langle \Phi \mid \hat{a}_2 \mid \Phi\rangle \tag{3.27}$$

This interaction will modify the complex field amplitude $s_{\mathrm{n,j}}$ $(j = 1, 2)$ of two co-propagating and overlapping optical beams of the same frequency, identifiable by their respective optical waveguides $(j = 1, 2)$. From. (3.22*a*) we have for the expectation values of the optical fields

$$\langle \Phi \mid \hat{a}_j \mid \Phi \rangle = 0.5\, e^{-i\,(\omega\, t + \varphi(0)_j)}\; s_{\mathrm{n,j}} \tag{3.28}$$

After converting to number of photons, i.e., $|\, s_{\mathrm{n,j}}|^2 = N_j$ and corresponding phases φ_j, the equation of motion (3.27) provides the rates of change of N_j and φ_j as follows:

$$\frac{\partial}{\partial\, z}\, N_1 = g_1\, N_1 \tag{3.29a}$$

$$g_1 = -\,\kappa \left(\frac{N_2}{N_1}\right)^{1/2} \sin\theta_{21} \tag{3.29b}$$

$$\frac{\partial}{\partial\, z}\,\theta_{21} = (\beta_2 - \beta_1) + \kappa\left[\left(\frac{N_1}{N_2}\right)^{1/2} - \left(\frac{N_2}{N_1}\right)^{1/2}\right]\cos\theta_{21} \tag{3.29c}$$

$$\frac{\partial}{\partial\, z}\,\varphi_1 = \kappa \left(\frac{N_2}{N_1}\right)^{1/2} \cos\theta_{21} \tag{3.29d}$$

$$\kappa = \frac{1}{\mathrm{v}_p}\,\frac{k_0}{2\,n}\int\int dx\, dy\, \chi_q^{(1)}\, f_1\; f_2\, \boldsymbol{e_1}\cdot\, \boldsymbol{e_2} \tag{3.29e}$$

$$\theta_{21} = (\,\beta_2 - \,\beta_1)\cdot z + \varphi_2 - \varphi_1 \tag{3.29f}$$

where the gain coefficient g includes an overall coupling coefficient κ and depends on the polarization states $\boldsymbol{e}_1$ and $\boldsymbol{e}_2$ of the photons. The phase difference between the two waves is θ_{21}, β being the propagation constant and $z/t = \mathrm{v}_\mathrm{p}$ is the phase velocity. In (3.29*e*), k_o and n specify the free-space wavevector and the effective refractive index, respectively. It should be noted that equations (3.29) are identical to the classical ones of Chapter

2 describing the physically meaningful process of quantum Rayleigh conversion of photons [6]. The quantum $\chi_q^{(1)}$ is related to the classical susceptibility by the coefficient of eq. (3.9) between the electric field operator and the creation operator. The coupling coefficient of Eq. (3.29*e*) indicates that the entire local value of the optically linear susceptibility $\chi^{(1)}$ is involved in the coupling process in the dielectric medium at any point where the two spatial distributions f_1 and f_2 overlap, each having units of m^{-1}, and the squares f^2 are normalized to a dimensionless unit over the cross-section area. This is in contrast to the physically impossible coupling between two optical waveguides apparently induced by a perturbation of the dielectric constant in the cladding.

Any two dynamic and coherent number states of (3.26*a*) co-propagating through a dielectric medium will couple photons from one state to the other depending on the relative phase between the two waves. This process, repeatedly, will eliminate optical waves whose phases diverge substantially from the phase of the surviving wave which will dominate the output of a lasing cavity.

Two groups of photons propagating simultaneously across the same dielectric medium would exchange photons, parametrically, with each other through the real part of the susceptibility – see (3.29) above – which is indicative of a beam splitter composed of a fibre-optic directional coupler.

3.4 The Spatial Field Profile of Photons

The instantaneous longitudinal and lateral field distributions of photons passing through an infinitesimal volume located at position $\boldsymbol{r}$ will be evaluated by combining the expectation value of the field operator and its definition in terms of the vector potential of the electromagnetic field.

3.4.1 The longitudinal distribution of photonic fields

We evaluate the intrinsic longitudinal field profile of a group of photons, or its coherence length, by using the wave function $|\Psi_n\rangle$ from (3.14*b*). Two equations can be identified for the expectation values of $\hat{a}$, or the corresponding *c* - numbers, by combining (3.9*a*) and (3.22), leading to:

$$\langle \Psi_n | \hat{a} | \Psi_n \rangle = b \langle \hat{E} \rangle + i s \langle \hat{B} \rangle \tag{3.30a}$$

$$\langle \Psi_n | \hat{a} | \Psi_n \rangle = q\ e^{-i(\omega t - \beta z)} \tag{3.30b}$$

where $q = 0.5\ \mathrm{n}^{1/2}$, $b = (\varepsilon / \hbar)^{1/2}$ and, $s = (\varepsilon\ c / \hbar)^{1/2}$. We point out that both quadratures of the field are represented in the phasor notation of (3.30). Eq. (3.30*a*) is obtained from (3.9*a*) and can be expressed in terms of the c – numbers $E = \langle \hat{E} \rangle$ and $B = \langle \hat{B} \rangle$. Recalling the relations [17] between the vector potential $\boldsymbol{A}(z, t)$ and the fields as:

$$\boldsymbol{E} = -\frac{\partial \boldsymbol{A}}{\partial t} \qquad and \qquad \boldsymbol{B} = \nabla \times \boldsymbol{A} \tag{3.31}$$

in the Cartesian frame of coordinates (x, y, z), the vectors have the notation, in the plane wave approximation: $\boldsymbol{A} = (A, 0, 0)$; $\boldsymbol{E} = (E, 0, 0)$; $\boldsymbol{B} = (0, B, 0)$ and the wave vector is $\boldsymbol{k} = (i\,k_x, i\,k_y, \beta)$ for a beam propagating in the z – direction in an optical waveguide. The complex amplitude of the vector potential is represented by

$$A(z,t) = A_p(z)\, f(x,y)\, e^{-i(\omega t - \beta z)} \tag{3.32}$$

where the lateral profile of the guided mode is given by $f(x, y)$ and the propagation constant by $\beta = 2\pi n_{eff} / \lambda$. The second term of the curl operation $\nabla \times f(x, y)\ \mathbf{x} = (\partial f / \partial z)\ \mathbf{y} - (\partial f / \partial y)\ \mathbf{z}$ does not lead to wave propagation and does not affect measurements in a plane perpendicular to the z - coordinate. The lateral field distribution is derived in the following sub-section.

Relating A_p to a moving source of photons would suggest a relative distance $\zeta = z - z_o$ with z_o being the instantaneous location of the photons, with the localization given by a Dirac delta function $\delta(z - z_o)$, resulting in this differential equation after substituting (3.31) and (3.32) into (3.30) to derive:

$$\frac{\partial}{\partial z} A_p + \sigma A_p = \gamma\, \delta(z - z_o) \tag{3.33}$$

where

$\sigma = b\,\omega / s + i\,\beta = (\omega / c)(1 + i\,n_{eff})$, and

$\gamma = -i\,q / s = i\,0.5\,(\mathrm{n}\,\hbar / \varepsilon)^{1/2}$.

Setting $A_p(z) = g(z)\ exp(-\sigma z)$ and inserting into the differential equation (3.33) leads to: $\int dg = \gamma \int exp(\sigma z)\ \delta(z - z_o)\, dz$. With $g = \gamma\ exp(\sigma z_o)$, and for reasons of physical symmetry, the longitudinal distribution of the

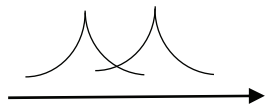

Fig. 3.2 Partially overlapping photon fields.

magnitude of the vector potential associated with photons of a wavefront is found to be:

$$A_p(z) = \gamma \, exp\ (-\sigma \mid z - z_o \mid) \tag{3.34}$$

The vector potential's decay constant is inversely proportional to the wavelength λ through $Re\ \sigma = 2\ \pi\ /\ \lambda$. Thus, the local optical field includes contributions from photons in the vicinity of z_o, as illustrated in Fig. 3. 2.

The normalised longitudinal optical field profile f_{ph} of one photon of wavelength λ, crossing point z_o, is obtained from (3.34) as:

$$f_{ph}(z = c\ t) = exp\ (-\frac{2\ \pi \mid z - z_o \mid}{\lambda}) \tag{3.35}$$

which has the form of a Wigner spectral component $S(\omega, t)$, that is, a time-varying spectral component [19] – as opposed to a time-constant amplitude and phase of a Fourier spectrum – crossing a surface perpendicular to the wavevector of propagation. The exponential decay of the spatio-temporal profile is identical to that obtained by Fourier transforming a fully populated transmission line of an interference filter [9].

3.4.2 The lateral distribution of photonic fields

The transversality condition [10] for a radiation field $\langle\ E\ \rangle \propto \langle \hat{a} + \hat{a}^{\dagger} \rangle$ and the dielectric constant ε, is given by the divergence of the displacement vector:

$$\nabla \cdot (\ \varepsilon\ \boldsymbol{E}\ ) = 0 \tag{3.36}$$

In cylindrical coordinates, the differential equation and its solution in the plane perpendicular to the wavevector are:

$$\frac{\partial}{\partial r}\,(r\,\varepsilon\,\boldsymbol{E}) = 0 \tag{3.37a}$$

$$\boldsymbol{E}\,(r) \;=\; \boldsymbol{E}_o\;\frac{r_o}{\varepsilon\,r} \tag{3.37b}$$

$$f_{ph;lat} = \frac{r_o}{\varepsilon\,r} \tag{3.37c}$$

where r_o is the reference position coordinate at the peak of $\boldsymbol{E}$, and r is the distance from the this position. This lateral distribution of the photonic field $f_{ph;lat}$ may explain the two-slit Young interference, as the broad lateral field splits at the slits and recombines behind them.

3.5 Coherence of Dynamic Number States

The Heisenberg uncertainty principle [16] has to do with the joint statistical distribution of the measured values of two variables corresponding to repeated measurements of identically prepared systems [8-9], and applies to the *simultaneous* measurements of two dynamic variables whose quantum operators do not commute in a given set of state wave functions, the variables being incompatible observables.

The principle of uncertainty does not preclude the existence of well-defined numerical values for either variable [16]. Limited information about one variable is associated with a variance in the measured values, with more information being available about the other variable. Measurements yield precise *instantaneous* values – within the constraints of the equipment – by "collapsing" the system's wave function into a specific value [16]. A quantum "spread" implies that measurements on identically prepared systems do not return identical results because of system-related fluctuations such as spontaneous emission, time-varying losses, temperature variations, background radiation, etc.

One should not confuse prediction with measurements. It is the measured values that come into play when plotting the joint distribution of two observable physical variables. A measurement of only one variable will still have its own variance of values but it is not subject to the Heisenberg uncertainty principle, because the physical system is not disturbed by the measurement of another variable. One can easily measure a well-defined eigenvalue of an operator [16] at a given time.

In free space, the degree of coherence of an optical monochromatic wave would be characterized by the statistical phase variance of the ergodic evolution of the wavefront phases. Their measured statistical distribution –

if detected in conjunction with another observable physical quantity or variable – will be subject to the Heisenberg uncertainty principle characterizing statistical measurements of ensembles. However, each *instantaneous* wave front has, possibly, a time-varying, and – as a result of interacting with the dielectric medium which collapses the wave function – a well-defined phase which will be involved in the optically linear parametric interactions in a dielectric medium [3 -6].

Two dynamic number states – derived in the previous Section 3.3 – co-propagating through a dielectric medium will couple photons from one state to the other depending on the relative phase between the two waves. This process, repeatedly, will eliminate optical waves whose phases diverge substantially from the phase of the surviving wave which will dominate the output of a lasing cavity.

3.6 Sub-Poissonian Distribution of Photons

The statistical properties of a stochastic and ergodic optical beam will unfold in time upon detection at a point in space. Intensity measurements absorb photons leaving nothing for phase-measurements. Splitting a beam in two and measuring quadrature phase values of $\cos\varphi$ and $\sin\varphi$ will leave nothing for intensity measurements. A stable reference beam is needed for all types of measurements. Its fluctuations, in fact, may be mistaken for proof of the uncertainty principle.

The interaction between a steady-state pump beam and a signal beam inside a dielectric medium can bring about a change in the initial Poisson distribution of signal photons leading, possibly, to a narrower sub-Poisson variance [1]. Such a distribution is commonly described and characterized in terms of mixtures of coherent states spanning the continuous phase-space by converting the field operators into complex eigenvalues of the *mathematically* generated coherent states of the various quasi-probabilities [1], [12],14].

The nature of the measurement would determine the type of quantum state used to model the experimental measurement. For light-matter interaction which require an optical field, the dynamic and coherent number states developed above would be required. In contrast, for statistical description of an overall distribution of measurements, the conventional number (or Fock) states will be more practical.

Two radiation modes carrying n and m photons, represented by the dynamic and coherent number states of Section 3.3, and propagating simultaneously across the same dielectric medium would exchange photons, parametrically, with each other through the real part of the susceptibility –

see eqs. (3.29) above – with the possibility of creating the n + m number state.

A criterion for generating sub-Poissonian distributions of photons through differential amplification of photons was outlined in [4] involving the phase-dependent gain coefficient, and this sub-Section presents a straightforward description of such photon distributions.

With the evolution of an optical wavefront being described by Eqs. (3.29), the number state is identified by the number of photons emerging from a parametric interaction, i.e., $n = N_1$, so that the overall statistical distribution of the beam is given by the elements ρ_{nn} of the density matrix of the mixed state.

For the "input" and "output" corresponding to one photon interaction, the probability coefficients of eq. (3.7) take on the values:

One lost photon: input $c_n = 1$; $c_{n-1} = 0$;
output $c_n = 0$; $c_{n-1} = 1$;

One gained photon: input $c_n = 0$; $c_{n-1} = 1$;
output $c_n = 1$; $c_{n-1} = 0$;

so that, the orthogonality of the number states can be used to specify clearly the pure state and mixed states of light, which is not the case with the coherent states of light which lack orthogonality.

At the detection stage, it is convenient to use the photon number states [8] as they provide a state density matrix ρ_{mn}. The photon number variance in the basis of number states is calculated from:

$$\langle (\triangle n)^2 \rangle = \langle \hat{N}^2 \rangle - \langle \hat{N} \rangle^2 = Tr\left(\hat{\rho}\,\hat{N}^2\right) - \left[Tr\left(\hat{\rho}\,\hat{N}\right)\right]^2 =$$

$$= \Sigma_n \rho_{nn}\, n^2 - (\Sigma_n \rho_{nn}\, n)^2 \qquad (3.38)$$

For a pure number state of the wavefront $\rho_{nn} = \delta_{nm}$, leading to the well-known result of $\rho_{mm} = 1$ and $\langle (\Delta n)^2 \rangle = 0$. For the mixed state of the beam $\rho_{nn} < 1$ and the variance broadens as more states are occupied. For a sub-Poissonian distribution, the reference Poissonian state will have the same mean number of photons, and the variance difference is given by

$$\langle (\triangle n)^2 \rangle - \langle n \rangle = \Sigma_n (\rho_{nn} - \rho_{nn}^{(P)})\, n^2 \qquad (3.39)$$

where $\rho^{(P)}_{nn}$ is the Poissonian distribution for which $\langle (\Delta n)^2 \rangle^{(P)} = \langle n \rangle$.

In this way, the spread is determined by the difference between the density matrix elements, and no quasi-probabilities are needed as in ref. [1].

The relative relation of Eq. (3.39) stems from the fact that the number states are eigen-functions of the photon number operator, which is not the case for the coherent states of light as they are destroyed by the creation operator. This shortcoming of the coherent states of light was handled by re-arranging the order of the field operators [1], [12], 14] leading to three types of quasi-probabilities on the complex phase-space of the eigenvalues α.

Additionally, deficiencies of the formalism based on the Bogoliubov solution [12] for the parametric amplification are detailed in [4-5]. This physically impossible solution for the optical field operators was used in the Wigner quasi-probability (WQP) [12], [14] to distort the circular distribution of a coherent state into an elliptic distribution – on the phase-space of eigenvalues α of the coherent states – for noise squeezing. But, the WQP itself distorts the point-like distribution of a pure coherent state in the context of the *P* quasi-probability. By contrast, a physically meaningful process of photonic coupling between two quadratures of an optical field was identified in [6, Eq. (5)], brought about by the quantum Rayleigh stimulated emission amplifying one quadrature while attenuating the other one.

3.7 Conclusions

Field quantization without quantum harmonic oscillators leads to the intrinsic field of photons. As a consequence, a quantum product state of photons requires both space and time overlaps.

A time-varying number of monochromatic photons are described by the classical mixed time-frequency representation of signals.

Based on the physical process of photon detection triggered by the optical field, quantum two-component number states are identified. These states deliver through their equation of motion a non-vanishing expectation values for the field operators and the phase quadratures. Additionally, the longitudinal and lateral profiles of a group of photons have been derived.

The possibility of evaluating directly, without the need for quasi-probabilities, the evolution of an optical wavefront regardless of the photon statistics of the overall beam, will facilitate the design and operation of functional integrated photonic circuits and devices.

Appendix -Alternative derivation of the dynamic and coherent number states

The expansion coefficients $c_j(t)$ in eq. (3.14*a*) with $j = \mathrm{n}$ and $\mathrm{n}-1$, will change as a result of a transition between the states $|\,\mathrm{n}-1\,\rangle$ and $|\,\mathrm{n}\,\rangle$ as determined by the Schrödinger equation of motion driven by a free background Hamiltonian $\widehat{H}_f$ of eq. (3.10) , so that:

$$i\,\hbar\,\frac{\partial}{\partial\, t}\,|\,\Psi_{\mathrm{n}}\,(\boldsymbol{r},t)\rangle = \widehat{H}_f\,(\boldsymbol{r},t\,)\,|\,\Psi_{\mathrm{n}}\,(\boldsymbol{r},t)\rangle \qquad (A\,3.1)$$

Since an operator remains unchanged in the Schrödinger picture, the rate of change for the expectation value in the Schrödinger picture contains only a commutative term between the operator and the Hamiltonian:

$$i\,\hbar\frac{\partial}{\partial t}\,\langle\,\Psi_{\mathrm{n}}\,(t)|\,\hat{a}\,|\,\Psi_{\mathrm{n}}\,(t)\rangle = \\ = \langle\,\Psi_{\mathrm{n}}\,(t)|\,\big[\,\hat{a},\widehat{H}_f\,\big]|\,\Psi_n\,(t)\rangle \qquad (A\,3.2)$$

The commutative relations involving the field Hamiltonian in free space are:

$$[\,\hat{a},\ \widehat{H}_f\,] = \hbar\,\omega\,\hat{a}\ \ ;\ \ \text{and}\ \ \ [\,\hat{a}^{\dagger},\widehat{H}_f\,] = -\,\hbar\,\omega\,\hat{a}^{\dagger} \qquad (A\,3.3)$$

The expectation value of the *quadrature operator* $(\hat{a} + \hat{a}^{\dagger})$ for the wave function of eq. (3.14*a*), is given, at time t , by

$$\langle\,\Psi_{\mathrm{n}}\,(\,t\,)\,|(\,\hat{a}\ +\ \hat{a}^{\dagger})|\,\Psi_{\mathrm{n}}\,(\,t\,)\,\rangle = \\ = c_{\mathrm{n}}(t)\,c^{*}_{\mathrm{n}-1}(t)\,s_{\mathrm{n}}(t) + c^{*}_{\mathrm{n}}(t)\,c_{\mathrm{n}-1}(t)\,s^{*}_{\mathrm{n}}(t) \qquad (A\,3.4)$$

We note that the last equality contains two complex conjugate terms and define:

$$\eta\,(\,t\,) = \ c_{\mathrm{n}}(t)\,c^{*}_{\mathrm{n}-1}(t) \qquad (A\,3.5)$$

to obtain from eq. (*A* 3.4)

$$\langle\,\Psi_{\mathrm{n}}\,(\,t\,)\big|\ \hat{a}\ \big|\,\Psi_{\mathrm{n}}\ (\,t\,)\,\rangle = \ \eta\,(\,t\,)\ s_{\mathrm{n}} \qquad (A\,3.6)$$

The solution for $\eta(t)$ is found from the equation of motion derived by combining eqs. (*A* 3.2 - 3.3) and (*A* 3.5 -3.6), leading to:

$$\frac{\partial}{\partial t}\,\eta\,(t) = -i\,\omega\;\eta\,(t) \qquad (A\,3.7a)$$

$$\eta\,(t) = \eta_{\mathrm{o}}\,e^{-i\,(\,\omega\,t\,+\,\varphi\,(0))} \qquad (A\,3.7b)$$

From the condition $|\,\mathrm{c_n}\,(t)\,|^2 + |\mathrm{c_{n-1}}\,(t)\,|^2 = 1$, one estimates the peak value of $\eta_{\mathrm{o}} = 0.5$, and eq. (*A* 3.6) becomes:

$$\langle\,\Psi_{\mathrm{n}}\,(\,t\,)|\,\hat{a}\,|\Psi_{\mathrm{n}}\,(\,t\,)\rangle = 0.5\,e^{-i\,(\omega\,t\,-\,\beta\,z+\,\varphi\,(0))}\,\mathrm{n}^{\,1/2}\,e^{-i\,\varphi_n} \qquad (A\,3.8)$$

delivering, along with its complex conjugate from eq. (*A* 3.4) above, an instantaneous expectation value for an optical field of any level of photon number, and associated phase, regardless of the overall beam distribution, and corresponding to a classical field representation.

The conventional expectation number of photons for the dynamic state $|\,\Psi_{\mathrm{n}}\,(t)\,\rangle$ of eq. (*A* 3.6) is found to be:

$$\langle\,\Psi_{\mathrm{n}}\,(t)|\;\hat{a}^{\dagger}\,\hat{a}\;|\,\Psi_{\mathrm{n}}\,(t)\,\rangle \;=\; \mathrm{n}\;-|\,c_{\mathrm{n}}(t)|^{\,2} \qquad (A\,3.9)$$

The factor $|\,c_2(t)^{\,2} = 0.5$ balances out the "half-photon" noise.

References

1. L. Davidovich, "Sub-Poissonian processes in quantum optics," Rev. Mod. Phys., **68**, 127-173, (1996).
2. K. Kikuchi, "Fundamentals of Coherent Optical Fiber Communications," J. Lightwave Technol., **34**, 157-178, (2016.
3. A. Vatarescu, Instantaneous Quantum Description of Photonic Wavefronts for Phase-Sensitive Amplification, *Frontiers in Optics/Laser Science Conference (FiO/LS),* paper JW4A.109, Washington, Sept. 2018.
4. A. Vatarescu, "Photonic Quantum Noise Reduction with Low-Pump Parametric Amplifiers for Photonic Integrated Circuits", Photonics, **3**, article 61, (2016).
5. A. Vatarescu A, "Phase-Sensitive Amplification with Low Pump Power for Integrated Photonics", OSA Advanced Photonics Congress, paper ID: IM3A.6., 2016
6. A. Vatarescu, "Photonic coupling between quadrature states of light in a homogeneous and optically linear dielectric medium", J. Opt. Soc. Am. B, **31**, 1741–1745, (2014).

7. A. Vatarescu ,“Photonic quadrature-wave pulses generated by a single electro-optic waveguide modulator for digital transmission”, J. Opt. Soc. Am. B, **32**, 555-561, (2015).
8. G. Breitenbach, S. Schiller, and J. Mlynek, “Measurement of the quantum states of squeezed light", Nature **387**, 471-475, (1997).
9. A. I. Lvovsky and M. G. Raymer, “Continuous-variable optical quantum-state tomography," Rev. Mod. Phys., **81**, 299-332, (2009).
10. R. J. Glauber and M. Lewenstein, “Quantum optics of dielectric media”, Phys. Rev. A, **43**, 467- 491, (1991).
11. D. T. Pegg and S. M. Barnett, “Phase properties of the quantized single-mode electromagnetic field”, Phys. Rev. A, **39**, 1665 – 1675, (1989).
12. J. C. Garrison and R.Y. Chiao, *Quantum Optics*, Oxford University Press, 2008.
13. U. Fano, “Description of States in Quantum Mechanics by Density Matrix and Operator Techniques”, Rev. Mod. Phys., **29**, 74-93, (1957).
14. D. A. Steck, *Quantum and Atom Optics*, University of Oregon, available online at http://steck.us/teaching (revision 0.11.0, 18 August 2016).
15. R. B. Griffiths, “Nonlocality claims are inconsistent with Hilbert-space quantum mechanics”, Phys. Rev. A **101**, 022117, (2020).
16. D. J. Griffiths, *Introduction to Quantum Mechanics*, Publisher: Pearson Prentice Hall, 2005.
17. K. J. Blow, R. Loudon, S. J. D. Phoenix and T. J. Shepherd, “Continuum fields in quantum optics”, Phys. Rev. A, **42**, 4102- 4114, (1990).
18. P. Carruthers and M. M. Nieto, “Phase and Angle Variables in Quantum Mechanics”, Rev. Mod. Phys., **40**, 411-440, (1968).
19. L. Cohen, “Time-frequency distributions-a review”, Proc. IEEE, **77**, 941–981, (1989).

CHAPTER FOUR

PHOTONIC QUANTUM NOISE REDUCTION

Optical interferometric measurements will benefit from using optical sources possessing reduced temporal fluctuations in their intensities and phase variations. These fluctuations are commonly associated with the Heisenberg uncertainty principle and referred to as quantum noise, involving canonically conjugate operators of observable, physical variables or quantities. The possibility of reducing the quantum noise variance of one observed variable below the Poissonian level while increasing it for its conjugate pair variable, constitutes the main approach to noise squeezing (Schnabel [1]; Andersen *et al*. [2]).

However, both optically linear and nonlinear parametric interactions provide physical mechanisms for operating or acting to separately limit the fluctuations in the number of photons and their phases. In Chapter 2, optical power was found to couple between the quadrature components of an optical wave through the quantum Rayleigh conversation of photons, as a wave propagates in a dielectric medium.

Small scale integration of photonic devices holds the prospect of overcoming speed limits associated with back and forth conversions between the electrical and optical domains for signal processing and transmission. Integrated photonic platforms (Thylén and Wosinski [3]; Zhang *et al.* [4]; Hendrickson *et al.* [5]) will contain their own low power optical sources which will be used for on-chip signal processing. However, the low levels of power rule out any significant nonlinear effects for $\chi^{(2)}$ and $\chi^{(3)}$, the second and third order susceptibilities. For instance, a recently reported phase-sensitive amplifier (Li *et al*. [6]) operating on $\chi^{(3)}$ in semiconductor materials can only deliver output signal powers of less than -31 dBm for input pump powers of -1 dBm .

In Chapter 2 above, the process of optically linear inter-quadrature coupling of power was pointed out and in Chapter 3 the quantization of the optical field, without invoking harmonic oscillators, led to the disappearance of the physically impossible half-photon noise. This Chapter presents a phase-sensitive gain coefficient which evolves throughout the propagation across a second-order optically nonlinear crystal, and in doing

so can bring about different levels of power between quadrature states. It is the intrinsic phase-shifting effect of a parametric coupling of photons that underpins the noise squeezing rather than a superposition of optical field operators.

4.1 Parametric Processes for Quantum Noise Reduction

Two specific parametric processes (Vatarescu [7-10]) have the potential to operate as integral parts of a photonic integrated circuit (PIC) with a high degree of photonic conversion (> 90%), as they require low pump powers (< 10 mW) and very short interaction lengths.

Parametric amplification and phase shifts can be performed with first-order susceptibility quantum Rayleigh emissions [7] in the form of optically linear parametric (OLP) effects and the corresponding electro-optic susceptibility-based conversion of photons in the form of electro-optic parametric (EOP) processes [10], both of which require low optical pump powers and short interactions lengths of a few microns for OLP interactions and a few centimetres for EOP devices. These interactions can be highly efficient and require only a pair of a pump and a signal optical waves, and functional devices can be fabricated with well-established technologies (Yamazaki *et al.* [11]).

As parametric processes of photonic conversions constitute a major mechanism for generating nonclassical states of light [1-2], any new insights into such interactions should be of particular interest in the design and operation of functional devices. Quantum optic noise reduction and phase-sensitive amplification will benefit an optical transmission system throughout the entire link and, in particular, at the receiver and detection stages of operation (Kikuchi [12]). Quantum noise stems from fluctuations in the distribution of numbers of photons and/or the distribution of associated phases of the optical fields [12], and include: the background (or vacuum) fluctuations of any electromagnetic field of radiation, the spontaneous emission of photons by an excited electric dipole polarization, the Poisson distribution as a function of time, of the number of photons in a coherent beam of light, fluctuations in the state of polarization, etc.

Experimentally, given the very low efficiency of parametric conversion of photons carried out by $\chi^{(2)}$ and $\chi^{(3)}$ - based materials, the undepleted pump approximation becomes a critical aspect of the interaction, along with the phase-matching condition. Theoretically, photonic noise reduction through variance squeezing – below the standard quantum limit (SQL) of an optical coherent state (Davidovich [13]) – is implemented by simultaneous amplification of a field quadrature of phase ϕ (defined by adding two output

fields or phasor modes) and attenuation of the corresponding conjugate quadrature $\phi + \pi/2$. This leads to the definition of a *virtual* photon annihilation operator (Yuen [14]; Henry and Glotzer [15]) which is the superposition of various levels of a photon annihilation operator a and a photon creation operator a^*. This type of quadrature noise squeezing requires a two-photon output per interaction [14] and it is linked to the Bogoliubov transformation for boson particles. For example, the output annihilation operator of the signal mode a_s is given as a superposition of the input operators weighted by c – number functions, i. e.,

$$a_s(z) = c_1(z)\, a_s(0) + i\, e^{i\varphi_p}\, c_2(z)\, a^*_i(0) \tag{4.1}$$

where the subscripts denote signal (s) and idler (i) waves, and φ_p identifies the pump phase(s) of the interaction term. This expression is based on the approximation of the undepleted pump which is treated classically by ignoring its operators, resulting in a gain coefficient g_o which is not allowed to vary at all, leading to many significant properties being discarded as a result of the linearization of the rate equations.

While the cross-coupling between a^*_i and a_s arises from the parametric conversion of photons, the self-coupling term has no physical origin being a mathematical artefact as a result of the conventional solution containing, *simultaneously*, an amplifying ($+ g_o = \chi^{(2)} \sqrt{P_p}$ and an attenuating ($- g_o$) exponential factors defined by the product of a susceptibility and the pump power P_p. Commonly used functions are: $c_1(z) = \cosh(g_o z)$ and $c_2(z) = \sinh(g_o z)$ for a phase-matching condition (Louisell *et al.* [16]). But no explanation has ever been provided as to how the same parametric process can, physically, amplify and attenuate *simultaneously* the signal wave. Indeed, a formal integration of Eq. (22) of [16] yields:

$$a_s(z) - a_s(0) = i\, e^{i\varphi_p}\, g_o \int a^*_i(z)\, dz \tag{4.2}$$

indicating that $c_1 = 1$ for any conditions and remaining unchanged throughout the propagation. Whether the input signal operator is amplified or attenuated at a particular point z in the dielectric medium will depend on the local value of the relative phase between the pump(s) and, the signal and idler waves. This is not the case with the Bogoliubov-type solution which has a phase-independent gain coefficient g_o.

Furthermore, if the classical pump amplitude, in the driving term of the formal integral in eq. (4.2) is replaced by its quantum optic representation, i.e., $c_p\, a_p$, then the driving force $a_p\, a^*_i$ on the right-hand side of that eq. (4.2) would oscillate at an angular frequency $-(\omega_p - \omega_i) = -\omega_s$ indicating

that only a_s is changed without any appearance of a positive frequency creation operator a_s* as suggested by the Bogoliubov transformation. Additional physical deficiencies of the Bogoliubov solution are outlined in the Appendix A below.

Consequently, an approximation-free and fully quantum optic formalism for parametric processes is needed, and it is developed in this Chapter based on the concepts outlined in (Vatarescu[8-9]). The parametric amplification consists of stimulated emission of photons which adopt the same characteristics as the stimulating beam. The direction of photon coupling, e.g., for the three photon–mixing interactions between the pump's frequency and the down-converted frequencies of the signal and idler waves, depends on the phase difference between the three waves. This process is also accompanied by spontaneously emitted photons which have arbitrary phases and states of polarization – (see Inoue and Mukai [17]) for the equivalent case of four-wave mixing). The spontaneous emission provides the seed photons to be amplified in the absence, at the input, of another stimulating optical wave.

The critical role of the parametrically engendered phases has been demonstrated experimentally [17]. A physically meaningful phase sensitive (PS) gain coefficient was identified in (Vatarescu [18]) along with its spectral bandwidth.

This Chapter involves no approximations and presents in Section 4.2, a fully quantum optic derivation of the parametric equations of motion describing the evolution of the complex *c* - number functions of the photon annihilation and creation operators, based on the concepts outlined in Chapter 3. Section 4.3 presents a generalized phase-dependent (PD) gain coefficient for parametric interactions, and a physically meaningful explanation for the generation from spontaneous emission of an idler wave phase-conjugated to the signal, and quadrature waves for maximal amplification and attenuation. Applications are outlined in Section 4.4, followed by a discussion, in Section 4.5, of new features emerging from a fully quantum optic approach to parametric amplification.

4.2 Quantum Optic Second-Order Parametric Equations of Motion

Quantum optically, in the Heisenberg picture, the evolution of a physical process is described by relevant varying operators while the initial state wave functions are kept unchanged. A varying operator itself is the product of a basic operator and a *c* - number complex function whose values are determined by the Heisenberg equations of motion. (Glauber and

Lewenstein [19]; Anderson *et al*. [20]). The initial conditions are determined by the expectation values of the basic operator. The *c*-number functions for coherent states of light are the eigenvalues α (alpha) numbers, and combinations of them can be measured experimentally (Townsend and Loudon [21]).

The phase dependence of the parametric gain coefficient and the related phase pulling effect – presented in (Vatarescu [8-9]) for the classical fields – can also be derived quantum optically by means of the Ehrenfest theorem presented in Chapter 3, including the annihilation and creation operators of all the optical fields (signal, idler and pump)- involved in the interactions.

For a second-order nonlinearity, or a $\chi^{(2)}$–based interaction, the frequencies are related by the equality: $\omega_1 + \omega_2 = \omega_3$, the pump being identified with ω_3 . Quantum mechanically, e.g., [19-20], the Hamiltonian of interaction $\widehat{H}_{int}$ which describes the exchange of photons by stimulated emission, has the expression:

$$\widehat{H}_{int,j} = \hbar\, \omega_j\, \chi_q^{(2)} \left(\hat{a}_1 \hat{a}_2\, \hat{a}_3^{\dagger} + \hat{a}_1^{\dagger} \hat{a}_2^{\dagger} \hat{a}_3 \right) \tag{4.3}$$

where the reduced Planck constant and the relevant susceptibility are, respectively, denoted by $\hbar$ and $\chi_q^{(2)}$, the latter including the constant of proportionality relating the Hamiltonian expressed in terms of the electric field operators to the Hamiltonian $\widehat{H}_{int}$ associated with photon annihilation and creation operators, $\hat{a}_j$ and $\hat{a}_j^{\dagger}$, of the ω_j field (j = 1, 2, 3), as defined in equation (3.9).

The equations of motion for the expectation values are found from the Ehrenfest theorem presented in Section 3.3.2. The composite wave function of the three interacting waves or photonic beams is:

$$|\Phi(\boldsymbol{r},t)\rangle = |\, \Psi_{\mathrm{n},1}\, (\boldsymbol{r},t)\, \rangle\, |\, \Psi_{\mathrm{n},2}\, (\boldsymbol{r},t)\, \rangle\, |\, \Psi_{\mathrm{n},3}\, (\boldsymbol{r},t)\, \rangle \tag{4.4}$$

Analogously to the linear wave interactions of Section 3.3.2, one obtains the following coupled wave equation of motion:

$$\frac{\partial}{\partial t}\, s_1 = -\, i\omega_1 \kappa\, s_3\, s_2^{\dagger} \tag{4.5}$$

After converting to number of photons, i.e., $|\, s_{\mathrm{n,j}}|^2 = N_j$ and corresponding phases φ_{j}, the equation of motion (4.5) provides the rates of change of N_j and φ_j as follows:

$$\frac{\partial}{\partial z} N_1 = g_1 N_1 \tag{4.6a}$$

$$g_1 = -\kappa_1 \left(\frac{N_2 N_3}{N_1}\right)^{1/2} \sin\theta \tag{4.6b}$$

$$\frac{\partial}{\partial z}\theta = (\beta_3 - \beta_2 - \beta_1) + \\ + \kappa_1 \left[\left(\frac{N_1 N_2}{N_3}\right)^{1/2} - \left(\frac{N_1 N_3}{N_2}\right)^{1/2} - \left(\frac{N_2 N_3}{N_1}\right)^{1/2}\right] \cos\theta \tag{4.6c}$$

$$\frac{\partial}{\partial z} \varphi_1 = \kappa_1 \left(\frac{N_2 N_3}{N_1}\right)^{1/2} \cos\theta \tag{4.6d}$$

$$\kappa_1 = \frac{1}{\mathrm{v}_p} \frac{k_{0;1}}{2n} \int\int dx\, dy\, \chi_q^{(2)} f_1 f_2 f_3 \tag{4.6e}$$

$$\chi_q^{(2)} = \left(\frac{\hbar}{\varepsilon}\right)^{3/2} \chi_{classic}^{(2)} \tag{4.6f}$$

$$\varphi_{1;2}(L) = \varphi_{1;2}(0) + \int_0^L r_{1;2}(z) \cos\theta(z)\, dz \tag{4.6g}$$

$$r_{1;2}(z) = \left(\frac{N_{2;1} N_3}{N_{1;2}}\right)^{1/2} \tag{4.6h}$$

$$\theta = \theta_{321} = (\beta_3 - \beta_2 - \beta_1)\cdot z + \varphi_3 - \varphi_2 - \varphi_1 \tag{4.6i}$$

$$\theta_{op} = \varphi_3 - \varphi_2 - \varphi_1 = -\frac{\pi}{2} \tag{4.6j}$$

where the gain coefficient g_1 includes an overall coupling coefficient κ_1 that depends on the polarization states of the photons through the tensorial structure of the classical nonlinear susceptibility $\chi^{(3)}$. The phase difference (or the relative phase) between the three waves is θ_{321}, β being the propagation constant and $z / t = \mathrm{v_p}$ is the phase velocity. In (4.6*e*), $k_{o;1}$ and

n specify the free-space wavevector and the effective refractive index, respectively, while *f* identifies the field distribution.

The condition for optimal amplification is found from eqs. (4.6), for $\Delta\beta = 0$, to be $\theta_{op} = -\pi/2$ of eq. (4.6 *j*).

The mixing of three photons of different frequencies can lead to quadrature-dependent coupling of photons, with one pump photon splitting into a signal photon of the same quadrature state (p), and the idler photon coupled into the second quadrature state (q). As a consequence of the relative phase being –π/2 in the phase -dependent coefficient of eq. (4.6*b*), i.e., $\varphi_p - \varphi_{p\,s} - \varphi_{q\,i} = -\pi/2$, these quadrature waves will be amplified, whereas those shifted by π/2 will be de-amplified. This is a much weaker version of the optically linear parametric exchange of power between quadrature waves of the same frequency identified in Chapter 2.

4.3 Phase-dependent Gain Coefficients and Phase-pulling Effects

An input-output transfer function for the expectation values of the signal or idler powers $P_{1;2}$ can be found by recalling the relation between the flux of photons *N* and the optical power of a beam (Blow *et al.* [22]), i.e., $P = \hbar\,\omega\,N$. This will unify the classical and quantum optic rate equations.

A formal integration of eq. (4.6*a*) will define a gain factor $G_{1;2}(z, \theta)$ and an output number of photons $N_{1;2}(z)$, that are:

$$G_{1;2}(z,\theta) = exp\int_0^z g_{1;2}\,(v,\theta)dv \qquad (4.7a)$$

$$N_{1;2}(z,\theta) = G_{1;2}(z,\theta)\,N_{1;2}(0,\theta) \qquad (4.7b)$$

The phase - dependence of the parametric conversion of photons is determined by the gain coefficient *g* of eq. (4.6*b*) through the relative phase θ of eqs. (4.6*c* and 4.6*d*). Signal and idler waves photons will be absorbed by the pump for $0 < \theta < \pi$, and will be amplified for $-\pi < \theta < 0$. The minimum level of input optical power corresponds to the spontaneous emission.

The power ratio $r_{1;2}(z)$ of eq. (4.6*h*) also plays the role of a saturation factor, reducing the gain coefficient for higher input levels of $N_{1;2}$. A higher power ratio $r_{1;2}(z)$ leads to a higher gain coefficient *g* but also speeds θ towards $-\pi/2$. This is a parametric phase pulling effect which, for $N_{pump} >>$

$N_{signal/idler}$, can overcome a phase-mismatch induced by $\Delta\beta \neq 0$ as explained in the next paragraph.

The parametric phase pulling (PPP) effect undergone by the signal wave emerges from the rate of change of φ_1 which dominates the shift in the relative phase θ in eq. (4.6*c*) for $N_3 > N_2 >> N_1$. This is illustrated in

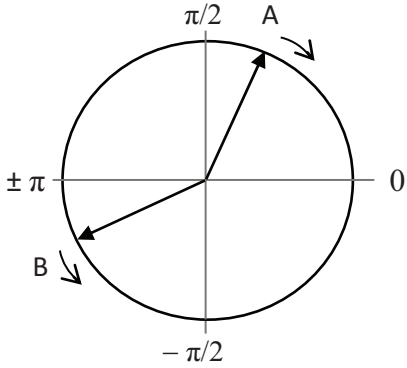

Fig. 4.1. The role of the parametric phase pulling effect for $N_3 > N_2 >> N_1$, in shifting θ towards $-\pi/2$, for any input signal phasor.

Fig. 4.1. From eq. (4.6*c*), for $-\pi/2 < \theta < \pi/2$, the relative phase will rotate clockwise on the phasor circle (in the negative direction) towards $-\pi/2$, and for $\pi/2 < \theta < 3\pi/2$, it will rotate in the positive direction as $-\cos\theta > 0$. This field phasor rotation suggests the possibility of reducing phase fluctuations as the relative phase, if dominated by the ratio r_1 of eq. (4.6*h*), is shifting towards the optimal phase of $-\pi/2$, regardless of the initial phase value. Therefore, parametric amplification of single photons is unavoidable. In the process, the gain coefficient g_1 increases in value and becomes locked-in at the optimal value of θ resulting in a phase-matched interaction.

For a vanishing total phase mismatch, with $N_3 > N_2 >> N_1$ and spontaneous emission initiating one sideband wave N_1, its phase φ_1 change will dominate the shift of the relative phase to bring about $\theta = -\pi/2 = \varphi_3(0) - \varphi_2(0) - \varphi_1$ at the output. By adjusting the initial pump phases $\varphi_3(0)$, a conjugate phase $\varphi_2 = -\varphi_1(0)$ can be obtained.

From eqs. (4.6) we find that by setting $\varphi_3(0) = 0$, the propagating quadrature waves of $\varphi_{1;2} = \pm\pi/4$ and $\varphi_{1;2} = \pi \pm \pi/4$ are, respectively, amplified (+) and attenuated (−), being separated by π rad. Their nonlinearly induced phases are obtained from eq. (4.6*g*). Other input phases are pulled towards these values by the parametric phase-pulling effect of the last term

of eq. (4.6*c*). The parametric phase-pulling effect will shift the arbitrary phases of photons towards a common value, thereby reducing the level of phase-noise as demonstrated experimentally in (Lundström *et al*. [23]).

A particular case that will be of interest in the following Chapters deals with the amplification of spontaneously emitted photons. This process will be initiated with $N_3 >> N_2 = N_1 = 1$ and arbitrary phases.

4.4 Simultaneous Amplification of a Signal and Sub-Poissonian Distributions of Photons

We have identified in previous sections of this Chapter the parametric phase-dependent gain coefficient and the related parametric phase-pulling effect as fundamental mechanisms underpinning two-photon output per interaction for $\chi^{(2)}$ (and $\chi^{(3)}$) parametric processes for any level of optical powers and conditions. In this Section, we consider the possibility of generating sub-Poissonian distributions of photons with the assistance of optically linear parametric (OLP) [6] and electro-optic parametric (EOP) [7] interactions which involve only one-photon output per interaction – with one-photon input – although the EOP conversion requires one microwave photon. The rate equations for these processes are similar, both having a phase-dependent gain coefficient and the related phase-pulling effect, and are derived by setting the appropriate electric dipole operators.

Let us consider a strong optical pump of angular frequency ω_o in the form of a conventional coherent state of light which is characterized by an α eigenvalue possessing a large average number of photons $\langle N \rangle = N_o$ and a narrow phase-dispersion (Carruthers and M. Nieto [24, Sec. 8a]) centred on its average value φ_o. Although the optical pump is commonly considered to remain undepleted, its temporal waveform $N(t)$ displays photon number fluctuations which should fall within the Poisson distribution, with a quantum noise standard deviation of $\sqrt{N_o}$. A simple method for reducing the fluctuations of a strong pump would have its beam split into two equal parts and each part launched into one branch of an optical time-delay (τ) interferometric filter, so that, at the output, the number of photons will be proportional to $N_{out} = 0.5\,[N(t) + N(t+\tau) + 2\sqrt{N(t)}\sqrt{N(t+\tau)}\,cos\,(\omega_o \tau)]$. The cosine term can be eliminated by adjusting the time delay so that $cos\,(\omega_o \tau) = 0$, leading to a Fourier transform of the superposition of two replicas of the photon number waveform, and their spectral power $S(f)\,cos^2\,(\pi f \tau)$ being shaped by a filter profile which will attenuate high electrical frequencies or photon-number sinusoidal waves associated which sharp rises and falls in the photon number fluctuations.

4.4.1. Optically linear parametric directional couplers

An optical directional coupler (ODC) composed of two parallel and identical optical waveguides can operate as a phase-sensitive (PS) amplifier when the signal power launched into one waveguide is much smaller than the pump power propagating in the other waveguide. This operation would be described by the coupled photon equations of Chapter 3 indicating that the phase-sensitive gain coefficient g_s of a signal is inversely proportional to the square root of the signal's number of photons, i.e. $\sqrt{N_s}$, thereby reducing the level of fluctuations in the output number of photons by enhancing the gain for the smaller number of photons. As a result, a sub-Poissonian distribution of photons is generated through the saturation-like amplification which is the consequence of the stimulating field being different from the pumping field.

The possibility of generating a sub-Poissonian distribution of photons through signal-dependent differential gain can be assessed by imposing the condition that the input range [0.7 N_o ; 1.4 N_o] of the number of signal photons N_s (0) – covering most of a Poissonian distribution of average N_o – is reduced to the interval of the standard deviation, i.e., [N_o (L) – $\sqrt{N_o}$ (L); N_o (L) + $\sqrt{N_o}$ (L)] at the output after an interaction length L.

An estimate of the reduced range can be assessed by inserting the gain coefficient from eqs. (3.29) into the eqs. (4.7) to obtain the equality

$$N_{s,j}(L) = N_{s,j}(0) \times G_{s,j}(L)$$

(with input $j = 1$ for 0.7 N_o and $j = 2$ for 1.4 N_o) and, requiring $N_p >> N_{s,j}$ to find from the ratio $\mu_j = N_{s,j} / N_o$ the expressions:

$$ln\,\mu_j(L) = ln\,\mu_j(0) + \int_0^L [\,g_{s,j}(z) - g_o(z)]\,dz \qquad (4.8a)$$

$$ln\,\mu_j(L) = ln\,\mu_j(0) + \int_0^L g_o'(z)\left(N_{s,j} - N_o(z)\right)dz \qquad (4.8b)$$

where

$$g_o'(z) = \frac{d\,g_s}{d\,N_s} = \frac{2\cdot(-0.5)\,\gamma\sqrt{N_p}}{[N_o(z)]^{3/2}} \qquad (4.8c)$$

is the gain derivative evaluated at $N_s = N_o(z)$ from eq. (3.29) for maximal gain, and having used the linear relation

$$g_{s,j}(z) \approx g_o(z) + g'_o(z) \cdot (N_{s,j} - N_o(z)),$$

i. e., a truncated power series expansion of $g_s(N_s)$. The design parameters include the coupling coefficient between the waveguides [7], the pump number of photons N_p, and the length of interaction L. An attempt to reduce $ln\ \mu_j$ to a target value close to zero may require more than one amplifying stage.

As an additional application, the gain coefficient can rotate the state of polarisation of an optical beam through differential amplification of the x–polarised and y –polarised components if the optical powers are not equal, with the pump being polarised at an angle of 45° relative to the axes.

For low levels of signal powers, the phase-pulling effect of eqs. (3.29*c*) and (3.29*d*), illustrated in Fig. 4.1, brings all signal phases towards the optimal value of their relative phase of $\theta = -\pi / 2$ for maximum amplification, thereby reducing phase fluctuations. Thus, photons with a broad range of phases have their phases brought together by the phase-pulling effect, resulting in a coherent beam of photons. As an application, a binary phase-encoded signal $\{-\pi/2, \pi/2\}$ can be converted into an amplitude binary {"1", "0"} with a phase-sensitive optical directional coupler amplifier.

Another saturation-like mechanism which further increases the gain for weaker signals is the phase dependence of the gain coefficient. The phase-pulling effect tends to equalise the levels of powers – or corresponding numbers of photons – between the pump power and the signal and idler powers particularly so for an input phase difference of $\varphi_p - \varphi_s = m\,\pi$ (where $m = 0, \pm 1, \pm 2, \ldots$ an integer). A weaker signal will reach the maximum gain condition faster than a stronger signal as indicated by eqs. (4.6).

The phase-sensitive optical directional coupler device can support only degenerate frequency amplification, i.e., ($\omega_{pump} = \omega_{signal}$) but one optical directional coupler will amplify any wavelength of a wavelength division multiplexed signal provided a suitable pump frequency comb is available. Non-degenerate frequencies amplification can be delivered by electro-optic parametric (EOP) waveguides as outlined in the next section.

4.4.2 Electro-optic converters

The parametric amplification of a signal whose frequency is different from that of an available pump can be implemented with an appropriately designed electro-optic modulator. The electro-optic parametric (EOP) interaction [10] provides external control of the phase-sensitive amplification through the phase of the microwave modulating signal.

An electro-optic phase-sensitive amplifier (EO-PSA) will consist of an electro-optic waveguide with electrodes designed for travelling microwave modulating signals. By adjusting the phases of the microwave field and of the optical pump wave, a frequency downshifted input signal can be amplified or attenuated [10] as illustrated in Fig. 4.2. An optical pump with a narrow spectral bandwidth can amplify and filter out a similarly narrow

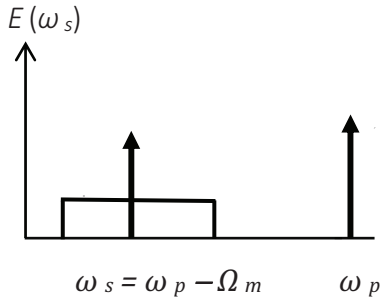

Fig. 4.2 Electro-optic parametric amplification filtering out a narrow band of the signal spectrum through frequency downshifting of pump photons (ω_p) by a modulating frequency Ω_m.

signal bandwidth through the electro-optic parametric process of frequency translation [10], (Riaziat *et al*. [24]). The frequency downshifting $\omega_p - \Omega_m = \omega_s$ would be easy to implement because it generates microwave photons, requiring only a limited level of input microwave power. Broadband amplification with EOP devices is possible by operating multiple optical pump waves.

The equations of motion for OLP and EOP interactions involve only two optical waves [6 -7] and can be reformulated similarly to the optically linear parametric conversion of photons – see Appendix B below – having the form:

$$\frac{\partial}{\partial z} N_1 = g_a N_a - \alpha N_a \qquad (4.9a)$$

$$g_{a;b} = -\kappa_a\, r_{a;b}(z)\ \sin\theta \tag{4.9b}$$

$$r_{a;b}(z) = \left(\frac{N_{b;\,a}}{N_{a;\,b}}\right)^{1/2} E_m \tag{4.9c}$$

$$\frac{\partial}{\partial\, z}\,\theta_{ba} = (\beta_b - \beta_m - \beta_a\,) + \kappa_a\,(r_b - r_a)\cos\theta_{ba} \tag{4.9d}$$

$$\theta_{ba} = (\,\beta_b - \beta_m - \beta_a)\cdot z + \varphi_b - \varphi_m - \varphi_a \tag{4.9e}$$

$$\varphi_{a;\,b}(L) = \varphi_{a;b}(0) + \int_0^L r_{a;b}\,(z)\cos\theta_{ba}\ dz \tag{4.9f}$$

$$\kappa_a = \frac{1}{\mathrm{v}_p}\,\frac{k_{0;\,a}}{2\,n}\int\int dx\,dy\,\chi^{(2)}_{q;EO}\,f_a\,f_b\,f_m \tag{4.9g}$$

where a loss factor α is included in eq. (4.9*a*)), and the modulating microwave field $E_{m,}$ phase and frequency Ω_m are identified by the subscript *m*. Additionally, $\omega_a = \omega_b - \Omega_m$.

The phase-sensitive gain coefficient of eqs. (4.9) will reduce amplitude fluctuations, while the parametric phase-pulling effect will narrow the range of phase variations carried by the signal – see Fig. 4.1.

A distinction is made between time-domain quadrature states of light, i.e., *cos (ω t)* and *in (ω t)*, and space-domain or propagation (longitudinally varying) quadrature states which will exhibit maximum or minimum gain for $\theta_{b\,a} = \pm\,\pi/2$ or no gain for $\theta_{b\,a} = 0$ or $\pm\,\pi$, as seen from eq. (4.9*b*).

The propagation quadrature states evolve as a result of parametric phase shifts as specified in eqs. ((4.9*d*) and (4.9*f*). For a phase-matching condition, $\Delta\beta = 0$, they will tend towards the maximum gain, while for a phase mismatch $\Delta\beta \neq 0$ they will depend on the interaction length as well.

4.5 Physical Aspects of Phase-sensitive Gain Coefficients

The conventional method of experimental noise reduction through the interference between a signal and its phase-conjugate replica, e.g., [21], (Levenson *et al*. [25-26]) relies on parametric conversions of photons in $\chi^{(2)}$ and $\chi^{(3)}$-based materials. These techniques, however, constitute only a particular case of a broader picture of parametric processes.

The approximated mathematical solution reproduced in Appendix A below – eqs. (A4.1-2) – is inconsistent with the rigorous and physically meaningful solution published in 1962 in (Armstrong *et al*. [27]) – and expanded in 2013 in (Marhic [28]) – and which was largely overlooked because of its complexities involving elliptic functions. Nevertheless, its physical features can be extracted from the interlinked rate equations of motion for the powers and phases of the optical waves involved in the parametric processes as presented in (Vatarescu [7-10], [18]). As a result, one identifies, both classically and quantum optically, a phase-dependent gain coefficient and a related phase-pulling effect. The rigorous solution rules out *simultaneous* amplification and attenuation of the signal and idler waves as indicated in eqs. (A4.1-2) of Appendix A below.

Equally, an approximation-free and fully quantum optic analysis of parametric processes – presented in this Chapter– reveals that the conversion of photons involves a parametric gain which depends on the relative phase between the pump waves and, the signal and idler waves and is inversely proportional to the square root of its power, as well as identifying a parametric phase-pulling effect, for any levels of optical powers.

The parametric phase-pulling effect is capable of countering a phase-mismatch condition and tends to equalize the levels of power among the waves taking part in the mixing of photons. Amplitude noise reduction is achievable for any levels of signal power as the gain coefficient displays a saturation-like property. The same characteristic is also exhibited by the related parametric phase-pulling effect.

The similarities between optically linear parametric and electro-optic parametric processes, on the one hand, and the three- or four-photon mixing interactions, on the other hand, are evident as all these processes belong to the same group of physical phenomena whereby the optical fields drive the atomic electrons into oscillation with no absorption of energy between resonant energy states.

The mathematical technique of linearizing – on the basis of assumptions and approximations [29] – the parametric nonlinear coupled wave equations brings about a loss of physical properties and the appearance of physical inconsistencies as pointed out in the Introduction to this Chapter and the Appendix A below. The differential equations derived under the condition of undepleted pump approximation do not include the variation of the conversion-related phase, or the possibility of power coupling reversal which is a major feature of parametric processes.

Possible operations of carrying out phase-sensitive amplification at low levels of optical power and over short interaction lengths may benefit from

the versatility offered by parametric processes involving only two optical waves. Functional operations can be implemented at low levels of pump power and over short distances of a few wavelengths for optically linear parametric interactions and centimetres for electro-optic parametric interactions.

Equally, a combination of optically linear parametric and electro-optic parametric devices will also involve only two interacting optical waves with the electro-optic parametric effect providing direct interfacing between the electrical and optical domains through the electro-optic effect of a suitable crystal interleaved with silica waveguides.

For applications in the following Chapters, we emphasize that the parametric amplification of a spontaneously emitted photon is unavoidable and that the propagation, in a dielectric material, of one photon per radiation mode is directionally random involving absorption and spontaneous re-emission.

4.6 Conclusions

A physical analysis of parametric processes reveals a common feature of phase dependent gain coefficients accompanied by a phase pulling effect. Phase-sensitive amplification can be achieved at low levels of optical power and over short interaction lengths by means of optically linear and electro-optic parametric conversions of photons. With only two optical waves needed for signal processing, e.g., amplification, noise reduction, filtering, etc., the electro-optic parametric–based devices will have the advantage of direct external control for different signal and pump frequencies.

These physical mechanisms can generate sub-Poissonian distributions of photons through a saturation-like effect and using only integrated photonic circuits.

Appendix A - The deficiencies of the Bogoliubov-type solutions

The evolution of the operators is given by the following equations of motion for a phase-matched nonlinear interaction [25]:

$$a_{s,\,i}(z) = \cosh(g_o z)\, a_{s,\,i}(0) + i\, e^{\,i\,\varphi_{p\,r}}\, \sinh(g_o z)\; a^*_{i,\,s}(0) \qquad (A\,4.1)$$

$$\frac{d}{dz}\, a_{s,\,i}(z) = 0.5\, g_o\, [a_{s,\,i}(0) + i\, e^{\,i\,\varphi_p} a^*_{i,\,s}(0)]\, e^{\,g_o\, z} -$$

$$- 0.5\, g_o\, [\, a_{s,\,i}(0) - i\, e^{\,i\,\varphi_p} a^*_{i,\,s}(0)]\, e^{\,-\,g_o\, z} \qquad (A\,4.2)$$

These expressions of the optical field operators and their rates of change – eq. (*A* 4.2) – also apply to the corresponding classical optical fields [21], [25 - 26], [29] where the complex amplitudes of the signal and idler waves are denoted by a_s and a_i, respectively, with the asterisk indicating complex conjugation and z being the longitudinal distance of propagation. The reference phase φ_p is (the sum of) the pump phase(s). The gain coefficient is given by $g_o = \kappa^{(2m+1)} P_p^m$ for a small signal, and phase-matching conditions, with κ and P_p corresponding, respectively, to the nonlinear coefficient and the pump power for $\chi^{(2)}$, the second-order susceptibility ($m = ½$), and $\chi^{(3)}$, the third-order susceptibility ($m = 1$).

The self-coupling term $g_o\, a_s\,(0)$ of the rate equation eq. (A4.2) above, would be generated by an electric dipole polarization oscillating at the angular frequency $\omega_{pump} + \omega_s$ instead of $\omega_{pump} - \omega_i$ which is required for an exchange of photons of ω_s in a second-order nonlinearity. Such a dipole frequency $\omega_{pump} + \omega_s$ cannot couple photons into the signal.

Classically, for a zero-input idler wave, i.e., $a_i\,(0) = 0$, the signal seems unaffected by the cross-coupling or interaction term. Equally, quantum optically, the expectation values of eqs. (A4.1-2) contain the creation operator a^* which, in the context of coherent states of light $|\alpha\rangle$, results in the complex conjugate value α^* of the eigenvalue of the annihilation operator. Consequently, the zero-photon state with $\alpha = 0$ cannot trigger a parametric conversion of photons in eq. (A4.2). This will be role of the spontaneous emission [7].

As the same number of stimulated photons is gained, or lost, by both the signal and the idler waves through stimulated emission, e.g. [7 - 9], the rate of power change should incorporate the product of all the optical powers taking part in the parametric conversion, i.e.,

$$\frac{d}{dz}\, P_{s,i} = \kappa^{(2m+1)}\, P_p^m\, \sqrt{P_s\, P_i}\, \sin\theta\,(z) \qquad (A4.3)$$

where $P_{s,i} = |\, A_{s,i}\,|^2$, A being the corresponding field amplitude, $\theta(z)$ the relative phase between the pump(s), and the signal and idler waves including the photonic conversion-induced phases [14], [20-21]. Eq. (A4.3) requires a non-zero input for both the signal and the idler waves in order for the conversion of photons to be initiated. The minimum input power will correspond to the spontaneous emission which depends on the strength of the electric dipole [7] and is distinct from the background (or vacuum) fluctuations which are much weaker and independent of the parametric process.

Appendix B – The Quantum Regime of Electro-optic Modulation

The analysis of one optical wave of frequency ω_o co-propagating through an electro-optic waveguide alongside a microwave of frequency $\boldsymbol{\Omega}$, will results in both frequency-upshifted and downshifted sidebands. These sidebands are generated through amplification of spontaneously emitted photons, and the derivation of Section 4.2 can be readily adapted to this case.

The corresponding Hamiltonian of interaction between adjacent sidebands $n-1$ and n takes the form:

$$\hat{H}_{int,n} = \hbar\, \omega_n\, \chi_q^{(2)} \left(\hat{a}_{n-1}\, \hat{a}_m\, \hat{a}_n^{\dagger} + \hat{a}_{n-1}^{\dagger}\, \hat{a}_m^{\dagger}\, \hat{a}_n \right) \qquad (B4.1)$$

The subscript m identifies the microwave photon annihilation and creation operators, and the first term in the brackets corresponds to an up-shifted optical frequency, while the Hermitian conjugate term indicates the down-shifting of the optical frequency.

An upshifted sideband denoted by an integer $n = 1, 2, 3...$gains photons from the $(n-1)$-th sideband and loses photons to the next $(n+1)$-th sideband. The frequencies are related by the equality: $\omega_{\,n} \pm \boldsymbol{\Omega} = \omega_{\,n\pm1}$. A downshifted sideband denoted by a negative integer $n = -1, -2, -3...$gains photons from the $(-n+1)$-th sideband and loses photons to the next $(-n-1)$-th sideband.

The equations of motion for the expectation values of the number of photons are found from the Ehrenfest theorem presented in Section 3.3.2. The composite wave function of the three interacting waves or photonic beams is:

$$|\Phi(\boldsymbol{r},t)\rangle = |\,\Psi_{n-1}\,(\boldsymbol{r},t)\,\rangle\,|\,\Psi_{\mathrm{n}}\,(\boldsymbol{r},t)\,\rangle\,|\,\Psi_m\,(\boldsymbol{r},t)\,\rangle \qquad (B4.2)$$

Analogously to the linear wave interactions of Section 3.3.2, one obtains the following coupled wave equation of motion for the number of photons N and corresponding phases φ of the optical sidebands [10], similarly to eq. (4.6):

$$\frac{\partial}{\partial\, z}\, N_{\pm n} = -\kappa_{\pm n} \sqrt{N_{\pm(n-1)}\, N_{\pm n}\, N_m}\, sin\, \theta_{\pm(n-1),\pm n} +$$

$$+ \kappa_{\pm n} \sqrt{N_{\pm n}\ N_{\pm(n+1)}\ N_m}\ sin\ \theta_{\pm\, n,\pm(n+1)} \qquad (B4.3)$$

$$\frac{\partial}{\partial\, z}\varphi_{\pm n} = \kappa_{\pm \mathrm{n}} \left(\frac{N_{\pm(n-1)}}{N_{\pm n}}\right)^{1/2} \sqrt{N_m}\ cos\ \theta_{\pm(n-1),\pm n}\ +$$

$$+ \kappa_{\pm n} \left(\frac{N_{\pm(n+1)}}{N_{\pm n}}\right)^{1/2} \sqrt{N_m}\ cos\ \theta_{\pm n\,,\pm(n+1)} \qquad (B4.4)$$

$$\theta_{\pm(n-1),\pm \mathrm{n}} = \varphi_{\pm(n-1)}\ \pm \varphi_m - \varphi_{\pm\, n}$$

$$\kappa_{\pm n} = \frac{1}{\mathrm{v}_p}\ \frac{k_{0;\,n}}{2\ n_{ref}} \int\int dx\ dy\ \chi^{(2)}_{q;EO}\ f_n\ f_{n\pm1}\ f_m$$

where $\kappa_{\pm \mathrm{n}}$ is the nonlinear coupling coefficient determined by the spatial overlap of the three field distributions *f*'s.

The optimal relative phase for both upshifting and downshifting cases is $\theta_{\pm} = -\pi / 2$. After converting the number of photons into the optical field magnitude $E_{\pm\, n} = \gamma_p \sqrt{N_{\pm\, n}}$ using eq. (3.28), the rate of change for both the upper and the lower sidebands of the optical field is found as:

$$2\frac{d}{dz}\ E_{\pm\, n} = s' E_{\pm\,(n-1)} - \ s' E_{\pm\,(n+1)} \qquad (B4.5a)$$

$$s = 2\kappa_{\pm n} \frac{1}{\gamma_p} \int E_m\ sin\ \theta(z)\ dz \qquad (B4.5b)$$

after defining a modulation index *s*, and its derivative *s′*, in the approximation of an undepleted pump and microwave power for any sideband, i.e., so long as photons are shifted away from the input pump wave. And for a continuous wave input, i.e., n=0, the pump loses power to both first order sidebands:

$$2\frac{d}{dz}\ E_{\mathrm{o}} = -s' E_{+1} - \ s' E_{-1} = 2\ - s' E_{+1} \qquad (B4.6)$$

The rate equations (*B*4.5) and (*B*4.6) provide, in the undepleted pump approximation, the evolution of the sideband fields $E_{\pm n}$, and their initial phase quadratures are found from the optimal phase for the amplification of the spontaneous emission:

$$\theta_{\pm(n-1),\pm n} = \varphi_{\pm(n-1)} \pm \varphi_m - \varphi_{\pm n} = -\frac{\pi}{2} \qquad (B4.7)$$

For φ_m = 0 or π, the modulating tone corresponds to $\pm\, cos\ (\Omega\, t)$, and for $\varphi_m = -\pi/2$ or $\pi/2$, to $+/-\ sin\ (\Omega\, t)$. The solutions to eqs. (*B*4.5) and (*B*4.6) lead to the Bessel functions of the first kind, i.e. $E_{\pm n} = J_n(s)$, through the equality:

$$\mathcal{E}_{\pm n} = E_{\pm n}\, e^{i\,(\omega_o \pm n\,\Omega)t} = J_n(s) e^{i\,\varphi_{\pm n}}\, e^{i\,(\omega_o \pm n\,\Omega)t} \qquad (B4.8)$$

where $\varphi_{\pm n} = \{0,\ \pi/2\ ,\pm\pi\ ,-\pi/2\ \}$. The initial quadrature phase $\varphi_{\pm n}$ is determined from the condition for optimal amplification of spontaneous emission of eq. (*B*4.7)) after setting $\varphi_0 = 0$. A superposition of fields $\mathcal{E}_{\pm n}$ multiplied by the corresponding sinusoidal tone reproduces the mathematical expansions in terms of Bessel functions of a phase modulated wave by the corresponding time single tone, i.e., $exp(\pm\, i\, s\ cos\ (\Omega\, t))$ and $exp(\pm\, i\, s\ sin\ (\Omega\, t))$.

The undepleted pump approximation can be somewhat relaxed because of the phase-mismatch compensation brought about by the parametric phase shifts in eq. (*B* 4.4). The approximation $sin\ \theta \approx -1$ holds at low levels of converted power because $\Delta\beta \cdot z$ is partially offset by the nonlinearly induced $\Delta\varphi$, for a strong and undepleted pump. The phase mismatch function $sinc\ (\Delta\beta \cdot z)$ is obtained from eq. (*B*4.5*b*) if the parametric phases are ignored, that is, $\Delta\beta \cdot z >> |\Delta\varphi|$ and initially $\theta = \pm\ \Delta\beta \cdot z - \pi/2$.

References

1. R. Schnabel, "Squeezed states of light and their applications in laser interferometers", Phys. Rep. **684**, 2017, 1-51, (2017).
2. U. L Andersen, T. Gehring, C. Marquardt1, and G. Leuchs, "30 years of squeezed light generation ", Phys. Scr. **91,** 053001, (2016).
3. L. Thylén and L. Wosinski, "Integrated photonics in the 21st century", Photon. Res*.,* ***2*****,** 75-81, (2014).

4. Z. Zhang, D. Felipe, V. Katopodis, P. Groumas, C. Kouloumentas, H. Avramopoulos, J-Y. Dupuy, A. Konczykowska, A. Dede, A. Beretta, A. Vannucci, G. Cangini, R. Dinu, D. Schmidt, M. Moehrle, P. Runge, J.-H. Choi, H.-B. Bach, N. Grote, N. Keil, and M. Schell, "Hybrid Photonic Integration on a Polymer Platform", Photonics **2,** 1005-1026, (2015).
5. S. M. Hendrickson, A. C. Foster, R. M. Camacho, and B. D. Clader, "Integrated nonlinear photonics: emerging applications and ongoing challenges", J. Opt. Soc. Am. B, **31**, 3193-3202, (2014).
6. W. Li, M. Lu, A. Mecozzi, M. Vasilyev, S. Arafin, D. Dadic, L. A. Johansson, and L. A. Coldren, "First Monolithically Integrated Dual-Pumped Phase-Sensitive Amplifier Chip Based on a Saturated Semiconductor Optical Amplifier", IEEE J. Quantum Electron*.,* **52***,* 0600212*,* (2016).
7. A. Vatarescu, "Photonic coupling between quadrature states of light in a homogeneous and optically linear dielectric medium", J. Opt. Soc. Am. B**, 31**, 1741–1745, (2014).
8. A. Vatarescu, "Phase-Sensitive Amplification with Low Pump Power for Integrated Photonics", *OSA Advanced Photonics Congress*, paper ID: IM3A.6, 2016.
9. A. Vatarescu, "Photonic Quantum Noise Reduction with Low-Pump Parametric Amplifiers for Photonic Integrated Circuits", Photonics, **3**, article 61, (2016).
10. A. Vatarescu, "Photonic quadrature-wave pulses generated by a single electro-optic waveguide modulator for digital transmission", J. Opt. Soc. Am. B, **32,** 555-561, (2015).
11. H. Yamazaki, T. Yamada, T. Goh, and A. Kaneko, "PDM-QPSK Modulator with a Hybrid Configuration of Silica PLCs and $LiNbO_3$ Phase Modulators", J. Lightwave Technol., **29,** 721–727, (2011).
12. K. Kikuchi*,* "Fundamentals of Coherent Optical Fiber Communications", J. Lightwave Technol., **34**, 157-178, (2016).
13. L. Davidovich, "Sub-Poissonian processes in quantum optics", Rev. Mod. Phys., **68**, 127-173, (1996).
14. H. P. Yuen, "Two-photon coherent states of the radiation field", Phys. Rev. A, **13,** 2226 – 2243, (1976).
15. R. H. Henry, and S. C. Glotzer, "A squeezed-state primer", Am. J. Phys., **56**, 318-328, (1988).

16. W. H. Louisell, A. Yariv, and A. E. Siegman, "Quantum Fluctuations and Noise in Parametric Processes", Phys. Rev., **124,** 1646 – 1654, (1961).
17. K. Inoue, and T. Mukai, "Signal wavelength dependence of gain saturation in a fiber optical parametric amplifier", Opt. Lett. **26**, 10–12, (2001).
18. A. Vatarescu, "Light conversion in nonlinear monomode optical fibers", J. Lightwave Technol., **5**, 1652–1659, (1987).
19. R. J. Glauber, and M. Lewenstein, "Quantum optics of dielectric media", Phys. Rev. A, **43**, 467- 491, (1991).
20. M. E. Anderson, D. McAlister, and M. G. Raymer, "Pulsed squeezed-light generation in $\chi^{(2)}$ nonlinear waveguides", J. Opt. Soc. Am. B, **14,** 3180-3189, (1997).
21. P. D. Townsend, and R. Loudon, "Quantum-noise reduction at frequencies up to 0.5 GHz using pulsed parametric amplification", Phys. Rev. A, **45**, 498 -510, (1992).
22. J. K. Blow, R. Loudon, S. J. D. Phoenix, and T. J. Shepherd, "Continuum fields in quantum optics", Phys. Rev. A, **42**, 4102-4114, (1990)
23. C. Lundström, Z. Tong, M. Karlsson, and P. A. Andrekson, "Phase-to-phase and phase-to-amplitude transfer characteristics of a nondegenerate-idler phase-sensitive amplifier", Opt. Lett., **36**, 4356–4358, (2011).
24. M. L. Riaziat, G. F. Virshup, and J.N. Eckstein, "Optical Wavelength Shifting by Traveling-Wave Electrooptic Modulation", IEEE Photon. Technol. Lett., **5,** 1002-1005, (1993).
25. M. D. Levenson, R. M. Shelby, A. Aspect, M. Reid, and D. F. Walls, "Generation and detection of squeezed states of light by nondegenerate four-wave mixing in an optical fiber", Phys. Rev. A, **32**, 1550-1562, (1985).
26. J. A. Levenson, I. Abram, T. Rivera, and P. Grangier, "Reduction of quantum-noise in optical parametric amplification", J. Opt. Soc. Am. B**, 10,** 2233–2238, (1993).
27. J. A. Armstrong, N. Bloembergen, J. Ducuing, and P, S. Pershan, "Interactions between Light Waves in a Nonlinear Dielectric", Phys. Rev., **127**, 1918 – 1939, (1962).

28. M. E. Marhic, “Analytic solutions for the phases of waves coupled by degenerate or nondegenerate four-wave mixing”, J. Opt. Soc. Am. B, **30**, 62-70, (2013).
29. C. McKinstrie, and S. Radic, “Phase-sensitive amplification in a fiber”, Opt. Express, **12**, 4973–4979, (2004).

CHAPTER FIVE

THE QUANTUM REGIME OPERATION OF DIELECTRIC DEVICES

The common approach in Quantum Optics (Garrison and Chiao [1]) for the prediction and explanation of experimental outcomes employs global quantum states which describe the distribution of a large ensemble of measurements. These quantum states, or wavefunctions associated with the state density operator, are independent of the position and time of each of the many measurements.

In this way, the explanation of the measured outcomes appears to confirm the concept of quantum nonlocality leading to the assumption of quantum interference between probability amplitudes which are complex values. It is suggested that a lack of information about the propagation pathway of one photon at any given time, between the source and the photodetector, underpins the quantum interference.

Nevertheless, one single photon entering a dielectric device such as a beam splitter or an optical fibre, will be deflected from its straight-line propagation by the quantum Rayleigh scattering.

Additionally, the spatial distribution of one photon is assumed to be generated by a superposition of Fourier components of a wave packet of which only one single component can exist at any given time. As a result, mysterious and counter-intuitive quantum processes are alleged to come about.

Single-photon sources (SPSs) would be a crucial component of quantum optic schemes for the processing and transmission of data or information (Hepp *et al*. [2]); (. Lodahl *et al*. [3]). The performance of SPSs is assessed by means of intensity correlation with a Hanbury Brown and Twiss (HBT) measurement, and two-photon coherence properties are specified with a Hong-Ou-Mandel (HOM) setup. Nevertheless, it is the rather questionable definition of a single photon per radiation mode that gives rise to the optical illusion of single photon interference. A typical experiment (Schneider and LaPuma [4]) is set up based on "… a figure of merit, the average photon occupancy, defined as the incident photon rate in photons per second times

the transit time (length divided by the speed of light) of the interferometer. For our nine-orders of magnitude attenuation, the average photon occupancy in the interferometer is approximately 10^{-2} photons." However, it is the number of photons present in the same group that is physically meaningful rather than disparate photons reaching the photodetector at different times.

The physical process of two optical waves interfering with each other – at the detection stage – can enhance or diminish the photon-dipole interaction of photon absorption.

In a 1999 review paper Mandel [5] wrote: "…about the quantum state of a system: in an experiment the state reflects not what is actually known about the system, but rather what is knowable, in principle, with the help of auxiliary measurements that do not disturb the original experiment. By focusing on what is knowable in principle, and treating what is known as largely irrelevant, one completely avoids the anthropomorphism and any reference to consciousness that some physicists have tried to inject into quantum mechanics. "[5, p. S279]. Therefore, in line with the concept of knowable elements of the experimental configuration suggested by Mandel, this Chapter identifies a range of physical processes that impact significantly on the experimental outcomes and their interpretations.

In the quantum regime of one photon per radiation mode and only one mode being present at any given time at the photodetector, the photon-photon interference cannot take place and it is replaced, *mathematically*, by probability amplitude-based interference. Yet, the photodetection is induced by the intrinsic fields of photons for each individual measurement included in the overall distribution, and the photonic intrinsic fields were derived in Chapter 3. Additionally, the unavoidable parametric amplification of spontaneously emitted photons was identified in Chapter 4.

Recent developments in the integration of photonic devices for quantum information processing [2-3] are characterized by their capability to generate two-photon destructive interference for temporally overlapping– but spatially separate – indistinguishable photons, which is commonly known as the Hong-Ou-Mandel (HOM) dip [1]. The reduction in the counting rate of coincident detection of photons at two spatially separated photodetectors is explained by opposite sign amplitudes for the probabilities of detecting each photon pair after having been reflected or transmitted by a beam splitter. Yet, with only one pair of photons present in the experimental setup, at any given time, the two types of detection cannot take place simultaneously.

This Chapter deals with the quantum regime operation of dielectric devices which are commonly used in various experiments such as beam

splitters of various configurations, interference filters, and "single" photon sources.

5.1 The Role of the Rayleigh Quantum Scattering

The core element of the photonic coincidence measurements is a symmetric beam splitter (BS) which provides two alternative pathways – A and B – for *one single photon* of number state $|1\rangle$ entering the beam splitter to reach a photodetector. When the two branches are brought jointly to the same detecting area, the emerging state describing an *ensemble* distribution would be (Walls [6]):

$$|\Psi\rangle_{out} = (|1\rangle_A |0\rangle_B + |0\rangle_A |1\rangle_B) / 2^{1/2} \tag{5.1}$$

giving rise to a *mathematical*, non-vanishing interference term, in the form of

$$\langle \hat{a}^{\dagger}_A \hat{a}_B \rangle = Tr (\rho \hat{a}^{\dagger}_A \hat{a}_B) \neq 0 \tag{5.2a}$$

$$_{out}\langle \Psi | \hat{a}^{\dagger}_A \hat{a}_B | \Psi \rangle_{out} = ({}_A\langle 0|_B \langle 0|) (|0\rangle_A |0\rangle_B) = 1 \tag{5.2b}$$

where the density matrix operator is $\rho = |\Psi\rangle_{out\,out}\langle\Psi|$, and the photon creation and annihilation operators are, respectively, $\hat{a}^{\dagger}$ and $\hat{a}$ of the two propagating modes. "The observed intensity pattern results from the interference of the probability amplitudes of a single-photon to take either of two possible paths" (Walls [6]). However, some physical contradictions arise: As $\hat{a}^{\dagger}_A$ and $\hat{a}_B$ operate simultaneously on mutually exclusive states, $|1\rangle_A |0\rangle_B$ and $|0\rangle_A |1\rangle_B$, the operator $\hat{a}_B$, acting to the right, absorbs a photon, while a second photon needs to be absorbed by $\hat{a}^{\dagger}_A$ as it acts to the left. Therefore, the two photons are associated with the mixed state of the ensemble of measurements, but they reach the beam splitter and the photodetector at separate times.

Any probability amplitude of a quantum event should be evaluated from wavefunctions that reflect the physical reality. Discarding temporal information – which becomes a lack of information – about the propagation pathway of a single photon does not create a physical effect; it can only mask or obscure the existence of physical interactions.

One such overlooked process is the quantum Rayleigh spontaneous emission (QRSE) in a dielectric medium, which scatters and replaces photons and entangled photons with independent ones (Vatarescu [7]).

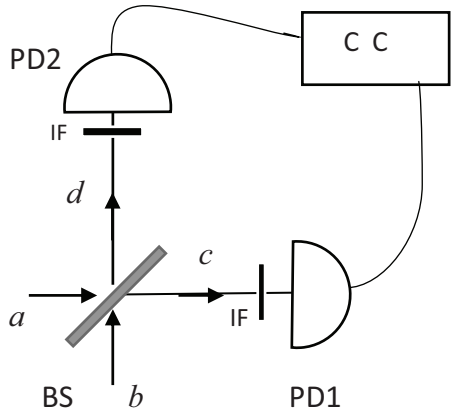

Fig. 5.1 The HBT detection setup ($b = 0$). The HOM setup ($b \neq 0$); BS beam splitter; C C coincidence counting of photons; PD photodetector; IF interferometric filter.

A single photon cannot propagate in a straight line because of the QRSE. Only a group of monochromatic photons propagating together can maintain their line of propagation and properties because the absorbed photon may be recaptured through stimulated emission by the other photons in the group.

A beam splitter does not conserve the number of photons passing through it because of the QRSE. For example, three photons entering through one input port of the beam splitter (BS) are split at the dividing dielectric interface with two photons being reflected and one transmitted to the output ports of the BS. The latter photon will most likely be scattered randomly by QRSE and will not emerge from the second output port. As a result, the HBT measurement will indicate no coincidence for zero-time delay even though a few photons were initially impinging onto the beam splitter.

5.1.1. The pure quantum state of individual measurements

In the case of an HBT measurement with a stream of single photons launched into one of two inputs *a* or *b* of a lossless cubic prism beam splitter (BS), illustrated in Fig. 5.1, the outgoing annihilation operators from ports *c* and *d* are conventionally given by [1]:

$$\hat{a}_c = r\,\hat{a}_a \quad \text{and} \quad \hat{a}_d = t\,\hat{a}_a, \tag{5.3a}$$

or

$$\hat{a}_c = t\,\hat{a}_b \quad \text{and} \quad \hat{a}_d = r\,\hat{a}_b, \tag{5.3b}$$

with the reflection and transmission coefficients $|r|^2 = |t|^2 = 0.5$ and a relative phase of $\varphi_r - \varphi_t = \pm\pi/2$. With an input state $|\Psi\rangle_{in}$, the *ensemble* probability P of each HBT detector recording a single photon is [1]:

$$|\Psi\rangle_{in} = |1\rangle_a\,|0\rangle_b \tag{5.4a}$$

$$P = {}_{in}\langle\Psi|\,\hat{a}_j^{\dagger}\,\hat{a}_j\,|\Psi\rangle_{in} = |r|^2 = |t|^2 = 0.5 \tag{5.4b}$$

where $j = c$ or d. If the two output states are combined to interfere at one photodetector, then the joint detection probability is given by:

$$P_{joint} = {}_{in}\langle\Psi|\,(\hat{a}_c^{\dagger} + \hat{a}_d^{\dagger})\,(\hat{a}_c + \hat{a}_d)\,|\Psi\rangle_{in} = |r + t|^2 \tag{5.5}$$

and the interference term is $2|r||t|\cos(\varphi_r - \varphi_t) = 0$. The relative phase condition is arbitrarily chosen – without any physical mechanism being identified – in order to comply with the quantum interference postulate of adding the complex probability amplitudes for alternative quantum trajectories. If the BS is replaced with a symmetric optical waveguide Y-junction, then physically there would be no phase difference and the probability would exceed unity.

Another type of operator transformation by the BS has been suggested (Kuhn and Ljunggren [8]; Reiserer and Rempe [9]) with an output of

$$\hat{a}_c = -r\,\hat{a}_a \quad \text{and} \quad \hat{a}_d = t\,\hat{a}_a \tag{5.6a}$$

$$\hat{a}_c = t\,\hat{a}_a \quad \text{and} \quad \hat{a}_d = r\,\hat{a}_a \tag{5.6b}$$

For $r = t = \sqrt{0.5}$, the probability of one photon detection over the ensemble becomes for the first option $P_{joint} = 0$, which is physically impossible.

Probabilities of a quantum event, such as photo-detection of a photon, are determined from a large ensemble of measurements carried out on identically prepared systems. Photonic *ensembles* for an HBT configuration will be described by a time-independent mixed state

$$|\Psi\rangle_{en} = \sqrt{p_\alpha}\;|1\rangle_A\,|0\rangle_B + \sqrt{p_\beta}\;|0\rangle_A\,|1\rangle_B \tag{5.7}$$

where the two ensemble distribution probabilities satisfy: $p_{\alpha} + p_{\beta} = 1$. For this state, the interference term may be non-zero [3].

By contrast, a *single* HBT measurement will be represented by a time-dependent pure quantum state

$$|\Psi(t)\rangle_m = \alpha(t)\,|1\rangle_A\,|0\rangle_B + \beta(t)\,|0\rangle_A\,|1\rangle_B \tag{5.8}$$

with $|\alpha(t)|^2 + |\beta(t)|^2 = 1$, and the two *mutually exclusive* options, for one measurement, are:

$$|\alpha(t)| = 1 \quad \text{and} \quad |\beta(t)| = 0 \tag{5.9a}$$

or

$$|\alpha(t)| = 0 \quad \text{and} \quad |\beta(t)| = 1 \tag{5.9b}$$

Each HBT measurement indicates, at any given time, the existence of a photon in one of two branches and the *absence* of a joint interference term. These inconsistencies are eliminated in this Chapter with a field-based approach, as the pure state describes the physical reality. The intrinsic fields of photons were presented in Chapter 3.

5.1.2. The Hong-Ou-Mandel experiments

Following Mandel [5],

> "Let us consider the quantum state $|\Psi\rangle$ of the photon pair emerging from the beam splitter (BS). With two photons impinging on the BS from opposite sides there are really only three possibilities for the light leaving BS: (a) one photon emerges from each of the outputs 1 and 2; (b) two photons emerge from output 1 and none emerges from output 2; (c) two photons emerge from output 2 and none emerges from output 1. The quantum state of the beam-splitter output is actually a linear superposition of all three possibilities in the form
>
> $$|\Psi\rangle = (|R|^2 - |T|^2)\,|1\rangle_1\,|1\rangle_2 +$$
>
> $$+ \sqrt{2}\,i\,R\,T\,|^2\,(|2\rangle_1\,|0\rangle_2 + |0\rangle_1\,|2\rangle_2)$$
>
> where R and T are the complex beam-splitter reflectivity and transmissivity."

But, the possibility of other physical processes is ignored.

The assumptions made in relation to an optical beam splitter – operating in the quantum regime – would have the total number of photons entering the beam splitter input ports equal the number of photons emerging from the two output ports, leading to a unitary transformation for the input-output relation [1] of the field operators and a $\pm\pi/2$ phase difference between the coefficients *R* and *T*.

However, the quantum Rayleigh conversion of photons presented in previous Chapters may give rise to additional output states, such as: $|0\rangle_1 |0\rangle_2$, $|1\rangle_1 |0\rangle_2$, and $|0\rangle_1 |1\rangle_2$ as photons are absorbed and spontaneously re-emitted, randomly, and, most likely, not in the direction of interest. The Hamiltonian of interaction between the electric dipoles and the optical field is [7]:

$$\hat{H} = \kappa \left(\hat{d}^{\dagger} \cdot \hat{a} + \hat{d} \cdot \hat{a}^{\dagger} \right) \tag{5.10}$$

where $\hat{d}$ is the electric dipole operator raising the atomic electron from one level to the next, and $\hat{a}$ is the photon annihilation operator, with $\hat{a}^{\dagger}$ its conjugate operator, the photon creation operator. The optically linear susceptibility $\chi^{(1)}$ is included in the spatial coupling coefficient κ.

The absorption of one photon through quantum Rayleigh conversion leads to the disappearance of an entangled state, that is:

$$\hat{a}_1 \left(|0\rangle_1 |0\rangle_2 + |1\rangle_1 |1\rangle_2 \right) = |0\rangle_1 |1\rangle_2$$

which is a product state. A similar annihilation occurs for the second photon. Alternatively, the dipole-field interaction of absorption projects the state onto the zero-photon state:

$$_1\langle 0 | \hat{a}_1 |1\rangle_1 |1\rangle_2 = |1\rangle_2$$

resulting in one single photon surviving as soon as the entangled pair was created in a parametric spontaneously down-converted emission in an optically nonlinear crystal. Additionally, unless two state functions or relevant operators overlap in the space-time of their configuration, i. e. $f_1(\boldsymbol{r}, t) \neq 0$ and $f_2(\boldsymbol{r}, t) \neq 0$, their product will be zero, preventing any interference.

In a nonlinear crystal pumped, e.g., with a continuous wave (cw) and for frequency down-converted photons of angular frequencies satisfying $\omega_s + \omega_i = \omega_p$, the gain-providing medium generating the spontaneous emission, will also amplify the initially single photons of the signal and the idler, particularly so in the direction of wavevector matching conditions. As a result, the commonly assumed one single photon output does not, in reality, physically happen. At least several photons will be associated with

each individual and discrete electronic "click". The gain coefficient of such amplification and the relative phase change are found from eqs. (4.6) to be:

$$g_{1;2} = -\kappa_{1;2}\sqrt{N_3}\ \sin\theta \qquad (5.11a)$$

$$\frac{\partial}{\partial z}\theta = -(\kappa_1 + \kappa_2)\sqrt{N_3}\cos\theta \qquad (5.11b)$$

after setting $N_1 = N_2 << N_3$ and recalling the phase pulling effect that will lead to $\theta = -\pi/2$.

Based on the analysis of (Glauber and Lewenstein [10]), with the Fresnel formulas for the optical reflection and transmission coefficients corresponding to probability amplitudes of the two events, the photonic conservation would apply only to one interface between two dielectric media. As additional internal reflections inside the glass plate of a beam splitter – see Fig. 5.2 – would take place, the assumption of photon number conservation is questionable. Furthermore, because of the quantum Rayleigh conversion or coupling of photons occurring inside a dielectric medium (Vatarescu [11]), one single photon can only be re-emitted spontaneously in a random direction, preventing a straight-line propagation. Only a group of photons propagating together can maintain their direction of propagation and characteristics through stimulated emission induced by the other photons which are not temporarily absorbed and re-emitted.

We can apply the Fresnel formulas if a pure state vector, or wavefunction, can be identified for the optical field – measured instantaneously – of the time-varying photonic wavefront, i.e., its amplitude in terms of the flux of photons and its phase. Such a function was developed in Chapter 3, taking the form of

$$|\Psi_n\rangle = (|n\rangle + |n-1\rangle)/\sqrt{2}$$

and delivering, classically compatible, *c* - number values for observable expectation values (Vatarescu [12]).

A pure state corresponds to one single measurement (Breitenbach *et al*. [13]: (Fano [14]) whereas a mixed state describes the statistical distribution of an ensemble of measurements [14]. A photonic wavefront carries a number of photons across a plane hosting dipoles and its duration will be determined by the response time of the photon-dipole interaction [13].

The physical process of quantum Rayleigh conversion of photons (QRCP) is associated with the real part of the first-order optical susceptibility and involves a group of electric dipoles interacting simultaneously with two photonic wavefronts carrying an arbitrary number

of photons across a plane over a short time $\Delta t \rightarrow 0$. The excited dipoles will emit either spontaneously or stimulatedly, depending on the circumstances. The spontaneous emission will affect the operation of dielectric interface-based beam splitters, while the stimulated emission will be active in a fibre-optic beam splitter configured as an optical directional coupler.

A mixed state of one-photon excitation as presented by Smith and Raymer [15, p. 8] is commonly used to describe the extent of a photon in space and time, but this is physically impractical for the description of the dipole-photon interactions because the photon wave packet $|1\rangle_{j,\sigma}$ describes a spectral superposition of temporally separate "single" photons associated with an output-measured spatial- and temporal-localized packet distribution which is time-independent. "An example is the deterministic generation of a single photon from an atom in a cavity-QED system. If the packet is dispersed spectrally by a prism and detected by an array of photon counters, only one counter will click, although which one clicks will be random. Such a state is expressed as

$$|1\rangle_{j,\sigma} = \int d^3k \, U_j^{(\sigma)}(\mathbf{k}) \, |1\rangle_{\mathbf{k},\sigma}/(2\pi)^3$$

where $|1\rangle_{j,\sigma}$ is a state with a single excitation having particular monochromatic wave vector-polarization state labelled by the pair ($\mathbf{k}$, σ). We see that the function $U_j^{(\sigma)}(\mathbf{k})$ fully specifies the state." [15, p. 8]. This state is of no utility for evaluating the optical field involved in a dipole-photon interaction as the expectation values vanish, i.e., ${}_{j,\sigma}\langle 1| \, \hat{a} \, |1\rangle_{j,\sigma} = 0$. For the single-photon wave packet, only one radiation mode is taking part in the detection or photon coupling processes. Yet, as derived in Chapter 3, an intrinsic photonic field distribution is carried by each (interacting) photon without any dependence on the measured statistical distribution of the ensemble of the mixed state.

The intrinsic field of one photon is neither an infinite plane wave, nor a wave packet (Mandel [5]) composed of an overall distribution of propagation wavevectors measured at the output as suggested in (Smith and Raymer [15]). Physically meaningful longitudinal and transverse distributions were derived in Chapter 3 based on the intrinsic field of photons.

The spectral expansion of the global function of the single photon mixed state in the case of a product state of two parametrically down-converted photons is equally physically questionable (Walborn *et al*. [16]; Schneeloch and Howell [17]). Once again, a global superposition of single photons – emitted one at a time – in the form of a mixed state containing contributions

from temporally and spatially separate measurements is a mathematical construct without any physical justification, leading to impossible and counterintuitive theoretical conclusions.

The interactions associated with quantum Rayleigh conversions of photons require a wavefunction capable of delivering transient or instantaneous expectation values for a pure state. These elements will underpin the analysis of various types of beam splitters, and interference filters in the following Sections.

5.2 Interference Patterns between Dynamic and Coherent Number States

Another useful effect is the interference between two waves reaching a photodetector. In the context of this analysis, one obtains that, in so far as localized and instantaneous detection of photons of two dynamic and coherent number states is concerned, the photocurrent I_{ph} generated by the interference output of a balanced homodyne detector is calculated by combining the expectation values of the quadrature field operators given in equality (3.22) of Chapter 3 to obtain:

$$\langle I_{ph}(t)\rangle = K\,(\langle Q_1\rangle + \langle Q_2\rangle)^2 = K\,[\,N_1\cos^2(\xi_1) + N_2\cos^2(\xi_2) + \\ + 2\sqrt{N_1 N_2}\cos(\xi_1)\cos(\xi_2)\,] \qquad (5.12)$$

with the constant of proportionality K corresponding to the quantum efficiency of photon-to-electron conversion. The phases are defined by $\xi_j = \omega_j\, t - \beta_j\, z - \varphi_j$ for j=1 or 2.This approach of making use of initially evaluated expectation values links the quantum regime to the classical one (Mandel and Wolf [18]). After time-averaging over a large number of optical frequency periods, namely, with the averaging time interval T satisfying $2\pi/\omega_j << T << 2\pi/|\omega_1 - \omega_2|$ we find that $\langle \cos^2(\xi)\rangle = 1/2$ and $\langle \cos(\xi_1 + \xi_2)\rangle = 0$, as well as $\langle \sin\xi\rangle = 0$, to retrieve the conventional interference pattern:

$$I(t)_{ph} = \frac{K}{2}\,[N_1(t) + N_2(t) + \\ + 2\sqrt{N_1(t)N_2(t)}\cos(\xi_1(t) - \xi_2(t)] \qquad (5.13a)$$

$$\langle I(t)_{ph}\rangle = \frac{K}{2}\,\langle\, N_{tot}(t)\,[1 + \sigma\,\Gamma\cos(\xi_1(t) - \xi_2(t)]\,\rangle \qquad (5.13b)$$

$$\langle N(t)\rangle = \frac{1}{T}\int_{-T/2}^{T/2} N(t)\,dt \qquad (5.13c)$$

$$\sigma = \frac{2\sqrt{N_1 N_2}}{N_1 + N_2}\,\hat{\boldsymbol{e}}_1 \cdot \hat{\boldsymbol{e}}_2\,; \qquad \Gamma(\tau) = \frac{\int_0^T f_{ph}(t)\, f_{ph}(t+\tau)dt}{\int_0^T f_{ph}^2(t)\;dt} \qquad (5.13d)$$

$$N_{tot}(t) = N_1(t) + N_2(t) \qquad (5.13e)$$

where $\hat{\boldsymbol{e}}_j$ specifies the polarisation of the group of photons, and the definition of Γ follows from the longitudinal profile of photons derived in eq. (3.35). Equality (5.13*b*) will be applied to two-detector correlations in the following Section. Thus, the formalism of Chapter 3 based on the intrinsic field of photons leads to eqs. (5.13) enabling a smooth transition between the quantum and classical regimes for any level of optical power and any related phase. The question of measured variances induced by system fluctuations will be addressed later in this Chapter.

5.3 The Beam Splitter

The quantum regime of photonic interference would involve only one photon per radiation mode (Mandel [5]). Yet, one single photon propagating by itself, in a dielectric medium, will not follow a straight line inside a dielectric medium because of the quantum Rayleigh spontaneous emission. Only a group of monochromatic photons propagating together can maintain a straight line of propagation as a photon absorbed by an electric dipole will be immediately recaptured through stimulated emission by the other photons in the group.

The appearance of temporarily discrete groups of photons in the process of parametric down-conversion is due to the unavoidable amplification of spontaneously emitted photons, particularly so, in the phase-matching direction. Such optical signals are best described by means of the mixed time-frequency (or Wigner-type) spectrum (Cohen [19]), with the frequency amplitude itself being a function of time, i. e., $S(\omega, t)$ specifying, in other words, a time-varying number of monochromatic photons being carried simultaneously by a photonic wavefront.

The analytic elements derived in the previous Sections will be applied hereafter. These elements include the wavefunctions of the dynamic and coherent number states which deliver the correct expectation values for the number of photons carried by a photonic wavefront and its associated complex amplitude, as derived in Chapter 3, eqs. (3.22). Equally, the optical

field profile of a group of photons is shown in eqs. (3.34) and (3.37) to be independent of the type of source that emitted them.

Given a photonic optical field, the Fresnel coefficients of reflection and transmission can be interpreted as probability amplitudes for the respective effects at a dielectric boundary [10]. At least three types of beam splitters can be identified: the glass plate of Fig. 5.2, the cubic prism of Fig 5.4, and the optical waveguide directional coupler composed of optical fibres (Agnesi *et al.* [20]; Semenenko *et al*. [21). Their operations involve the quantum Rayleigh spontaneous and stimulated emissions.

5.3.1 The glass plate beam splitters and the HOM dip

For a plate beam splitter sketched in Fig. 5.2, the primary reflected and transmitted optical fields will lead to the transformation:

$$\hat{a}_c^\dagger = -r_{01}\hat{a}_a^\dagger + t_{01}\, t_{10}\, \hat{a}_b^\dagger \tag{5.14a}$$

$$\hat{a}_d^\dagger = t_{01}\, t_{10}\, \hat{a}_a^\dagger + t_{01}\, r_{10}\, t_{10}\, \hat{a}_b^\dagger \tag{5.14b}$$

where the subscripts of the reflection r and transmission coefficients t indicate the boundary interface, with the first subscript corresponding to the incoming direction of the photons.

To illustrate an application of this approach, two groups of photons generated as the signal (s) and idler (i) waves in a parametric down-conversion are impinging, from opposite sides, onto a glass plate operating as an optical beam splitter which is placed in the xy plane - see Fig.5.2. With the upper boundary used as the synchronization place for the two groups, i.e. $\tau = 0$, the output field operators are:

$$\hat{a}_c = -\, r_s\, \hat{a}_s + t_i\, \hat{a}_i \tag{5.15a}$$

$$\hat{a}_d = t_s\, \hat{a}_s + r_i\, \hat{a}_i \tag{5.15b}$$

with reflection (r) and transmission (t) coefficients identified by the type of photons. The relative phases of these photonic wave fronts are:

$$\theta_{sr}(t,\tau) = -\omega\,\tau + \varphi_s(t) - \pi \tag{5.16a}$$
$$\theta_{it}(t) = \varphi_i(t) + \gamma \tag{5.16b}$$
$$\theta_{st}(t) = \varphi_s(t) + \gamma \tag{5.16c}$$
$$\theta_{ir}(t,\tau) = \omega\,\tau + \varphi_i(t) + 2\gamma \tag{5.16d}$$

where the random phases of the spontaneously emitted photons are denoted by $\varphi(t)$ and γ is the phase added during one transit propagation between the boundaries of the beam splitter and a $(-\pi)$ phase shift is due to the upwards reflection from a higher refractive index.

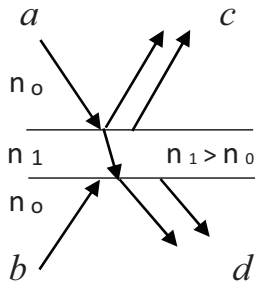

Fig. 5.2 A typical glass plate beam splitter. Photons arrive simultaneously at the upper dielectric boundary.

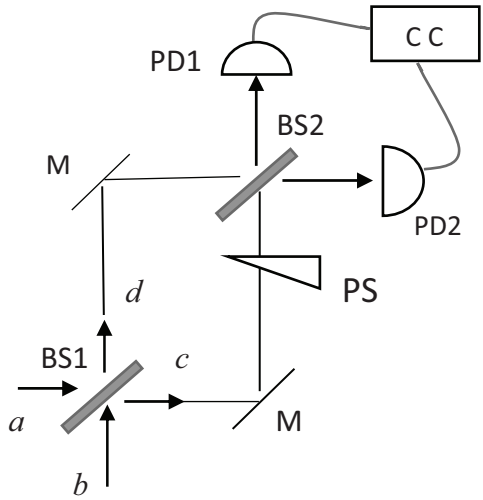

Fig. 5.3 Correlation setup for two intensities generated at two separate photodetectors with a Mach-Zehnder configuration. BS beam splitter; M mirror; PS phase shifter; PD photodetector; CC coincidence counting of photons.

Moving the beam splitter in the vertical direction will bring about a time delay $\pm\tau$ between the two wavefronts reaching the same photodetector – see Fig. 5.1. The number of photons $N_j(t)$ detected by photodetector j =1; 2 is

evaluated from the interference pattern of the instantaneously measured flux of photons presented above in eqs. (5.13):

$$N_j(t) = \frac{K}{2}\,[N_{sj}(t) + N_{ij}(t) + \\ + 2\sqrt{N_{sj}(t)N_{ij}(t)}\,cos[\theta_{sj}(t) - \theta_{ij}(t)] \qquad (5.17)$$

where the phases are given by (5.16 *a-d*), e. g., $\theta_{sl}(t) = \theta_{sr}(t, \tau)$ and $\theta_{il}(t) = \theta_{ir}(t, \tau)$. The inline letter *t* denotes time.

The correlation function $C_{12}(\tau)$ for the coincidence counting of photons is specified by the following averaging relations, with reference to Fig. 5.1:

$$C_{12}(\tau) = \langle N_1(t)\, N_2(t + \tau)\rangle \qquad (5.18a)$$

$$\langle N_1(t)\, N_2(t + \tau)\rangle = \frac{1}{T}\int_{-T/2}^{T/2} N_1(t)N_2(t + \tau)\, dt \qquad (5.18b)$$

$$\langle \cos\theta(t) \cos\theta(t + \tau)\rangle = \\ = \frac{1}{T}\int_{-T/2}^{T/2} \cos\theta(t) \cos\theta(t + \tau)\, dt \qquad (5.18c)$$

The coincidence counting of photons for the transient interference patterns of the two separate photodetector intensities, over the coincidence time interval *T* (a few ns) is derived, after denoting the total number of photons reaching each photodetector as $N_{oj} = N_{js} + N_{ji}$, to be:

$$C_{12}(\tau) = N_{01}\, N_{02}[\,1 + \sigma_1\sigma_2\,\Gamma_1\Gamma_2\, cos\,\Theta\,] \qquad (5.19a)$$

$$\sigma_j = \frac{2\sqrt{N_{js}N_{ji}}}{N_{js} + N_{ji}} \qquad (5.19b)$$

$$\Gamma_j(\tau) = \frac{\int_0^T f_{ph}(t)\, f_{ph}(t + \tau_j)dt}{\int_0^T f_{ph}^2(t)\, dt} \qquad (5.19c)$$

for photodetector $j = 1$ or 2, and the normalised overlap integral Γ_j involves the longitudinal profile f_{ph} of eq. (3.35) specifying the optical field

distribution of one photon as a mixed time-frequency distribution [19], to be compared to the conventional approach of a Fourier transform of a spectral distribution of an ensemble whose constituent elements arrive one at any given time. This latter mathematical superposition is physically impossible.

With the phase difference Θ for the intensity correlation given by

$$\Theta = [\theta_{sr} - \theta_{it}] - [\theta_{st} - \theta_{ir}] = (\omega_i - \omega_s)\,\tau - \pi \qquad (5.20)$$

there are two statistical possibilities for the random phases φ_s and φ_i of the spontaneously emitted photons. These two random phases can interchange values without affecting the result, and the cosine term 0.5 *cos* Θ of the expansion of the cosine products

$$cos\,(\alpha)\,cos\,(\beta) = 0.5\,[cos\,(\alpha + \beta) + cos\,(\alpha - \beta)]$$

should be counted twice when calculating, "classically", the correlation function $C_{12}(\tau)$ of eq. (5.18).

From (5.20), $\Theta = -\pi$ for $\tau = 0$, and with equal numbers of photons in the interfering waves, so that, $\sigma_1 = \sigma_2 = 1$, we find from (5.18) a vanishing correlation $C_{12}(0) = 0$, which corresponds to the Hong-Ou-Mandel (HOM) dip (Hong *et al*. [22]; Ou and Mandel [23]).

Therefore, there is no need for entangled photons – apparently created by the beam splitter – which transcend time and space to have their probability amplitudes somehow interfere in order to explain the coincidence counting of photons by two separate photodetectors. The only requirement is that the two groups of photons are split between the two detectors and are synchronized at a chosen interface.

Other combinations of the relative phases Θ are possible by setting up a Mach-Zehnder interferometer configuration with two identical 50:50 beam splitters as sketched in Fig. 5.3, placing one at the input and the other at the output of the interferometer (Halder *et a*l. [24]). Basically, there are four waves or groups of photons reaching each of the two photodetectors. We will denote them as *s1* for the unmodulated signal wave and *s2* for the modulated signal wave, and as *i1* for the unmodulated idler wave and *i2* for the modulated idler wave.

Next, we choose, for degenerate frequencies of the signal and idler waves, the interference term $cos\,(-\omega\,\tau + \varphi_{s1} - \varphi_{s2})$ from one of the detectors and the $cos\,(-\omega\,\tau + \varphi_{i1} - \varphi_{i2})$ term from the other, and recall

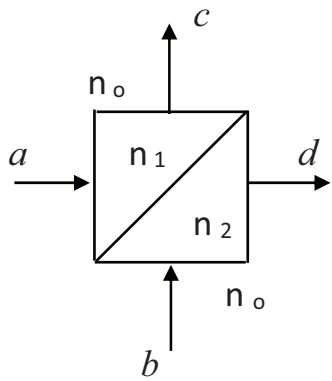

Fig. 5.4 A typical cubic prism beam splitter. Photons arrive simultaneously at the diagonal boundary interface. $n_2 > n_1 > n_0$

that the parametric phase-pulling effect (see Sections 4.2 and 4.3) leads to the condition for optimal amplification, given by eq. (4.6 *j*) as

$$\varphi_s + \varphi_i = \varphi_p + \pi/2$$

for any initial phases of weak waves, with the coherent phase of the pump photons given by φ_p. Taking all this in consideration in eqs. (5.17) leads to the statistical average value of the fourth-order in the field, numerical interference:

$$\langle cos(-\omega\,\tau + \varphi_{s1} - \varphi_{s2})\, cos(-\omega\,\tau + \varphi_{i1} - \varphi_{i2})\rangle = cos(-2\omega\,\tau) \quad (5.21)$$

which oscillates with the pump frequency (Halder *et al*. [24]). Similar expectation values may be derived for any combination of any two interference patterns, one from each photodetector, e.g. ([24]; Kim *et al*. [25-26]). It is noteworthy that the phases of the spontaneously emitted photons do not appear in the conventional quantum descriptions of two-photon beats, e.g. [22-26], but they are critical in introducing a factor of 2 to the statistical average because of the two possible options of obtaining the phase condition of maximal amplification, i.e., $\varphi_s + \varphi_i = \varphi_p + \pi/2$.

5.3.2 The cubic prism beam splitter

For a cubic beam splitter made up of two butting prisms of different refractive indexes as sketched in Fig. 5.4, the field transformation becomes:

$$\hat{a}_c^\dagger = -t_{01} r_{12}\, t_{10}\, \hat{a}_a^\dagger + t_{01}\, r_{12}\, t_{10}\, \hat{a}_b^\dagger \quad (5.22a)$$

$$\hat{a}_d^\dagger = \; t_{01}t_{12}\, t_{20}\, \hat{a}_a^\dagger + t_{02}\, r_{21}\; t_{20}\, \hat{a}_b^\dagger \qquad (5.22b)$$

The subscript 0 indicates free space, and subscripts 1 and 2 refer to the refractive index of each of the two prisms.

In the case of the cubic prism beam splitter, any two external surfaces can form a resonant cavity through reflection or transmission at the diagonal interface. The output states will be affected by photons temporarily trapped inside the beam splitter, leading to the possibility of additional quantum states, as well as quantum Rayleigh coupling of photons as described in Chapter 3.

5.3.3 The fibre-optic beam splitter

The longitudinal optical field profile of a group of monochromatic photons was derived in Chapter 3 and has the form of a Wigner spectral component $S(\omega, t)$, that is, a time-varying spectral component [19] – as opposed to a time-constant amplitude and phase of a Fourier spectrum – crossing a surface perpendicular to the wavevector of propagation.

For the optical directional coupler, the evolution of the photons is governed by eqs. (3.29) with the possibility of one waveguide capturing most of the photons resulting in an asymmetric output. The coupling coefficient κ will have to take into consideration the temporarily discrete nature of the groups of photons by including the longitudinal field profile $f_{ph}(z)$ next to the transverse spatial field f, that is:

$$\kappa = \frac{1}{\mathrm{v}_p}\frac{k_0}{2\,n}\,\Gamma_{12}\,(z_o)\iint dx\,dy\,\chi_q^{(1)}\,f_1\;f_2\,\boldsymbol{e_1}\cdot\boldsymbol{e_2} \qquad (5.23a)$$

$$\Gamma_j\,(z_{o1};z_{o2}) = \int_0^z f_{ph}\,(z-z_{o1})\,f_{ph}(z-z_{o2})\,dz \qquad (5.23b)$$

This spatio-temporal overlap is characteristic of the quantum regime of discrete groups of photons. The phase-dependent coupling of photons of eqs. (3.29) is critical in the operation of the optical fibre beam splitters by creating, with the adjustable phase difference, an asymmetric output [25-26]. Future integration of photonic components will replace the optical fibre splitter with integrated waveguides.

5.4 The Interference Filter

Experimental configurations for two-photon quantum beats, e.g. [22-26], employ interference filters in order to control the "coherence length of the photon".

The extent of the correlation fringes is determined by the coherence length of the photons, which can be shaped by an interference filter, apparently operating on the *output* spectral distribution Φ (ω_1, ω_2) of the ensemble of photons generated by an active source over a long time, such as the spontaneous parametric down-conversion mechanism [16-17].

However, from a physical perspective, a Fourier transform – or a superposition of spectral components – necessitates the simultaneous presence of the entire range of spectral components. But this is not the case when only one photon, at any given time, crosses an interference filter. A single monochromatic photon propagating through a Fabry-Perot type filter, or a Bragg refractive index grating in a waveguide, will be delayed randomly by repeated internal reflections and will acquire an integer multiple of a bias phase or time-delay. The higher the internal reflectivity of the cavity, the longer some photons may bounce back and forth inside the cavity resulting in a "longer photon" output, which is interpreted as a longer coherence length. Such optical signals are best described by means of the mixed time-frequency (or Wigner-type) spectrum, e.g. [19] with the frequency amplitude itself being a function of time $S(\omega, t)$ specifying, in other words, a time-varying number of monochromatic photons being carried by different photonic wavefronts. The time-stretching of the photonic group will be equivalent to pulse expansion for a narrower Fourier spectrum.

Thus, a group of photons entering, simultaneously, a resonant cavity of an interference filter, will exit at different times as the higher the internal reflectivity, the longer the time that some photons will bounce back and forth inside the cavity. This process will cause the initially bunched photons to spread out in time and give rise to a longer coherence length for photon coincidence counting (Halder *et al*. [27]). The wavefunction describing this output would take the form:

$$|\Phi_{out}(\boldsymbol{r},t)\rangle = \Sigma_m \, c_{\mathrm{n}}(\boldsymbol{r},t)\, f_{\mathrm{n}}(\boldsymbol{r})\, \delta\,(t - t_m)\, |\Psi_{\mathrm{n}}(\omega,t)\rangle \qquad (5.24)$$

where the times t_m specify the existence of a group of n photons at location $\boldsymbol{r}$. The pure state of a photonic wavefront is monochromatic and time-dependent as detailed in Chapter 3, whereas the overall mixed state of the

ensemble is multi-chromatic and time-independent (e.g. the bi-photon wavefunction [25-26]).

The temporal profile of the optical field carried by a photon or any instantaneous photonic wavefront should be determined from a pure quantum state wavefunction because it should be unaffected by the spectral distribution of an ensemble of measurements. However, for interference to take place, at least two coefficients c_n ($n > 0$) have to be non-zero in eq. (5.24).

5.5 The Distorted Outputs of Single-Photon Sources

Inside a resonant (micro-)cavity, the photon can bounce back and forth many times (Reiserer and Rempe [9]). With the quality of the resonator being characterized by its finesse $\mathscr{F}$, the average number of bounces is given by $\mathscr{F}/\pi$. As a result, groups of initially single photons can emerge from the resonator as each photon of a regular input sequence would undergo different numbers of reflections.

It is pointed out by (Senellart *et al*. [28]) that a quantum dot "emits a cascade of photons and a single photon is obtained only through *spectral filtering* of one emission line". "Bright sources have been obtained using micropillar cavities where the optical field is confined vertically by two distributed Bragg mirrors (DBR) and laterally by the high refractive index contrast. The mode volume is of the order of few λ^3 (wavelength)^3 and the quality factor can reach values of a few 10^5." In micro-cavities, a spontaneously emitted photon can be reflected from DBR gratings and return to stimulate the emission of another photon – thereby creating a small group of identical photons – even for several picoseconds-long exciting pulses.

A quantum dot (QD) placed in a high finesse micro-cavity of a few wavelengths long and excited with a picosecond pulse, can emit a photon spontaneously and be re-excited within the duration of the same pulse. If the photon was reflected towards the QD, stimulated emission may occur due to the small dimensions of the micro-cavity. This will result in two, or more, photons leaving the emitter simultaneously in a group, as well as a reduced lifetime of the excited state of the QD, manifesting itself as a higher decay rate overshadowing the Purcell effect.

"Resonators with small mode volume and high-quality factors (Q-factors) enhance the light–matter coupling." (R. Trivedi *et al*. [29]). However, a high Q-factor indicates a build-up of energy inside the cavity, i.e., a large number of photons do not leave the cavity after being emitted and reaching the output facet for the first time. The early photons emitted

by a QD embedded in a resonant cavity of a dielectric structure of distributed Bragg reflectors (DBRs), may be reflected towards the excited quantum dot and be amplified, thereby giving rise to time-varying spectral or intensity distributions which emerges from the "single-photon source" in the form of discrete pulses.

The lifetime of the QD excited state for spontaneous emission inside a micro-cavity can be reduced by stimulated emission induced by resonant photons bouncing back and forth inside the cavity. As a result, temporarily discrete groups of monochromatic photons will build up and be partially emitted. These, however, will be mistaken for spontaneously emitted single photons because of the photodetector's inability to resolve the number of photons.

Equally, the quantum Rayleigh stimulated emission in a dielectric medium – described in Chapter 2 and 3 – can coalesce two counterpropagating photons into one group by having one photon excite a dipole, with the other photon capturing the absorbed photon into its radiation mode through stimulated emission.

High-finesse optical cavities incorporated in an HBT measurement setup distort the temporally regular sequence of single photons because of multiple internal reflections. The emerging stream may contain groups of a few overlapping photons, e.g. five, which may be unevenly split by a beam splitter and reduced in number through quantum Rayleigh spontaneous emission, so as to generate no coincidence for a zero time-delay in an HBT measurement.

For atoms inside cavities with highly reflective mirrors, the emission rate of discrete photons is much lower than the laser pump rate, e.g., 3.6 MHz versus 80 MHz (Loredo *et al*. [30]). This can be explained by the synchronisation condition between the pumping time-interval Δt_{pump} and the average exit time-interval of photons $\Delta t_{photon\ group}$, which may be related by the following equality

$$m \times \Delta t_{photon\ group} = p \times \Delta t_{pump} + \tau_{ex} \tag{5.25}$$

where τ_{ex} is the life time of the excited state that decays through stimulated emission. The integers m and p correspond to the respective number of intervals for synchronisation.

A monochromatic pulse-like field profile, derived in Chapter 3, is represented by a mixed time-frequency structure [19]. A spectral or interference filter may delay the photon's exit from the output facet by

repeated internal reflections, thereby spreading out the exit times of photons from an input group.

A sequence of groups of photons (pulses containing a low number of monochromatic photons) temporarily separated, can be transformed into a quasi-continuous stream (or wave) of photons by means of interference filters. A high internal reflectivity will retain, repeatedly, more photons inside the cavity than those exiting, for additional round-trip propagations, which will spread out the initial monochromatic pulse. The higher the number of photons inside a dielectric cavity hosting a quantum dot, the more likely it is that the quantum Rayleigh coupling interactions will create larger groups of photons, even for counter - propagating photons. As a result, the triggered clicks at the detector will count a lower number of photon groups rather than individual photons.

When another group of photons enters the interference filter of the DBR, the relative phase will determine the direction of photon- coupling through the phase-dependent quantum Rayleigh conversion of photons (QRCP). As a result, an output continuous wave beam is generated which can serve as an unmodulated or reference wave for interference.

5.6 Conclusions

The probability amplitude approach to photonic quantum interference leads to physical contradictions which are eliminated by using the intrinsic field of photons. The role of the quantum Rayleigh scattering of photons rules out single-photon propagation in a straight-line, raising serious doubts about the conventional interpretation of HOM experiments. These are explained physically, in a meaningful manner, by using the intrinsic fields of photons derived from the dynamic and coherent number states. Various types of beam splitters are analysed in this way.

The operation commonly used for extending the coherence length of photons by means of interference filters is explained in the context of multiple internal reflections of groups of monochromatic photons whose exit times are stretched over a period of time. These photons can also stimulated additional emission generating multi-photon discrete pulses.

References

1. J. C. Garrison and R.Y. Chiao, *Quantum Optics*, Oxford University Press, 2008.

2. S. Hepp, M. Jetter, S. L. Portalupi, and P. Michler, "Semiconductor Quantum Dots for Integrated Quantum Photonics", Adv. Quantum Technol., **2**, 1900020, (2019)..
3. P. Lodahl, S. Mahmoodian, and S. Stobbe, "Interfacing single photons and single quantum dots with photonic nanostructures", Rev. Mod. Phys., **87**, 347 – 400, (2015).
4. M. B. Schneider and I. A. LaPuma, "A simple experiment for discussion of quantum interference and which-way measurement ", Am. J. Phys. **70**, 266-271, (2002).
5. L. Mandel, "Quantum effects in one-photon and two-photon interference*,"* Rev. Mod. Phys*.,* **71**, S274-S282, (1999).
6. D. F. Walls, "A simple field theoretic description of photon interference", Am. J. Phys., **45**, 952 - 956, (1977).
7. A. Vatarescu, "The Scattering and Disappearance of Entangled Photons in a Homogeneous Dielectric Medium," Rochester Conference on Coherence and Quantum Optics (CQO-11), doi.org/10.1364/CQO.2019.M5A.19, (2019).
8. A. Kuhn & D. Ljunggren,"Cavity-based single-photon sources", Contemp. Phys., **51**, 289-313, (2010).
9. A. Reiserer and G. Rempe, "Cavity-based quantum networks with single atoms and optical photons", Rev. Mod. Phys., **87**,1379 – 1418, (2015).
10. R. J. Glauber and M. Lewenstein, "Quantum optics of dielectric media", Phys. Rev. A, **43**, 467- 491, (1991).
11. A. Vatarescu, "Photonic coupling between quadrature states of light in a homogeneous and optically linear dielectric medium", J. Opt. Soc. Am. B, **31**, 1741–1745, (2014).
12. A. Vatarescu, *"*Instantaneous Quantum Description of Photonic Wavefronts for Phase-Sensitive Amplification," *Frontiers in Optics/Laser Science Conference (FiO/LS),* paper JW4A.109, Washington, Sept. 2018.
13. G. Breitenbach, S. Schiller, and J. Mlynek, "Measurement of the quantum states of squeezed light," Nature, **387**, 471-475, (1997).
14. U. Fano, "Description of States in Quantum Mechanics by Density Matrix and Operator Techniques", Rev. Mod. Phys*.,* **29**, 74-93, (1957).
15. B. J. Smith and M G Raymer, "Photon wave functions, wave-packet quantization of light, and coherence theory ", New J. Phys*.,* **9**, 414-420, (2007).
16. S. P. Walborn, C. H. Monken, S. Pádua, and P. H. Souto Ribeiro, "Spatial correlations in parametric down-conversion", Phys. Rep.**, 495**, 87-139, (2010).

17. J. Schneeloch and J. C. Howell," Introduction to the transverse spatial correlations in spontaneous parametric down-conversion through the biphoton birth zone", J. Opt., **18**, 053501, (2016).
18. L. Mandel and E. Wolf, "Coherence Properties of Optical Fields", Rev. Mod. Phys., **37**, 231-287, (1965).
19. L. Cohen, "Time-frequency distributions-a review", Proc. IEEE, **77**, 941–981, (1989).
20. C. Agnesi, B. Da Lio, D. Cozzolino, L. Cardi, B. Ben Bakir, K. Hassan, A. Della Frera, A. Ruggeri, A. Giudice, G. Vallone, P. Villoresi, A. Tosi, K. Rottwitt, Y. Ding, and D. Bacco, "Hong–Ou–Mandel interference between independent III–V on silicon waveguide integrated lasers *",* Opt. Lett., **44**, 271-274, (2019).
21. H. Semenenko, P.Sibson, M. G. Thompson, and C. Erven, "Interference between independent photonic integrated devices for quantum key distribution ", Opt. Lett., **44**, 275-278, (2019).
22. Hong, C. K., Ou, Z. Y. & Mandel, L. Measurement of subpicosecond time intervals between two photons by interference", Phys. Rev. Lett., **59**, 2044–2046, (1987).
23. Z. Y. Ou and L. Mandel, "Observation of Spatial Quantum Beating with Separated Photodetectors ", Phys. Rev. Lett., **61**, 54 – 57, (1988).
24. M. Halder, S. Tanzilli, H. de Riedmatten, A. Beveratos, H. Zbinden, and N. Gisin, "Photon-bunching measurement after two 25-km-long optical fibers ", Phys. Rev. A, **71**, 042335, (2005).
25. H. Kim, S. M. Lee, and H. S. Moon," Generalized quantum interference of correlated photon pairs"*,* Sci. Rep. **5**, 9931-9936, (2015).
26. H. Kim, S. M. Lee and H. S. Moon, "Two-photon interference of temporally separated photons ", Sci. Rep. **6**, 34805-34810, (2016).
27. M. Halder, A. Beveratos, R. Thew, C. Jorel, H. Zbinden, and. N. Gisin, "High coherence photon pair source for quantum communication", New J. Phys., **10**, 023027, (2008).
28. P. Senellart, G. Solomon, and A. White, "High-performance semiconductor quantum-dot single-photon sources," Nature Nanotech., **12**, 1026- 1039, (2017).
29. R. Trivedi, K. A. Fischer, J. Vuckovic, and K. Müller, "Generation of Non-Classical Light Using Semiconductor Quantum Dots", Adv. Quantum Technol., **3**, 1900007, (2020).
30. J.C. Loredo *et al*.,"Scalable performance in solid-state single photon sources ", Optica, **3**, 433-440, (2016).

CHAPTER SIX

PHOTONIC COINCIDENCES AND CORRELATIONS

The excitation levels of an electromagnetic field were identified in Chapter 3 as the number of photons carried by an optical wavefront. In the quantum regime, a radiation mode carries one or, at most, a few photons at any given time. However, only a multi-photon excitation can maintain a straight-line propagation inside a dielectric medium where the quantum Rayleigh spontaneous emission may gradually reduce the number of photons with the possibility of having only one photon, or none, exit in the desired direction. Equally, the stimulated Rayleigh emission will preserve the physical properties of the monochromatic photons in the group.

Probability distributions are determined from an ensemble of measurements, but each non-zero measured value requires the presence of a photon. It is the photonic field that triggers the photodetector, and consequently, the interference pattern of probability amplitudes is underpinned by the intrinsic fields of photons. Therefore, the primary role is played, at the level of a single and individual measurement, by the intrinsic optical field of photons described in Chapter 3 rather than the probability amplitude which is the consequence of the field-dipole interactions involving an ensemble of measurements.

One type of experiments would have one pair of photons generated simultaneously by the same physical process – but detected separately with two photodetectors – interact with another similar pair of photons. As a result, pairs of photons generated at different times as well as detected at different times, would cancel each other out in the context of an ensemble of measurements, subject to some synchronisation conditions. This process involving no memory mechanism would transcend time, thereby creating a quantum "miracle" of nonlocality between detection coincidences of photons. This corresponds to the well-known Hong-Ou-Mandel dip.

This Chapter points out the physical flaws of such claims and provides physically meaningful explanations for the experimental outcomes involving radiation modes propagating through a dielectric medium such as

a beam splitter. Classical interference (Mandel and Wolf [1, Sec. 7.3]) can describe transient effects, whereas quantum optics is supposed to deliver expectation values of an ensemble of identically prepared systems. Yet, each measurement can be associated with a pure quantum state and the ensemble will be linked to a mixed state.

The analysis of this Chapter draws on findings of previous Chapters: 1) The quantum Rayleigh scattering of photons of Chapter 3; 2) The spatial profile of the intrinsic optical field of photons of Chapter 3 and its applications to beam splitters in Chapter 5; and, 3) The unavoidable parametric amplification of spontaneously emitted photons of Chapter 4, as well as the coalescing of initially single photons into groups of photons through the process of quantum Rayleigh stimulated emission of photons, presented in Chapter 3.

6.1 Deficiencies of the Ensemble Quantum State

A major discrepancy between the use of a global wavefunction to predict quantum probabilities, on the one hand, and the physical reality of each individual measurement which may be time- and space- dependent, on the other hand, would lead one to draw counterintuitive conclusions about the interpretation of those outcomes. An ensemble state appears to create interaction between non-overlapping states of single or individual measurements. But this interpretation arises from the lack of any spatial and/or temporal dependence of the ensemble distribution at the output of a long series of measurements.

Even in the case of "single photon" interference of probability amplitudes, two photons are required because the two optical field operators act on mutually exclusive photonic states, as explained in Section 5.1, eqs. (5.2).

The number or Fock states cannot interact with a dielectric medium because they do not deliver an optical field. Additionally, the coherent state is an ensemble-based distribution and cannot describe an instantaneous interaction which depends on the local number of photons and their local phase. Yet, these two categories of photonic states are widely used for their simplicity leading to erroneous and counterintuitive conclusions.

A particular case is the experimental configuration of a two-input and two-output beam splitter with two photodetectors measuring the discrete emerging photonic signals to determine coincidences between the electronic clicks and correlations – within a small-time interval – associated with those detections. This is illustrated in Fig. 6.1 where two input modes lead to two output combined modes.

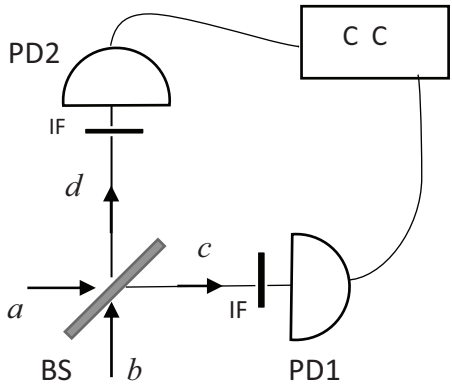

Fig. 6.1 The HBT detection setup ($b = 0$). The HOM setup ($b \neq 0$); BS beam splitter; C C coincidence counting of photon; PD photodetector; IF interferometric filter.

According to Mandel [2]:

> "The quantum state of the beam-splitter output is actually a linear superposition of all three possibilities in the form
> $| \Psi \rangle = (| R|^2 - | T |^2) |1\rangle_1 |1\rangle_2 + \sqrt{2}\, i\, (| R\, T |^2 [\, | 2 \rangle_1 | 0 \rangle_2 + | 0 \rangle_1 | 2 \rangle_2]$
> where R and T are the complex beam-splitter reflectivity and transmissivity."

While this statement is mathematically possible for an ensemble of measurements, from a physical perspective, at the level of one individual measurement this is impossible. The states $| R |^2 |1\rangle_1 |1\rangle_2$ and $| T |^2 |1\rangle_1 |1\rangle_2$ cannot cancel each other out because they do not exist *simultaneously* as only two photons are supposed to be present throughout the measurement at any given time.

As the field operators propagate through the dielectric beam splitter, the Rayleigh Hamiltonian of interaction $\hat{H}_R$ between the electric dipoles and the optical field comes into play in the form of (Glauber and Lewenstein [3]):

$$\hat{H}_R = \kappa \left(\hat{d}^\dagger \cdot \hat{a} + \hat{d} \cdot \hat{a}^\dagger \right) \tag{6.1}$$

where $\hat{d}$ is the electric dipole operator raising the atomic electron from one level to another, and $\hat{a}$ is the photon annihilation operator, with $\hat{a}^\dagger$ its Hermitian conjugate operator, the photon creation operator. The optically linear susceptibility $\chi^{(1)}$ is included in the coupling coefficient κ.

Once again, we emphasise that the absorption of one photon through quantum Rayleigh conversion – involving $\hat{H}_R$ of eq. (6.1) – leads to the disappearance of an entangled state, that is:

$$\hat{a}_1 \left(| 0 \rangle_1 | 0 \rangle_2 + | 1 \rangle_1 | 1 \rangle_2 \right) = | 0 \rangle_1 | 1 \rangle_2 \tag{6.2}$$

which is a product state. A similar annihilation occurs for the second photon. Alternatively, the dipole-field interaction of absorption projects the state onto the zero-photon state:

$$_1\langle 0 | \ \hat{a}_1 \ | 1 \rangle_1 | 1 \rangle_2 = | 1 \rangle_2 \tag{6.3}$$

resulting in one single photon surviving as soon as the entangled pair was created in a parametrically spontaneous down- converted emission in an optically nonlinear crystal.

The probability Pr over an ensemble of measurements, of joint or simultaneous detections by the two photodetectors in Fig. 6.1, in the time interval $\{t, t + \Delta t\}$ has the expression (Mandel [2]):

$$\Pr\ (\boldsymbol{r}, t) = \langle \Phi | \hat{E}_s^- (\boldsymbol{r}_1, t_1) \hat{E}_i^- (\boldsymbol{r}_2, t_2)\ \hat{E}_i^+ (\boldsymbol{r}_2, t_2) \hat{E}_s^+ (\boldsymbol{r}_1, t_1) | \Phi \rangle\ \triangle t \tag{6.4}$$

for two detectors located at $\boldsymbol{r}_{\mathrm{p}}$ (p =1, 2) and timed at t_{p}, with the integration interval $\Delta t \rightarrow 0$ tending to zero..

For two sources $j = 1; 2$ of spontaneous parametric down conversion, the composite two-photon state was given for an ensemble of measurements as (Mandel [2]):

$$| \Phi \rangle = | \Psi_1 \rangle\ | \Psi_2 \rangle\ | N_p \rangle \tag{6.5}$$

$$| \Psi_j \rangle = \frac{c_{oj} | 0\rangle|0\rangle + c_{1j}| 1\rangle |1\rangle}{\sqrt{\left| c_{oj} \right|^2 + \left| c_{1j} \right|^2}} \tag{6.6}$$

where the number state of the pump is given by $| N_{\mathrm{p}} \rangle$.

However, a single measurement of spontaneous emission into mode $\boldsymbol{k}$ will start with $c_0 = 1$ and $c_1 = 0$, and deliver either $c_{\mathrm{o}} = 0$ and $c_1 = 1$ for a successful transition, or $c_{\mathrm{o}} = 1$ and $c_1 = 0$ for no emission into the mode being measured.

The expectation value c_1 of the ensemble of measurements is derived from the formal integration of the Schrödinger wave equation to first order:

$$|\Phi\,(\boldsymbol{r},t)\rangle = -\frac{i}{\hbar}\;|\Psi\,(\boldsymbol{r},0)\rangle - \frac{i}{\hbar}\int_0^t \widehat{H}_{int}\,(\boldsymbol{r},t\,)\;dt\;\;|\Phi\,(\boldsymbol{r},0)\rangle \qquad (6.7)$$

or by solving the perturbation differential equation. The perturbation of expansion coefficients describes a sequential generation of photonic states.

$$i\hbar\frac{\partial}{\partial t}\,\mathrm{c}_{1j}\,(t) = \langle\,\Psi_j\,(t)\big|\;\widehat{H}_{int}\,\big|\,\Psi_j\,(0)\rangle\;\mathrm{c}_0(t) \qquad (6.8)$$

The Hamiltonian of interaction generating two photons from a pump photon through the second-order nonlinear susceptibility $\chi^{(2)}$ has the formal structure:

$$\widehat{H}_{int} = \iiint dx\,dy\,dz\,f_p\,f_s\,f_i\;\chi^{(2)}\left(\hat{a}_p\,\hat{a}_s^{\dagger}\,\hat{a}_i^{\dagger} + \hat{a}_p^{\dagger}\,\hat{a}_s\,\hat{a}_i\,\right) \qquad (6.9)$$

where $f_j\,(x, y, z)$ for $j = p, s, i$ is the respective spatial distribution of the related optical fields which should be evaluated from the intrinsic optical fields of photons of Chapter 3, as opposed to solutions of the Helmholtz equations (Glauber and Lewenstein [3]). The conservation of energy requires that the angular frequencies fulfil the equality $\omega_p = \omega_s + \omega_i$ and the wave vectors are linked by the relation $\boldsymbol{k}_p = \boldsymbol{k}_s + \boldsymbol{k}_i$ for optimal parametric amplification, although for spontaneous emission the electron involved in the dipole-photon interaction can contribute to the momentum conservation by moving inside its local potential of the surrounding atoms or molecule, and re-emit spontaneously in any arbitrary direction compatible with the emission pattern of an electric dipole.

For such sources, a global wavefunction $|\,\Phi\,\rangle$ labelled as a biphoton state of the signal and idler photons, was suggested for one single photon per radiation mode, which is space and time independent (Garrison and Chiao [4]):

$$|\,\Phi\,\rangle = \iint d\boldsymbol{k}_s\,d\boldsymbol{k}_i\,d\omega_s d\omega_i\,F(\,\boldsymbol{k_s},\boldsymbol{k_i}\,,\omega_s,\omega_s)\;\;|\,1_s\,\rangle\,|\,1_i\,\rangle \qquad (6.10)$$

The quantum description or representation of a single photon as a time-independent and $\boldsymbol{k}$-dependent distribution of wavefunctions $F\,(\boldsymbol{k}, \omega)$ creates an analogy with the classical structure of an optical pulse and a lateral wave front.

However, from eq. (3.6) we have for any two arbitrary indices i and j the wavefunction

$$|\Phi\,(\boldsymbol{r},t)\rangle = \;\;\Sigma_i\,\Sigma_j\;c_i\,(\,\boldsymbol{r},t)\,c_j{}^{*}(\,\boldsymbol{r},t)\,|\,S_i\;\rangle\,|\,S_j\;\rangle \qquad (3.6)$$

describing individual measurements. The composite wavefunction should have its product terms overlap in both time and space for a non-vanishing product, namely, at the same location $\boldsymbol{r}$ and the same time t both c_i and c_j are non-zero. With the signal and idler waves entering the beam splitter through different ports a and b (see Fig. 6.1), the input state is not represented physically by a product state. Rather, a superposition of states such as the following

$$|\Phi\,(\boldsymbol{r},t)\rangle = c_a\,(\boldsymbol{r}_a,t_a)\;\;|\,S_a\,\rangle + \;c_b\,(\boldsymbol{r}_b,t_b)\,|\,S_b\,\rangle \qquad (6.11)$$

is indicative of the physical reality, with the states $|\,S_j\,\rangle$ given by the dynamic and coherent number states $|\,\Psi_{\,n}\rangle = (\,|\,n\,\rangle + |\,n-1\rangle\,) / 2^{1/2}$ derived in Section 3.

A meaningful physical description is provided by the dynamic and coherent number states, taking also into consideration the unavoidable parametric amplification and the related phase-pulling effect. These effects will easily explain the "Striking, remarkable, and bizarre phenomena… of two-photon quantum interference, i.e. coincident photon counting at two separate photo-detectors" (Garrison and Chiao, Sections 10.2.1 – 10.2.3 of [4]). Nonetheless, those interpretations failed to consider the quantum Rayleigh scattering in a homogenous medium which has been extensively explained in previous Chapters and is illustrated in Fig. 6.2.

Additional views of quantum miracles associated with the two-photon experiments [2] have been expressed by Walmsley [5], namely:

> "The experiment consisted of sending two elementary particles of light photons, onto opposite sides of a piece of glass that had been coated with a thin film to give it a reflectivity of 50% (see the figure). They observed that the two photons always left by the same side at the output, though it was not possible to determine beforehand which side that would be."
>
> "The HOM phenomenon is a beautiful manifestation of the interference of a quantum field; in this case, the bosonic field associated with photons."
>
> "In their paper, Hong, Ou, and Mandel (HOM) emphasized the role of distinguishing information in determining the extent to which interference occurred, arguing that the mere presence of such information, whether measured or not, would abrogate the "bunching" effect."

This foregoing interpretation appears to make a virtue out of a lack of information about the system being observed. And it fails to even mention,

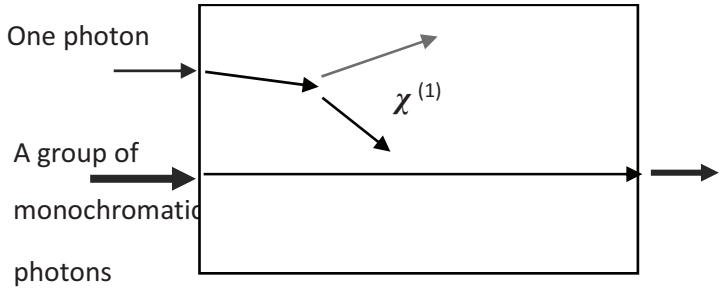

Fig. 6.2 The quantum Rayleigh scattering of a single photon in a homogeneous dielectric medium versus the propagation of a group of photons.

let alone consider, the role of the quantum Rayleigh scattering inside a dielectric medium.

The following statement made by Mandel [2] was meant to support the 'mysteries' of quantum optics, but it can also be adopted to rebut and disprove them. That statement reads [2]:

> "In an experiment the state reflects not what is actually known about the system, but rather what is knowable, in principle, with the help of auxiliary measurements that do not disturb the original experiment. By focusing on what is knowable in principle, and treating what is known as largely irrelevant, one completely avoids the anthropomorphism and any reference to consciousness that some physicists have tried to inject into quantum mechanics."

Indeed, many physically meaningful quantum processes and effects were ignored or overlooked in search of miraculous quantum phenomena.

In the following Section, these apparently time- and space- transcending phenomena will be explained by invoking well established physical interactions and processes which have been detailed in previous Chapters of this book.

6.2 The Pure State of Single Measurements

With reference to Fig.6.3, for two signal *(s)* beams and two idler (*i*) beams waves, the field operators were defined, after a beam splitter brings them jointly to a photodetector, as (Mandel [2]):

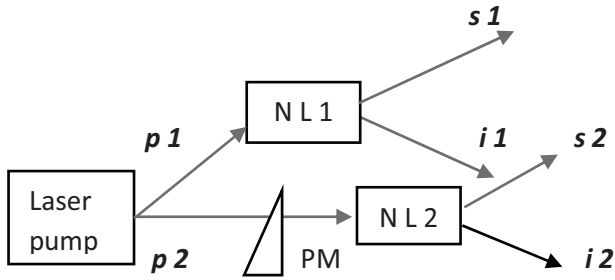

Fig. 6.3 The configuration for signal-signal interference with the idler *i1* bypassing the nonlinear crystal NL2 for interference with *i 2*. PM phase modulator.

$$\hat{E}_s^+ = -r\,\hat{a}_{s1}\,e^{i\phi_{s1}} + t\,\hat{a}_{s2}e^{i\phi_{s2}} \tag{6.12a}$$

$$\hat{E}_i^+ = \; r\,\hat{a}_{i1}\,e^{i\phi_{i1}} \; + \; t\,\hat{a}_{i2}e^{i\phi_{i2}} \tag{6.12b}$$

In a nonlinear crystal pumped with a large number of photons N_p and for frequency down-converted photons satisfying the condition of $\omega_s + \omega_i = \omega_p$, the gain-providing medium which generates the spontaneous emission, will also amplify the initially single photons, particularly so in the direction of wavevector matching conditions, even for a limited space-time overlap. Thus, the commonly assumed one single photon output does not physically happen. At least several photons will be associated with each individual and discrete electronic "click". A phase-pulling effect for each pair of photons, leading to the correlation of phases -see eq. (4.6 *j*):

$$\phi_s + \phi_i = \phi_p + \frac{\pi}{2} \tag{6.13}$$

also occurs as identified in Sections 4.2-3. So long as groups of photons coming out of the two nonlinear crystals reach the same photodetector simultaneously, a transient interference pattern occurs. Intensity first-order and second-order effects may appear provided phase correlations are generated as in eq. (6.13).

6.2.1 The second-order interference

Various options are possible when combining the signal and idler outputs of two nonlinear crystals pumped by the same laser output, as illustrated in Fig. 6.3. As in reference [1], we first consider the signal-signal interference between outputs *s1* and *s2*, drawing upon the analytic results of Chapters 3, 4 and 5.

The instantaneous photocurrent I_{ph} generated by the two signal beams of photons possessing parallel polarisations and impinging onto the same detecting area was presented in Section 5.2 as:

$$I_{ph}(t) = \frac{K_{ph}}{2} \; [N_1(t) + N_2(t) + \\ + 2\sqrt{N_1(t)\, N_2(t)}\, cos(\phi_{s1} - \phi_{s2})] \qquad (6.14)$$

The statistical average of the interference term in eq. (6.14) vanishes when integrated over one cycle $\{0, 2\,\pi\}$ because

$$\phi_{s2} - \phi_{s1} = random, spontaneously\ emitted\ photonic\ phases$$

Alternatively, for a static configuration sketched in Fig. 6.3, the only time-varying phase arises from the spontaneous emission of single photons which are amplified with a phase-pulling effect – see eq. (4.6 *j*) – leading to

$$\phi_{s2} = \phi_{p2} - \phi_{i2} + \frac{\pi}{2} \qquad (6.15a)$$

$$\phi_{s1} = \phi_{p1} - \phi_{i1} + \frac{\pi}{2} \qquad (6.15b)$$

Using these identities, we find:

$$\phi_{s1} - \phi_{s2} = \phi_{p1} - \phi_{p2} + (\phi_{i2} - \phi_{i1}) \qquad (6.16)$$

and integrating the random distribution of idlers' phases over the range $0 \leq (\phi_{i2} - \phi_{i1}) \leq 2\,\pi$, a vanishing average of the interference term in eq. (6.14) above is obtained for sampled values of the photocurrent in the context of photon counting.

Another possibility for a vanishing correlation of eq. (6.14) is to have the two optical fields reach one of the photodetectors in anti-phase, i.e. with a π-phase difference so that $E_{s1} - E_{s2} = 0$ for equal number of photons, causing the two optical fields to cancel each other out. This is, in fact, the operation of the glass plate beam splitter and is applicable to "classical" waves.

By setting up the configuration of Fig. 6.4 where the idler beam *i1* is strong enough because of the unavoidable amplification in NL1, and is injected alongside the pump *p2* into the nonlinear crystal NL2 to cause a fast

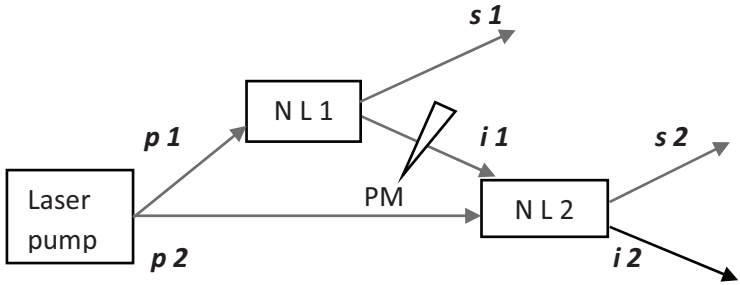

Fig. 6.4 The configuration for signal-signal interference with the idler *i 1* propagating through the nonlinear crystal NL2 alongside pump *p 2*. PM phase modulator.

phase shift of the spontaneously emitted signal photons in NL2 with very little of its own change, one finds from eqs. (4.6) and (6.15) that:

$$\phi_{i2} \approx \phi_{i1} + \Delta\phi_{i1} \qquad (6.17a)$$

$$\phi_{s2} - \phi_{s1} = \phi_{p2} - \phi_{p1} + \Delta\phi_{i1} \qquad (6.17b)$$

with $\Delta\phi_{i1}$ being the phase shift acquired by the beam *i1* as it propagates between the two nonlinear crystals through the phase shifter PM. Upon substitution into eq. (6.16), we thus find that the second-order interference of the two beams of signal photons depicted in Fig. 6.4 varies as the pump phase difference is changed. The two signal beams have their phases correlated through the seeding of the second nonlinear crystal by the idler *i1*.

6.2.2 The fourth-order interference

The case of the fourth-order interference was shown in Chapter 5, eq. (5.18) to correspond to a correlation of intensities:

$$C_{12}(\tau) = \langle I_{ph,1}(t)\, I_{ph,2}(t+\tau)\rangle \qquad (6.18a)$$

Identifying the two photocurrents of the two photodetectors, j = 1 or 2, reached by the signal beams (i_s) and the idler beams (i_i), we have from eqs. (5.18) and (5.19), the correlation function for an ensemble average of the case illustrated in Fig. 6.3 as:

$$\langle cos(\phi_{s1} - \phi_{s2})\, cos(\phi_{i1} - \phi_{i2})\rangle = \langle cos\,(\phi_{s1} - \phi_{s2} + \phi_{i1} - \phi_{i2})\rangle =$$

$$= \cos(\phi_{p2} - \phi_{p1}) \qquad (6.19a)$$

$$\phi_{s2} - \phi_{s1} + \phi_{i2} - \phi_{i1} = \phi_{p2} - \phi_{p1} + \Delta\phi_{i1} \qquad (6.19b)$$

where eq. (6.19*b*) is derived from eq. (6.13). As $\phi_{i2} \approx \phi_{i1} + \Delta\phi_{I1}$ from eq. (6.17), the fourth-order interference of eq. (6.19*a*) varies with the difference between the pump phases resulting from the phase relation of eq. (6.15) induced by the parametric amplification of weak numbers of photons, such as signal and idler spontaneous emissions. Additionally, as the two spontaneous phases ϕ_s and ϕ_i can be interchanged in eq. (6.13) or (6.15) without affecting the numerical value of the interference pattern, a factor of 2 multiplies the statistical average to obtain eq. (6.19*a*).

In both the second-order and fourth order-order interference patterns of discrete groups of photons, the statistical interference fringes are determined by the phase-pulling effect associated with the unavoidable parametric amplification of spontaneously emitted photons. The question of whether or not the observer has any information about the source of photons or their paths from the source to the photodetector is irrelevant as, at least, two photons arriving from different directions are needed to create the interference pattern, even in the case of "quantum" interference.

The statement made by Mandel in [2] that "After all, the signal photons *s1* and *s2* are emitted spontaneously and the spontaneous emissions are not really disturbed at all by the act of blocking *i1*" is physically incorrect because the seed idler wave *i1* does combine with pump *p2* to generate *s2* photons whose phase is correlated to that of *s1* through the optimal phase of eq. (6.13) for optimal amplification, as explained in Chapter 4. From Fig. 6.4 we see that for a phase shift $\Delta\phi_{i1}$ induced by a modulator placed in the path of beam *i1* before crystal NL2, a corresponding modulation of the interference pattern between *s1* and *s2* will emerge as indicated by the phase of eq.(6.19*b*). When this intensity of the interference of the signal beams is electronically multiplied by the intensity of the second idler wave, a correlation of the two separate photocurrents is recorded for properly synchronised arrivals of photons, and the correlation carries the modulation of the signals' pattern.

Another configuration known as the Franson interferometer replaces the two nonlinear sources pumped by the same laser light with one source but both the signal and the idler beams – propagating in different directions – are split into two partial beams by means of two separate Mach-Zehnder interferometers placed in their propagation paths from the source to their respective photodetector. The analysis of the coincidence counting of photons between the signal intensity and the idler intensity follows the same steps as in the case of Fig. 6.3. Once again, the unavoidable parametric

amplification is responsible for the propagation of a group of several photons per radiation mode that are needed for the photonic group to survive the transition though a dielectric medium. The initial group of photons splits into two sub-groups at the inputs to the Mach-Zehnder interferometers, and recombine at the outputs giving rise to two separate intensities which originated in the spontaneous emission of parametric down-conversion.

The two-path configuration may also be implemented by utilizing a electro-optic birefringent crystal with two orthogonal eigenstates of linear polarisations. Discrete groups of photons are generated through the unavoidable parametric amplification of a spontaneously emitted photon, or as a cluster of photons exiting an interferometric filter at the same time after bouncing back and forth for different periods of time. These discrete groups of photons which are mistaken for one photon per radiation mode, will each have their linear polarisation aligned with one of the eigenstates of the static modulator as well as the states of the beam splitter. A polarisation beam splitter, through quantum Rayleigh spontaneous emission, creates polarisation eigenstates and directs orthogonally polarised photons to separate photodetectors. When a varying voltage is applied to the electro-optic modulator that brings about a change in the optical path lengths, the beam polarisation is rotated by 45^{o} relative to the crystal's polarisation eigenmodes. As a result, the polarisation beam splitter will direct projected photons from both initial eigenstates to both photodetectors, mixing the beams and creating temporal interference patterns in each photodetector so that, over an ensemble of measurements, their correlated photocurrents will build up and be averaged.

Therefore, the Franson interferometer is no more mysterious than the HOM dip. Both are easily explained once is it realised that only groups of photons can overcome the Rayleigh scattering and propagate in a straight line in a dielectric medium.

6.2.3 The probability amplitude as a consequence of optical field detection

The second- and fourth-order, in the optical field, interferences are determined by the relation linking the spontaneous phases of the photons emitted parametrically in the nonlinear crystal as opposed to the assumption of a lack of knowledge about the propagation pathway between the source and the photodetector.

The concept of a relationship between interference and indistinguishability of optical pathways of the photons involved in the interference is a consequence that arises from the optical interference of

optical fields, which, in turn, leads to measured probabilities and associated probability amplitudes.

As pointed out by Mandel [2], the field operators propagate from the source to the photodetectors which are located far apart by comparison with the dimensions of the intrinsic fields of photons derived in Chapter 3. Consequently, the two detection processes described by the expectation value of the fourth-order interference as given in the Dirac notation [2]:

$$\Pr(\boldsymbol{r},t) = \langle\, \Phi \mid \hat{E}_s^-(\boldsymbol{r}_1,t_1)\, \hat{E}_i^-(r_2,t_2)\; \hat{E}_i^+(\boldsymbol{r}_2,t_2)\, \hat{E}_s^+(\boldsymbol{r}_1,t_1) \mid \Phi \,\rangle \quad (6.20)$$

would vanish because $\hat{E}_i^+(\boldsymbol{r}_1,t_1) = 0$ and $\hat{E}_s^+(\boldsymbol{r}_2,t_1) = 0$ and the space integral of the expectation value is non-zero only when the two Hilbert spaces of the measurements overlap (Griffiths [6]). This can be prevented by factorizing the product of the optical fields according to their positions, namely:

$$\Pr(\boldsymbol{r},t) = \langle\, \Psi_s \mid \hat{E}_s^-(\boldsymbol{r}_1,t_1)\; \hat{E}_s^+(\boldsymbol{r}_1,t_1) \mid \Psi_s \,\rangle \times$$
$$\times \left\langle\; \Psi_i \mid \hat{E}_i^-(r_2,t_2)\; \hat{E}_i^+(r_2,t_2) \mid \Psi_i \;\right\rangle \triangle t = Pr_s\; Pr_i \quad (6.21)$$

This expression (6.21) of probability products indicates that probability correlation should follow the "classical" interpretation of joint correlations by means of products of localised probabilities Pr_s and Pr_i, rather than a global joint detection which defies time and space disconnections.

As the energy of an electromagnetic wave is split equally between the electric and magnetic field, and with only the electric field interacting with electric dipoles, the number of photons detected with a fully efficient photodetector, is averaged over one cycle:

$$I_{ph} = N\,\langle cos^2(\omega\, t)\rangle = 0.5\, N \quad (6.22)$$

Interference with another optical wave may enhance or diminish the ensemble probability Pr of detection

$$\Pr = \frac{\langle N(t)\rangle}{\langle N_{tot}\rangle} = \frac{1}{2}\,\langle [1 + \langle \sigma\, \Gamma\rangle \langle cos(\xi_1(t) - \xi_2(t)\rangle]\rangle \quad (6.23)$$

after using eqs. (5.13). The ensemble average is represented by angled brackets, and each measurement delivers a unity value for the absorption of one or more photons.

An optical wavefront carrying simultaneously N photons can be decomposed into multiple partial wavefronts, each carrying one or several

photons. Partial wavefronts are generated by splitting the incoming wavefront, and they can be recombined at the output. The interference pattern is determined by the spatial distribution of the wave functions f_j ($\boldsymbol{r}$, t), while the "filling-up" of an interference pattern depends on how many photons are available over a given time interval.

A common interpretation would have one single photon per radiation mode being part of an ensemble of events so that every possible quantum propagation path will be activated statistically, but each event follows only one option. The interference pattern of spatially propagating waves f_j ($\boldsymbol{r}$, t) provides the probability distribution of an ensemble of photons which arrive sequentially in time, giving rise to the quantum "miracle" of interference of probability amplitudes. But since one single photon cannot propagate in a straight-line across a dielectric medium, this interpretation of multipath interference is questionable from a physical perspective. Once again, only a group of monochromatic photons can deliver the measured interference patterns as they can overcome the Rayleigh scattering through stimulated emission.

The mathematical treatment of classical interference of optical waves is carried over to the concept of interference of quantum probability amplitudes. However, time-independent ensemble probabilities contain elements of physical realisations which occurred at different times or locations. Attempts to link two temporarily or spatially separate photons, underlying two events, bring about the miracle of quantum nonlocality in time or space involving entangled number states which, by themselves, do not carry an optical field, and are, therefore, misrepresenting the physical reality.

The modelling of quantum interference by using Fourier transforms [2], [4] between the temporal profile of discrete photons and the spectral distribution $F(\boldsymbol{k_s}, \boldsymbol{k_i}, \omega_s, \omega_s)$ of the nonlinear crystal outputs implies the existence of simultaneous and spectrally distributed photons coming out of an interference filter, undermining the assumption that only one photon per radiation mode is present at any given time inside the experimental setup. Groups of photons are created even by a weakly pumped nonlinear crystal through the unavoidable amplification of a spontaneously emitted photon.

Groups of monochromatic photons are generated through stimulated emission even in the case of one atom trapped inside a high finesse resonant cavity. As a result of a very large number of internal reflections of the same photon, the synchronisation condition of eq. (5.25) applies between the excited atom and the group of photons bouncing back and forth inside the cavity, and partially exiting the cavity as groups of photons (Reiserer and Rempe [7]).

6.4 Correlations of the Balanced Homodyne Detection

The experimental setup for measuring the amplitude or any phase component of an optical radiation mode is illustrated in Fig. 6.5. The configuration is very similar to that for the HBT or HOM measurements, but is employed to deliver a statistical distribution of raw data for a weak signal which is mixed at the beam splitter with a strong reference wave in order to generate interference terms with opposite signs at the two photodetectors. The subtraction of the two photocurrents $\Delta I = I_1 - I_2$ is proportional to the interference value of the two optical beams.

The instantaneous photocurrent generated by detector j =1 or 2 is

$$I_j(t) = \frac{K_{ph}}{2}\ [N_{j\,LO}(t) + N_{j\,sig}(t) + \\ + 2\sqrt{N_{j\,LO}(t) N_{j;\,sig}(t)}\, cos(\theta_{LO}(t) - \theta_{sig}(t))] \qquad (6.24)$$

The current difference, with the number of photons of the local oscillator LO and the signal given, respectively, by $N_{LO}(t)$ and $N_{sig}(t)$ has the form:

$$\Delta I = \langle I_1 - I_2 \rangle = \frac{K_{ph}}{2}(T - R)\,[N_{LO}(t) - N_{sig}(t)] + \\ + 2\,K_{ph}\sqrt{R\,T\,N_{sig}(t)\,N_{LO}(t)}\,cos\left(\theta_{LO} - \theta_{sig}(t)\right) \qquad (6.25)$$

where $N_{LO}(t) \gg N_{sig}(t)$. The reflectivity and transmissivity are, respectively, denoted by R and T. The ensemble average of the reflectivity $\langle R \rangle$ and the transmissivity $\langle T \rangle$ coefficients may be set equal, but for each individual, single photon measurement their absolute values can be R=1 and T=0, and R=0 and T=1, because one photon is indivisible. An odd number of signal or local oscillator photons will split unevenly, that is: $2m + 1 = m + 1 + m$. As a result, the first term of the current difference in eq. (6.25) involving transmitted and reflected photons may not, physically, vanish even though, mathematically, $R = T = 0.5$.

For N_{sig}= 0, the only contribution to the temporal fluctuations ΔI would come from the local oscillator $(T - R)\,N_{LO}(t)$ which should *not* be taken as the expectation value of a coherent beam. The LO fluctuations are split unequally by the beam splitter, so that the current difference ΔI still recreates the noise statistics of the local oscillator.

The additional noise contribution from the interference term of eq.

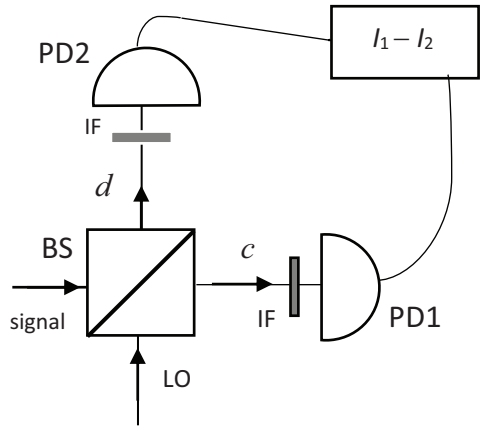

Fig. 6.5 The setup for a balanced homodyne detector. BS beam splitter; $I_1 - I_2$ difference of photocurrents PD photodetector; IF interferometric filter.

(6.25) adds significantly to the sides of the measured distributions (Lvovsky and Raymer [8]) which are averaged over $\theta_{sig}(t)$ for a given θ_{LO}. Defining $\Delta\theta \equiv \theta_{LO} - \theta_{sig}(t)$, the interference term adds to the positive side of the measured quadrature variable X for $-\pi/2 < \Delta\theta < \pi/2$, and to its negative side for $\pi/2 < \Delta\theta < 3\pi/4$, giving rise to a lateral peak of noise on either side of the statistical distribution of the quadrature X [8].

6.4.1 Continuous-variable optical quantum states

Having identified a physically meaningful explanation for the operation of the balanced homodyne detection of photons, we proceed now to point out a few physical processes missing from the 2009 review on "Continuous-variable optical quantum-state tomography" (Lvovsky and Raymer [8]).

We base our quest for a physically meaningful reality on the first paragraph of the review which reads:

> "A quantum state is what one knows about a physical system. The known information is codified in a state vector $|\psi\rangle$, or in a density operator $\hat{\rho}$, in a way that enables the observer to make the best possible statistical predictions about any future interactions (including measurements involving the system). [8, p. 299].

As mentioned in previous Chapters a few times already, the use of a global quantum state which is time- and space-independent has led in many

cases to physically impossible conclusions which were, nonetheless, taken as the "miracles" of quantum optics and quantum mechanics. This approach would seem rather puzzling when reading another paragraph from the 2009 review under scrutiny:

> "Quantum-information applications require measurement of optical modes that are localized in time. Homodyning has to be performed in the time domain: difference photocurrent is observed in real time and integrated over the desired temporal mode to obtain a single value of a field quadrature. Repeated measurements produce a quantum probability distribution associated with this quadrature". [8, p. 310].

In other words, even though information about the quantum system can be obtained from each individual measurement, the predictions of expected values of dynamic variables are based on global quantum states which discard a great deal of information.

The following paragraph is highly indicative of the shortcomings associated with an approach or formalism that deliberately overlooks physical elements and aspects of experimental setups. This paragraph reads:

> "In order to prepare a heralded photon, a parametric down-conversion (PDC) setup is pumped relatively weakly so it generates, on average, much less than a single photon pair per laser pulse (or the inverse PDC bandwidth). The two generated photons are separated into two emission channels according to their propagation direction, wavelength, and/or polarization. Detection of a photon in one of the emission channels (labeled trigger or idler) causes the state of the photon pair to collapse, projecting the quantum state in the remaining (signal) channel into a single-photon state." [8, p. 311].

As derived and explained in Chapter 4, the parametric amplification is unavoidable and is accompanied by a phase-pulling effect which leads to the optimal condition for amplification. The alleged collapse of the state of the pair of photons, upon detection of one of them, into a single-photon state of the photon assumes that a single photon per radiation mode can propagate across a medium, in a straight-line to the desired photodetector. As explained in previous Chapters, this assumption is ruled out by the existence of the quantum Rayleigh scattering in dielectric media such as optical fibres which are mentioned in the following paragraph:

> "Controlling the spatial mode of the signal photon is simplified if a single-mode optical fiber is used as an optical filter instead of a pinhole arrangement. Such a filter automatically selects a pure spatial mode in the

trigger channel, which transforms to a spatially pure signal photon. It is also advantageous in terms of the pair production rate." [8, p. 312]

The following two paragraphs describe a biphoton state and their alleged miraculous nonlocal influence on each other despite being separated and far apart beyond any spatial overlap of their physical extents.

"The biphoton is a complex entangled state with many parameters (spectrum, direction, polarization, etc.) of the two photons highly correlated, " [8, p. 311]

"Pulsed single photons were prepared by conditional measurements on a biphoton state generated via parametric down-conversion in the weak pumping regime. Narrow spatiotemporal filtering of the trigger photon was used as outlined in Sec. IV.B. The field state in the signal channel was characterized by means of optical homodyne tomography. "[8, p. 317]

While a pair of spontaneously emitted photons in a parametric down-conversion process does possess corelated values of various degrees of freedom, or parameters of the biphoton state, their correlations result from their common past and origin, having nothing to do with a collapse of the biphoton through a conditional measurement.

The global state involving the presence of one photon at any given time – but which, by means of the Dirac notation, appears to bring together two photons reaching the detectors at different time – plays a critical role in the conventional interpretation of quantum optics:

"A dual-rail qubit, described by the state

$$| \Psi_{\text{dual-rail}} \rangle = \tau \, |1_A, 0_B\rangle - \rho \, |0_A, 1_B\rangle, \qquad (62)$$

is generated when a single photon $|1\rangle$, incident upon a beam splitter with transmission τ^2 and reflectivity ρ^2, entangles itself with the vacuum state $|0\rangle$ present in the other beam splitter input. " [8, p.318]

Once again, a single photon cannot propagate through a dielectric medium such a beam splitter in a straight line because of the quantum Rayleigh scattering. Furthermore, despite a lack of experimental evidence at the level of an individual event being measured to yield the claimed results, it is suggested that, at the level of an ensemble distribution, the following statements identify accurately physical phenomena:

"Phase-dependent quadrature correlations are a consequence of the entangled nature of the state $|\psi_{\text{qubit}}\rangle$." [8, p.318]

"By performing a homodyne measurement on her part of the entangled state (62) and detecting a particular quadrature value $Q_{\theta A}$ at the local oscillator phase θ, Alice projects the entangled resource (62) onto a quadrature eigenstate $\langle Q_{\theta A}|$,

$$|\psi_B\rangle = \langle Q_{\theta A}, \theta_A| \Psi\rangle$$

$$= \tau \langle Q_{\theta A}, \theta_A| 1_A\rangle |0_B\rangle - \rho \langle Q_{\theta A}, \theta_A| 0_A\rangle |1_B\rangle,$$

which is just a coherent superposition of the single photon and vacuum states, i.e., a single-rail optical qubit. By choosing her LO phase θ_A and post-selecting a particular value of $Q_{\theta A}$, Alice can control the coefficients in the superposition, i.e., remotely prepare any arbitrary state within the single-rail qubit subspace." [8, p. 319].

The quadrature projection state $\langle Q_{\theta A}|$ corresponds to the harmonic oscillator, which is an arbitrary choice on the part of the observer as there are no harmonic oscillators being carried by the optical electromagnetic filed. The local photodetector projects, or reduces, the state to one of the eigenstates it measures, i.e. the detection of one photon – see eq. (3.5) for measurement-related projection of states. Thus, this type of projection is not physically possible.

Additionally, the spatial profile of photons was derived in Chapter 3, in eqs (3.35) and (3.37*b*) having the structure of a Wigner-type or time-varying single spectral component providing a physically meaningful explanation for synchronised interference and coincidence counting of photons as opposed to the assumption that a single photon state is made up of a wavepacket of Fourier components as suggested in this paragraph:

"If it is known a priori that only one photon elementary excitation of the field exists in a certain space-time volume, it is sensible to ask what is the temporal-spatial wavepacket mode that describes this photon. This task is close to that of finding the wave function of the photon treated as a massless particle. This notion is known to be controversial [see Smith and Raymer (2007) for a review]. However, if one restricts attention to the photon's transverse degrees of freedom in the paraxial approximation, the subtleties that arise can be circumvented. " [8, p. 323].

There are, in fact, no difficulties in so far as the longitudinal and lateral spatial distributions of a photon are concerned as these can be easily derived by means of the dynamic and coherent number states as explained in Chapter 3. In other words, unlike the spurious assumptions of time-independence underlying a global quantum state, a time-varying number of photons $N(\omega, t)$ for a given monochromatic frequency, as derived in

Chapter 3 from the dynamic and coherent number states, is a physically meaningful description of one photon or any number of photons possessing a spatial distribution of the optical field about its propagating peak, in both the longitudinal and lateral dimensions.

The question of "Remote state preparation using the nonlocal single-photon state" is rather problematic. The claim [8] of remotely collapsing a wave function is highly questionable. A single photon propagating through a beam splitter would be deflected from its planned pathway by quantum Rayleigh scattering. Furthermore, the maximum likelihood method of numerically reconstructing a quantum state from raw data "aims to find, among the variety of all possible density matrices, the one that maximizes the probability of obtaining the given experimental data set and is physically plausible" (Lvovsky and Raymer [8]). From the experimental point of view, the observer B's "photoreceivers do not have to be efficient, and he can post-select on finding his system in a particular subspace" [8]. The maximum likelihood method of reconstruction requires a target state, and the sign parameter *s* is delivered from observer A for the reconstruction of the quantum state by observer B. Therefore, the reconstruction is not independent. Indeed, the quantum Rayleigh scattering would deflect any single-photon crossing the beam splitter, and bearing in mind the slight parametric amplification inside the source, the two observers share the same photon phase from the same group of photons split at the beam splitters. There was no direct link at the level of a pure quantum state of a single measurement between the two observers, if only, because with only one photon in the experimental setup at any given time, only one detector can be triggered, whether or not the photon states are, mathematically, entangled. Consequently, the raw data measured (Fuwa *et al*. [9]) requires a great deal of numerical manipulation before it appears to produce a statistical correlation without any correlation being identified at the level of individual measurements.

6.4.2 The "miracle" of quantum imaging

Another example of the shortcomings of the global, and space- and time-independent ensemble quantum state is provided by the rather questionable explanation for the concept of "Induced coherence without induced emission" (Wang *et al*. [10]).

An imaging technique based on single-photon interference and not requiring coincidence detection was presented by Lemos *et al*. [11]. The experimental configuration is identical to Fig. 6.4 but with the idler beam *i1* passing through a transparent object before reaching the second nonlinear

crystal NL2. The experimental results are interpreted by suggesting that "Induced coherence without induced emission" (Wang *et al*. [10]) can be masterminded between two independent sources of entangled pairs of photons of degenerate frequencies $\omega_s \neq \omega_i$, so that "quantum mechanical interference between these two possible ways of reaching the detectors" takes place (Horne *et a*l. [12]).

> "The intensity image (non-constant transmittance) is due to transverse position-dependent which-source information carried by the undetected idler photons. The phase image is of a different nature: it is due to the fact that the position-dependent phase shift on the idler photons in path *d* is actually passed to the signal" [11].

These published articles claim that (Wiseman, and Mølmer [13])

> "there was no induced emission in their experiment, as the down-conversion rates were so low that the probability of both crystals producing a down-converted pair was negligible ".

It is recognized that "the phase sum of the signal and idler is locked to the pump phase", but the underlying physical mechanism remains elusive in those explanations, and that the condition applies only in the classical regime of, at least, many photons. Yet, this relation from eq. (4.6 *j*)

$$\phi_s + \phi_i = \phi_p + \frac{\pi}{2}$$

which holds for any number of photons spontaneously emitted and parametrically amplified, has been derived in Chapter 4, for the quantum dynamic and coherent numbers states identified in Chapter 3. As explained in Section 6.2.2. the interference pattern between the two signal beams as a result of the modulation of the seed idler beam is the result of the relative phase:

$$\phi_{s2} - \phi_{s1} + \phi_{i2} - \phi_{i1} = \phi_{p2} - \phi_{p1} + \Delta\phi_{i1} \qquad (6.19c)$$

after inserting

$$\phi_{i2} \approx \phi_{i1} + \Delta\phi_{i1} \qquad (6.17a)$$

Further scrutiny applied to the second-order conversion of photons presented in Chapter 4 and based on the dynamic and coherent number states of light analysed in chapter 3, clearly and directly indicates that the

parametric amplification of photons gives rise to the mechanism of phase-pulling effect leading to the optimal amplification of both the signal and idler photons. Indeed, if enough optical pump power is available to generate spontaneously emitted photons, then the same excited medium will unavoidable amplify the spontaneous emissions. Therefore, the physically meaningful explanation for the first-order interference presented in Section 6.2 above is based on interference of intrinsic fields of photons that emerge from the crystal as groups of photons which are separated into smaller groups by beam splitters and recombine to interfere at the output. As already pointed out in Section 6.2, the idler wave from the first nonlinear crystal seeds the idler wave in the second nonlinear crystal, thereby providing the induced stimulated transmission even for low levels of pump powers.

The existence of the amplification stage is demonstrated by the fact that the correlation between the wave vectors, i.e. $\boldsymbol{k}_p = \boldsymbol{k}_s + \boldsymbol{k}_i$ holds for the photons exiting the bulk crystal. This is physical evidence that only a group of monochromatic photons can propagate in a straight line in a dielectric medium. If only one photon per radiation mode was propagating inside the crystal, whether entangled with another photon or not, the quantum Rayleigh spontaneous emission would have scattered it. As the pump power into the second nonlinear crystal NL2 is increased, the more photons are added to each group, with the emission rate determined by the incoming beam *i2*. The first spontaneously emitted photons become amplified and deplete the parametric gain available in the second NL2, with the rate of emission being determined by the seed beams of idler photons.

6.5 Conclusions

The formalism of interference of probability amplitudes is based on mathematical operations acting on global quantum states which are time- and space-independent. This formalism involves transitions between number states which are present at different times. By contrast, the physically meaningful approach presented in this book identifies temporal and spatial properties, and aspects of an individual measurement, as well as photon-dipole interactions by means of the pure dynamic and coherent number states.

The “miraculous” outcomes of photon countings and correlations are physically and meaningfully explained by taking into consideration the nonlinear mechanism of parametric spontaneous emission of pairs of photons and their unavoidable parametric amplification. This process is accompanied by a phase-pulling effect leading to optimal conditions for

amplification even for weak pumps, which creates correlations between two interacting nonlinear crystal pumped by the same laser light.

In the situation of two separate photons colliding inside a dielectric medium such as a beam splitter, an interferometric filter, a polarising crystal, an optical fibre, etc. the quantum Rayleigh coupling of photons described in Chapter 3 could produce a group of two photons that will propagate together, at least initially.

Furthermore, given the indivisibility of one photon, the questions that have never been answered by the global approach to quantum optics are: 1. How can a single photon be filtered by an interferometric spectral filter which requires the simultaneous presence of many partial optical waves? and 2) How can a single photon have its state of polarisation varied by an electro-optic modulator as two perpendicular optical fields need to be differentially modulated?

References

1. L. Mandel and E. Wolf, “Coherence Properties of Optical Fields,” Rev. Mod. Phys., **37**, 231-287, (1965).
2. L. Mandel, “Quantum effects in one-photon and two-photon interference,” Rev. Mod. Phys., **71**, p. S274-S282, (1999).
3. R. J. Glauber, and M. Lewenstein, “Quantum optics of dielectric media,” *Phys. Rev. A*, **43**, 467- 491 (1991).
4. C. Garrison and R.Y. Chiao, *Quantum Optics*, Oxford University Press, 2008.
5. I. Walmsley, “Quantum interference beyond the fringe, *Science,* **358** (6366), 1001-1002, 2017.
6. R. B. Griffiths, “Nonlocality claims are inconsistent with Hilbert-space quantum mechanics”, Phys. Rev. A **101**, 022117, (2020).
7. A. Reiserer and G. Rempe, “Cavity-based quantum networks with single atoms and optical photons,” Rev. Mod. Phys., **87**, 1379–1418, (2015).
8. A. I. Lvovsky and M. G. Raymer, “Continuous-variable optical quantum-state tomography," Rev. Mod. Phys., **81**, 299-332, (2009).
9. M. Fuwa, S. Takeda, M. Zwierz, H. M. Wiseman, and A. Furusawa, “Experimental proof of nonlocal wavefunction collapse for a single particle using homodyne measurements”, Nat. Commun., **6**, 6665, (2015).
10. L. J. Wang, X. Y. Zou, and L. Mandel, ”Induced coherence without induced emission”, Phys. Rev. A **44**, 4614–4622, (1991).

11. G. B. Lemos, V. Borish, G. D. Cole, S. Ramelow, R. Lapkiewicz and A. Zeilinger, “Quantum imaging with undetected photons “, Nature, **512** (7515), 409–412, (2014).
12. M. A. Horne, A. Shimony, and A. Zeilinger, “Two particle interferometry”, Phys. Rev. Lett. **62**, 2209–2212, (1989); “Two particle interferometry”, Nature **347**, 429–430 (1990)
13. H. M. Wiseman, and K. Mølmer,” Induced coherence with and without induced emission”, Phys. Lett. A **270**, 245–248 (2000).

CHAPTER SEVEN

QUANTUM RAYLEIGH ANNIHILATION OF ENTANGLED PHOTONS

The interpretation of published experimental results intended to prove the existence of a quantum phenomenon of non-locality involving photonic entangled states did not take into consideration the existence of the quantum Rayleigh conversion of photons in dielectric media. This phenomenon leads to the existence of high levels of correlations between two independent photonic and linearly polarised quantum states generated after the entangled photons have been absorbed through the quantum Rayleigh conversion. Both pure and mixed individual states of polarisation result in expressions normally associated with entangled photonic states, providing support for the view that the physical concept of quantum non-locality is highly questionable.

In an opinion article written by Aspect [1] and published at the end of 2015, the question of quantum non-locality is all but settled on the basis of three experimental reports published earlier in the year apparently providing evidence of strong correlations between the two subsystem photonic components of entangled states.

For some particular reason though, as already pointed out in previous chapters of this textbook, over a period of more than three decades of experimental contributions apparently supporting the concept of quantum nonlocality, the quantum Rayleigh scattering or spontaneous emission taking place inside dielectric media (Vatarescu [2]) has been ignored or overlooked. Any experiment incorporating dielectric components such as beam splitters, optical fibres, interference filters, dichroic mirrors, etc. will involve quantum Rayleigh scattering. The quantum Rayleigh spontaneous emission (QRSE) in a dielectric medium replaces entangled photons with independent ones (Vatarescu [2]). A single photon cannot propagate in a straight line because of the QRSE. Only a group of monochromatic photons propagating together as a group, can maintain their line of propagation and properties because an absorbed photon may be recaptured through stimulated emission by the other photons in the group.

Additionally, a periodic stream of single photons is distorted statistically by optical cavities because of multiple internal reflections of various durations for different photons so that groups of photons may emerge from interferometric filters in addition to individual ones - see Chapter 5 above.

These effects will require a reassessment of the interpretations of the experimental results outlined by Aspect [1]. Two of the experiments (Giustina *et al*. [3]; Shalm *et al*. [4]) use optically nonlinear crystals which, as explained in Chapter 4, unavoidably amplify the spontaneously emitted photons generated through spontaneous, parametric down-conversion. Consequently, the polarisation properties of the initial photons are delivered to the detection stage by a group of photons. This fact enables the random polarisation modulation before the detection. The third experiment (Hensen, *et al*. [5]) uses single atoms as the source of photons but a dichroic mirror is placed at the output of the emitting source so that photons may be propagating back and forth inside the dielectric structure to coalesce, through the process of quantum Rayleigh coupling of photons described in Chapter 3, into groups of photons that will continue their propagation to the photodetector as a cluster of photons.

The relatively strong correlations between the detected states of polarizations of the two space-time separated photons [1] were considered to be a clear indication of an instantaneous collapse into an eigenstate of the wave function describing the two apparently entangled photons and, as a result, it was concluded that a non-local mechanism - of a yet unknown origin and nature - brings about a mutual influence between the two distant measurements. Overall, it is argued that those correlations disprove beyond any doubt the paradox pointed out by Einstein, Podolsky and Rosen (EPR), while complying with the uncertainty principle for each subsystem which would not allow simultaneous sharp values for two incompatible variables linked to the Pauli spin operators which do not commute. However, the role of the wave functions in the evaluation of the uncertainty relation is disregarded even though the derivation of the uncertainty principle (D. Griffiths [6]) is initiated with a given set of wave functions.

The measured events of correlated pairs of photons are “extremely rare” [1], with typical values of “slightly more than one event-ready signal per hour”. Nevertheless, the interpretation of the experimental results by Aspect [1] failed to take into account the role played by the quantum Rayleigh conversion of photons (Louisell [7]; Marcuse [8]) in their propagation through the dielectric media of optical fibres, beam splitters, polarization rotating devices and other dielectric elements comprising the experimental setups. While the classical Rayleigh scattering induced by perturbations of the refractive index is the major loss factor in optical fibres (Wang *et al*.

[9]), the quantum Rayleigh conversion of photons has been practically ignored although documented in early textbooks. Recently, however, the quantum Rayleigh conversion of photons has been identified as the physical process underpinning the forward propagation of an optical wave through a dielectric medium (Vatarescu [10]), as well as a practical way of implementing phase-sensitive amplification in the linear regime (Vatarescu [11-12]).

In the case of only one photon propagating through a dielectric medium, the only process occurring is that of absorption of the photon by an oscillating dipole and spontaneous emission of one photon, which corresponds to the quantum Rayleigh spontaneous emission of photons (QRSE). The QRSE would bring about various time-delays causing a photon to change direction, back and forth, inside an optical fibre or change its polarization state in any dielectric device such as optical fibres, beam splitters, crystal polarizers, etc.

From a physical perspective, the correlation between the polarisation measurements at the two distant stations can be easily explained by a combination of the quantum Rayleigh spontaneous emission and the molecular structures of polarisation-dependent components such as polarisation beam splitters, polarisation filters, birefringent crystal plates, etc. As the two measurement stations have similar, if not identical, device configurations, photons will keep propagating in their respective forward directions if they are repeatedly captured by the eigenmodes of a specific component; to a certain degree this mechanism mimics a quantum Zeno effect (Griffiths [6]) or a protective measurement preventing a quantum state from changing (Piacentini *et al*. [13]).

The physical concept of quantum nonlocality is inextricably linked to the existence of entangled states of pairs of photons (Edamatsu [14]; Garrison and Chiao [15]), These two photons are generated simultaneously by the same parametric conversion of one pump photon into two new photons commonly labelled signal and idler. Another alleged process for creating entangled photons would be a beam splitter across which two initially independent photons propagate from different input directions.

The prevailing criterion – allegedly proving the phenomenon of quantum nonlocality or remote influence between two sets of measurements performed on degrees of freedom of pairs of entangled photons – has the form of an inequality involving combinations of values of a correlation function and is commonly known as the Clauser-Horne-Shimony-Holt (CHSH) [16] scenario. In this context (Zeilinger [17]), it is claimed that:

> "It is this very independence of a measurement result on one side from what may be done on the other side, as assumed by EPR, which is at variance with

> quantum mechanics. Indeed, this assumption implies that certain combinations of expectation values have definite bounds. The mathematical expression of that bound is called Bell's inequality, of which many variants exist" (Zeilinger [17]).

Unfortunately, both analytical (Tipler [18]) and experimental results (Qian *et al*. [19]; Gonzales [20]) can do away with the quantum miracle of nonlocality. A statistical approach based on conditional and joint or simultaneous detections of two similar and spatially separate sets of binary data results in the same correlation function as for the entangled states (Tipler [18]).

Experimentally, the violation of CHSH-Bell inequality has been found to occur for classical variables which are mathematically "entangled", that is, they appear as sum of products which cannot be separated into a product of a sum of states. As outlined by Eberly *et al*. [21]:

> "In any event, the definition of entanglement is simply inseparability of sums of product states that exist in different vector spaces."

> "We should keep in mind that entanglement is a vector space property, present in any theory with a vector-space framework. Thus, there is no distinction between quantum and classical entanglements, as such. The important differences between the quantum and classical theories of light do allow quantum entanglements to be exhibited in a wider variety of ways, but of course these are never observed unless detection capability makes individual photons experimentally distinguishable." [21]

This Chapter analyses the propagation of entangled photons through a dielectric medium and the physical process of quantum Rayleigh scattering of photons through spontaneous emission which is bound to affect the propagation of the single photons originating from the same source and forming the components of entangled states (Edamatsu [14]). As outlined in Section 7.1, the initially entangled state of photons is destroyed in a quantum Rayleigh interaction through electric dipole excitation which is followed by spontaneous emission. The correlation functions – evaluated in Section 7.2 – are associated with the two spontaneously and separately emitted qubits of photons and deliver the same degree of high correlations for pure and independent states as for entangled states. Variable outcomes for mixed states have the potential to exceed the lower bound of the Bell inequalities. Additionally, each term of the commutative relations between the relevant Pauli operators in the context of the individual and separated photonic state vectors will vanish leading to the possibility of simultaneous measurements and the absence of an EPR paradox. The implications of

replacing the physically eliminated entangled states of photons with individual and independent qubits are discussed in Section 7.3, and support the view objecting to the existence of quantum nonlocality. Extensive references are identified in support of local realism.

7.1 Spontaneous Emission and Polarisation Rotation

A mathematically entangled polarization state of a pair of photons is conventionally generated by means of spontaneous parametric down-conversion of photons [(Edamatsu [14]). For type-I nonlinear crystals, the emerging two photons possess the same state of polarisation, HH or VV, while for a type-II nonlinear crystal, the pair photons have perpendicular states of polarisation, HV or VH, which are explicitly written in terms of horizontal and vertical states as:

$$|\Psi_{\mathrm{I}}\rangle = |1_{\mathrm{H}}\rangle_s |1_{\mathrm{H}}\rangle_i + |1_{\mathrm{V}}\rangle_s |1_{\mathrm{V}}\rangle_i \qquad (7.1a)$$

$$|\Psi_{\mathrm{II}}\rangle = |1_{\mathrm{H}}\rangle_s |1_{\mathrm{V}}\rangle_i + |1_{\mathrm{V}}\rangle_s |1_{\mathrm{H}}\rangle_i \qquad (7.1b)$$

where the subscripts s and i identify the signal and idler photons, respectively.

When acted upon with the absorption operator of the quantum Rayleigh Hamiltonian of eq (6.1), these states become product states because the empty, zero-photon state does not possess any property, i.e.,

$$\hat{a}\,|\Psi_{\mathrm{I}}\rangle = |0\rangle_s |1_{\mathrm{H}}\rangle_i + |0\rangle_s |1_{\mathrm{V}}\rangle_i = |0\rangle(|1_{\mathrm{H}}\rangle_i + |1_{\mathrm{V}}\rangle_i) \qquad (7.2a)$$

$$\hat{a}\,|\Psi_{\mathrm{II}}\rangle = |0\rangle_s |1_{\mathrm{V}}\rangle_i + |0\rangle_s |1_{\mathrm{H}}\rangle_i = |0\rangle(|1_{\mathrm{H}}\rangle_i + |1_{\mathrm{V}}\rangle_i) \qquad (7.2b)$$

Once again, as explained in Chapter 4, in a nonlinear crystal pumped, e.g., with a continuous wave (p) and for frequency down-converted photons of frequncies $\omega_s + \omega_i = \omega_p$, the gain-providing medium which generates the spontaneous emission, will also amplify the initially single photons, particularly so in the direction of wavevector matching conditions, even for limited space-time overlap. A phase-pulling effect leading to $\varphi_s + \varphi_i = \varphi_p + \pi/2$ also occurs. Thus, the commonly assumed one single photon output does not physically happen. At least several photons will be associated with each individual and discrete electronic "click". Only a group of monochromatic photons propagating together can overcome the quantum Rayleigh scattering by recapturing the absorbed photon through stimulating emission. Nonetheless, it is possible for only one photon to survive the

propagation across a dielectric medium of the polarisation filter and reach the photodetector.

The probability of emitting a photon with momentum $\boldsymbol{k}$ and polarization μ is related to the decay rate γ_s [1/s] of the excited dipole inside a dielectric medium, and was evaluated as (Glauber and Lewenstein [22]):

$$\gamma_s(\boldsymbol{k}, \mu, \omega) = \frac{9\,\epsilon^{5/2}}{(2\,\epsilon+1)^2}\frac{\omega^3}{\hbar\, c}\left(\frac{\boldsymbol{d}\cdot\boldsymbol{e}_{\boldsymbol{k}\mu}}{4\,\pi}\right)^2 \tag{7.3}$$

with $\boldsymbol{d}$ denoting the electric dipole moment which is excited by an optical field of the same polarisation, $\boldsymbol{e}_{\boldsymbol{k}\mu}$ being the polarization unit vector of the emitted photon, which is perpendicular to the direction of propagation $\boldsymbol{k}$, and μ identifies one of the two perpendicular polarisations. In a dielectric material of constant ϵ the decay rate is modified, but its angular distribution is the same as in free space.

The angular distribution of an accumulated number of spontaneously emitted photons $N_{sp}(\Delta z, \varphi_{em})$ over a distance Δz, is predicated on eq. (7.3), leading to:

$$N_{sp}(\Delta z, \varphi_{em}) = N_{sp}(\Delta z)\,(cos\,\varphi_{em})^2 \tag{7.4}$$

with φ_{em} the emission angle between the dipole $\boldsymbol{d}$ and the polarization unit vector $\boldsymbol{e}_{\boldsymbol{k}\mu}$ of the photons and $N_{sp}(\Delta z)$ is calculated as in Chapter 2, (Appendix). Spontaneously emitted photons with $\pm\varphi_{em}$ polarisation angles relative to the pump polarization $\boldsymbol{e}_p$, will be amplified through the optically linear parametric gain coefficient presented in Chapters 2 and 3. This amplification includes a polarisation dependence in the factor $\boldsymbol{e}_p\cdot\boldsymbol{e}_{\boldsymbol{k}\mu}$, bringing about a correlation between the state of polarisation and its number of amplified photons as found in (Qian *et al*. [19]).

For $\boldsymbol{e}_{\boldsymbol{k}\mu}\cdot\boldsymbol{x} = cos\,\varphi_{em}$ and $\boldsymbol{x}\cdot\boldsymbol{y} = 0$, a non-vanishing value along the $\boldsymbol{y}$ –polarisation is obtained by blocking off either $+\varphi$ or $-\varphi$ polarised photons as, for a large number of photons, the $\boldsymbol{y}$ –polarised photons cancel each other out. This corresponds to the use of a polarisation filter for the polarisation paradox which "rotates" photons from $\boldsymbol{x}$ to $\boldsymbol{y}$.

The generic eigenstates of polarisation associated with spontaneous emission through quantum Rayleigh conversion of photons on the two-dimensional Hilbert space $\mathcal{H}$ will take the form of single and independent qubits $|\Psi(\varphi_{em})\rangle$ identified as:

$$|\Psi(\varphi_{em})\rangle = cos\,\varphi_{em}\,|x\rangle + sin\,\varphi_{em}\,|y\rangle \tag{7.5}$$

These state vectors with polarization angles φ_{em} in the range

$$-\pi/2 \leq \varphi_{em} \leq \pi/2$$

will describe any possible polarisation perpendicular to the direction of propagation of the spontaneous emission and will be of practical interest in the next Section. Thus, incoming photons initially polarised in the x – direction will reappear with an angle θ – rotated polarisation, thereby enabling them to pass through a θ – rotated polarisation analyser.

It should be emphasised that the quantum state of eq. (7.5) is a mixed state on the two-dimensional Hilbert space $\mathcal{H}$ or a space- and time-independent global state describing an ensemble of measurements. The shortcomings of such global states were identified in previous Chapters as omitting the physical features associated with single and individual measurements describing the physical reality.

Using an alternative notation that is clearer for further analysis, the spontaneously emitted photon will have an arbitrary state of polarization

$$|\Psi\rangle_s = cos\,\theta_s\,|1_x\rangle_s + sin\,\theta_s\,|1_y\rangle_s \tag{7.6}$$

where θ_s indicates the angle of polarization in the plane perpendicular to the direction of propagation, and which is unrelated to the other photon of the initially entangled state.

7.2 Quantum Correlation Functions

As a photon enters a birefringent crystal and interacts with electric dipoles, the photon needs to be re-emitted into a polarization eigenstate so it can propagate in the same forward direction to reach the intended photodetector. If each of the individual photons of the initial pair is re-emitted into their original state of polarisation and reaches its respective detector within the designated time interval for a coincidence count to be registered, then this physical process can be mistaken for the physically impossible case of the entangled photons having survived their propagation through the dielectric media without interacting with electric dipoles. Nevertheless, as photons acquire a phase shift as a result of their propagation, the probability of no dipole-photon interactions taking place even for a short distance of millimetres, is nil.

7.2.1. Pure states of polarization

Although the conventional definition of the correlation function – see Eq.13 of Brunner *et al*. [23] – involves the same state of polarization reaching the two separate detectors, in the case of quantum Rayleigh spontaneous emission additional correlations can be defined between different states of polarization – possibly boosting the detection counts – for two different angles φ_1 and φ_2, relative to the x – axis of reference.

Correlation functions E_c for a quantum behaviour are defined [23] as the expectation value of the tensor product of two measurement operators for a set of initial state vectors which are projected onto the measurement Hilbert space $\mathcal{H}_m = \mathcal{H}_1 \otimes \mathcal{H}_2$ in the expression

$$E_c = \langle \Psi(\varphi_1) | \hat{p}(\theta_1) \otimes \hat{p}(\theta_2) | \Psi(\varphi_2) \rangle = \langle \Phi_1 | \otimes | \Phi_2 \rangle \tag{7.7}$$

The second line of eq. (6) indicates that the projected states $| \Phi(\varphi) \rangle$ lie in the measurement space of $\mathcal{H}_m$ which identifies the comparison of measured values with a localized measurement [18].

The polarisation eigenstates of the measured photons, rotated by an angle θ_j from the reference or generic states $|x\rangle$ and $|y\rangle$ are denoted as

$$|x(\theta_j)\rangle = \cos\theta_j |x\rangle + \sin\theta_j |y\rangle \tag{7.8a}$$

$$|y(\theta_j)\rangle = -\sin\theta_j |x\rangle + \cos\theta_j |y\rangle \tag{7.8b}$$

and the quantum operator measuring polarisation properties of the photons is the projector

$$\hat{p}(\theta_j) = |x(\theta_j)\rangle\langle x(\theta_j)| - |y(\theta_j)\rangle\langle y(\theta_j)| =$$

$$= \sin(2\theta_j)\,\hat{\sigma}_1 + \cos(2\theta_j)\,\hat{\sigma}_3 \tag{7.9}$$

where $\hat{\sigma}_1 = |x\rangle\langle y| + |y\rangle\langle x|$
is the real part of the two-dimensional Pauli transition operator, flipping the photon between the two generic eigenstates, and

$$\hat{\sigma}_3 = |x\rangle\langle x| - |y\rangle\langle y|$$

corresponds to the Pauli projection operator for the difference between the generic eigenstates. Using the identities of the operators:

$$\hat{\sigma}_1 |x\rangle = |y\rangle; \qquad \hat{\sigma}_1 |y\rangle = |x\rangle; \tag{7.10}$$

$$\hat{\sigma}_3 \mid x \rangle = \mid x \rangle ; \qquad \hat{\sigma}_3 \mid y \rangle = - \mid y \rangle$$
$$\hat{\sigma}_1 \hat{\sigma}_3 = - \hat{\sigma}_3 \hat{\sigma}_1$$
$$\hat{\sigma}_1 \hat{\sigma}_1 = \hat{\sigma}_3 \hat{\sigma}_3 = \hat{I} = |x\rangle\langle x| + |y\rangle\langle y|$$

we obtain from eq. (7.9) for the correlation operator:

$$\hat{p}(\theta_1) \otimes \hat{p}(\theta_2) = cos\, 2(\theta_1 - \theta_2)\ \hat{I} + sin\, 2(\theta_1 - \theta_2)\ \hat{\sigma}_1 \hat{\sigma}_3 \qquad (7.11)$$

By inserting Eq. (7.11)), along with the equalities

$$\langle \Psi(\varphi_1) \mid \Psi(\varphi_2) \rangle = cos\ (\varphi_1 - \varphi_2) \qquad (7.12a)$$

$$\langle \Psi(\varphi_1) | \hat{\sigma}_1 \hat{\sigma}_3 | \Psi(\varphi_2) \rangle = \langle \Psi(\varphi_1) \mid \Psi(\varphi_2 + \pi/2) \rangle =$$

$$= cos(\varphi_1 - \varphi_2 - \pi/2) = \sin\ (\varphi_1 - \varphi_2) \qquad (7.12b)$$

into eq. (7.7), we evaluate the correlation function as

$$E_c = cos\ 2(\theta_1 - \theta_2)\, cos(\varphi_1 - \varphi_2) + sin\ 2(\theta_1 - \theta_2)\, sin\ (\varphi_1 - \varphi_2)$$
or
$$E_c = cos[\, 2(\theta_1 - \theta_2) - (\varphi_1 - \varphi_2)] \qquad (7.13)$$

For $\varphi_1 = \varphi_2$, this expression of the correlation function for single and independent qubits of the same state of polarization reaching both detectors, is identical to the expression for photonic entangled Bell states [15] (Ch.19), reaching the two detectors. Equally, eq. (7.13) evaluates the correlation for the orthogonal detections, $\theta_1 - \theta_2 = \pi/2$, of two different states of photon polarizations. With adjustable settings of the detecting polarisation filters, i.e. θ_1 and θ_1, any values of the correlation functions can be obtained for corresponding values of the incoming photon polarisation angles, i.e., φ_1 and φ_2.

7.2.2 The Heisenberg uncertainty of predicted values

The expectation values of the operator products $\hat{\sigma}_1 \hat{\sigma}_3$ are found to vanish for pure states of eq. (7.5), i.e.,

$$\langle \Psi(\varphi) | \hat{\sigma}_3 \hat{\sigma}_1 | \Psi(\varphi) \rangle = 0 \qquad (7.14a)$$

$$\langle \Psi(\varphi) | \hat{\sigma}_1 \hat{\sigma}_3 | \Psi(\varphi) \rangle = 0 \qquad (7.14b)$$

because $\hat{\sigma}_1\hat{\sigma}_3\,|\Psi(\varphi)\rangle = |\Psi(\varphi+\pi/2)\rangle$. As a result, each term of the resulting commutative relation vanishes and we obtain

$$\langle\Psi(\varphi)|\,[\,\hat{\sigma}_1\,,\hat{\sigma}_3]\,|\,\Psi(\varphi)\rangle = 0 \tag{7.15}$$

for the lowest limit of uncertainty involving the two Pauli operators. The eigenstates of $\hat{\sigma}_1$ are superpositions of the eigenvectors of $\hat{\sigma}_3$ on the two-dimensional Hilbert space $\mathcal{H}$ and simultaneous measurements of well-defined values are possible as their product operator $\hat{\sigma}_1\hat{\sigma}_3$ flips the eigenstates $|\,\Psi(\varphi)\rangle$ and $|\Psi(\varphi+\pi/2)\rangle$ onto each other. Thus, the output value is indicative of the input one, and each term of the commutator vanishes for the wave functions $|\,\Psi(\varphi)\rangle$ of eq. (7.5) or eq. (7.6). Consequently, the simultaneous measurement of the two operators in the context of the single and independent qubit wave functions is capable of identifying the incoming state as well as the measured one.

The detection of photons having a polarisation direction $\boldsymbol{e}_{k\mu}$ which is not aligned with the polarisation filter $\boldsymbol{e}_f$ will occur due to the probability of a dipole excitation being proportional to the scalar product $\boldsymbol{e}_f \cdot \boldsymbol{e}_{k\mu}$ [7]. For photons to propagate in the same forward direction in a uniaxial crystal they need to be recaptured after spontaneous emission by the electric dipoles which are aligned with the principal axes of the crystal.

A relation can be derived between the correlation function of the measurements $E_c(\theta_1,\theta_2) = cos\ 2(\theta_1-\theta_2)$ and the overlap probability

$$P\,(\theta_1,\theta_2) = |\langle\Psi\,(\theta_1)\,|\,\Psi\,(\theta_2)\rangle|^2 = cos^2\,(\theta_1-\theta_2)$$

before the measurements of two independent photons having polarization angles of θ_1 and θ_2. As in [15, Ch.19] this relation is

$$E_c(\theta_1,\theta_2) = 2\,P\,(\theta_1,\theta_2) - 1$$

indicating that entangled states of photons do not possess any particular properties regarding quantum correlations associated with detections at two remote locations.

7.2.3 Mixed states of polarization

The overall correlation for one step of spontaneous emission will be found by adding up probability-weighted correlation functions of eq. (7.13) as the ensemble of polarisations states generated over a time interval corresponds to a mixed quantum state described by the density matrix elements

$$\rho_{mn}(\varphi) = p(\varphi)\langle m\,|\,\Psi(\varphi)\rangle\,\langle\,\Psi(\varphi)|\,n\rangle$$

where *m, n = x, y.* A possible probability density can be identified from eq. (7.4) above, that is,

$$p(\varphi) = \frac{cos^2\varphi}{0.5\,\pi}$$

for generating the state $|\,\Psi(\varphi)\rangle$ over the range $\varphi \in \{-\pi/2, \pi/2\}$. This leads to a higher probability for the interval $\{-\pi/4, \pi/4\}$ than for the intervals $\{-\pi/2, -\pi/4\}$ and $\{\pi/4, \pi/2\}$.

The correlation function for the mixed state of an ensemble is evaluated similarly to eq. (7.13) after using the transformation

$$|\,\Psi(\varphi)\rangle \rightarrow \sqrt{p(\varphi)}\,|\,\Psi(\varphi)\rangle$$

in eq. (7.7) to obtain:

$$E_c = cos\,2\,(\theta_1 - \theta_2) + \int d\varphi_2\,\sqrt{p(\varphi_2)}\;\times$$
$$\times \int_{-\frac{\pi}{2}}^{\frac{\pi}{2}} d\varphi_1\,\sqrt{p(\varphi_1)}\;cos[2\,(\theta_1 - \theta_2) - (\,\varphi_1 - \,\varphi_2)]\;\times$$
$$\times\,[1 - \,\delta\,(\,\varphi_1 - \,\varphi_2)] \quad (7.16)$$

where the first term reproduces the result for identical and independent qubits, i.e., $\varphi_1 = \varphi_2$, with δ being Dirac's delta function. The second term of (7.16) depends on the polarization state distribution of the mixed state, providing the possibility of controlling the level of correlation with various distributions of polarizations.

7.3 Physical Aspects of Simultaneous Measurements of Independent Photons

Since the same correlation functions of eq. (7.13) are derived for independent and single qubits generated through quantum Rayleigh spontaneous emission of photons – from initially entangled polarised photons – as for the initially entangled photons [15], it follows that the violations of any type of relevant Bell inequalities will also take place in the same way. The CHSH-Bell inequality consists of a linear combination of binary correlation values at four settings of the joint and simultaneous measurements involving, mathematically, entangled states of photons. A measurement performed on one photon of a jointly emitted pair would, through an unspecified mechanism, impact on an immediate measurement carried out on the second photon. Yet, the nature of this remote interaction

has never been specified if only because a Hamiltonian of interaction cannot be identified (R. B. Griffiths [24]). A projection operator does not act as a Hamiltonian of interaction in the Schrödinger wave equation.

By contrast, the correlations derived in this Chapter result from similar, if not identical, distributions of polarisation states as opposed to what is conceptually believed to be a non-local quantum effect. These correlations do not require the existence of entangled states of photons.

Once the same correlation functions are derived using only states of polarisations emitted spontaneously by the quantum Rayleigh conversion of photons, no other physical processes are required to explain the experimental results.

Furthermore, spatially separated Hilbert spaces rule out quantum nonlocality (R. B. Griffiths [24]). The wavefunction collapse, or more accurately reduction, provides a mathematical tool for calculating conditional probabilities involving no remote influence by one measurement over the other.

Statistical scrutiny of experimental outcomes satisfying Bell-type inequalities leads to explanations based on conditional probabilities for joint or simultaneous detections of random sets of binary values which are spatially separated. These probabilities do not require any nonlocal interactions, and the CHSH-Bell inequality can be derived from various considerations fully compatible with local realism (Boughn [25]; Khrennikov [26]; Kupczynski [27]).

7.4 Quantum Local Realism

Let us now consider a few characteristics associated with local realism [6] of quantum measurements in the context of quantum Rayleigh conversion of photons:

1. *Locality* of measurements is supported by the use of single and independent photonic qubits emitted separately by quantum Rayleigh spontaneous emission, to explain the experimental results of apparently enhanced correlations of outcomes.
2. *Randomness* of experimental parameters stems from the quantum Rayleigh spontaneous emission that generates the projection from the polarization state $| x \rangle$ of the input photons to the rotated polarization state $|\Psi(\varphi)\rangle = cos\ \varphi\, |x\rangle + sin\ \varphi\, |y\rangle$.
3. *Realism* of values carried by the detected photons is indicated by the physical effect of the measuring operators on the detected photons in the quantum states $|\Psi(\varphi)\rangle$ of eq. (7.5) or eq. (7.6), for which the two commutator terms of the two Pauli operators of eqs. (7.14-15) vanish

> independently of each other. Thus, a physically meaningful identification of wavefunctions will enable simultaneous measurements of well-defined values by recognising the operator-induced change of state upon measurement.

The common view [6] holds that "the measurement of one component of the entangled state collapses the total wave function into a certain value which, in turn, affects instantaneously the second measured value." Nonlocality is associated with the instantaneous collapse of the wave function. The "remarkable" correlation is revealed by a comparison of the two lists of measured data compiled at the two detection points, as ethereal influences are said to be associated with the collapse of the wave function upon measurement. Yet, the experimental results can be explained without entangled states of photons which are destroyed by propagating through a dielectric medium and replaced by independent qubits of photon polarisation.

The presentation of Garrison and Chiao [15, Ch.19] describes the Einstein, Podolsky and Rosen (EPR) view suggesting that there is no such thing as an uncaused random event, and the characteristic randomness of the quantum world originates at the very beginning of each macroscopic event. By contrast, the conventional view [1] would have a quantum description in which the state vector evolves in a perfectly deterministic way from its initial value, and randomness enters only at the time of measurements. The quantum Rayleigh spontaneous emission is, in fact, a random process at the generating stage followed by evolution described by the Schrödinger equation, thereby supporting the EPR view.

It is emphasized in [19] that

> "Bell violation has less to do with quantum theory than previously thought, but everything to do with entanglement."

Actually, there is no need for entangled states to measure strong correlations of polarisations between spontaneously emitted photons detected far apart from each other or non-locally. As derived in the foregoing Section 7.2.1, the same correlation function is found for single and independent qubits as was for entangled qubits.

It is claimed in [23] that

> "… the violation of Bell inequalities can be seen as a detector of entanglement that is robust to any experimental imperfection: as long as a violation is observed, we have the guarantee, independently of any implementation details, that the two systems are entangled."

Yet, this is not the case with single and independent qubits which can reproduce the same results.

For the entangled state of two polarised photons shown in the inset of [1, (Fig. 1)], quantum mechanics predicts that the polarisation measurements performed at the two distant stations will be strongly correlated [1]. But the same prediction also applies to two independent, single qubits which are generated through quantum Rayleigh spontaneous emission from initially identical photons propagating in different directions through dielectric media such as optical fibres.

Additionally, the article by Ringbauer *et al*. [28]

> "…rules out outcome-dependent causal models without additional assumptions in any scenario with more than two settings. A direct causal influence from one outcome to the other can therefore not explain quantum correlations."

The analysis presented in this Chapter is based on physically meaningful interactions of quantum Rayleigh conversion of photons and supports Tipler [18] in his statement that:

> "There is no mystery. There is no quantum nonlocality".

It is the physical process that gives rise to a wave function. The opposite approach of relying on mathematical complexities to conjure up physical processes is bound to generate "'quantum mysteries".

As for the quantum key distribution between the two measuring units (Ursin *et al*. [29]), it is determined by the local distribution of the mixed state of spontaneously emitted photons – see Section 7.2.3 above – and the measurement setup of the dielectric devices involved in the polarisation filtering with its eigenstates capturing the projected single qubits. However, errors will appear because of the statistical nature of the correlations between polarised photons.

7.5 The Deficiencies of the Concept of Quantum Nonlocality

As is often the case with the advocates of quantum nonlocality, a recently published review (Paneru *et al*. [30]) omits every rebuttal of the concept of quantum nonlocality despite a multitude of experimental and analytic results.

One such review that completely ignores any possibility of quantum nonlocality being physically impossible has been presented by Paneru *et al*. [30]. This Section outlines the deficiencies of many of their statements.

We begin with this statement:

> "…entanglement is the fundamental feature of quantum physics between two (or more) systems and the consequences drawn from the obtained correlations do not apply to any classical system, i.e. classical correlations cannot lead to the same conclusions as quantum entanglement. While analogies might be seen in the mathematical formulation, the possibility of spatial separation, which is the key aspect of entanglement, does not hold for the classical counterpart." (Paneru *et al*. [30]).

This paragraph implies that entangled photons can influence each other regardless of how far apart from each other they propagate. This statement does not identify any Hamiltonian of interaction between non-overlapping Hilbert spaces as pointed out by R.B. Griffiths [24]. It is rather puzzling that the quantum process of Rayleigh scattering through spontaneous emission has been totally ignored, as already emphasised in early Chapters of this textbook.

The next quotation is:

> "Numerous experiments performed on multiparticle entangled states, such as the Hong-Ou-Mandel effect [50], the Franson interferometer [51], etc., have exhibited correlations that do not have any classical counterparts, thus showing entanglement to be purely a quantum effect." (Paneru *et al*. [30]).

This statement fails to explain the difference between an ensemble of measurements described by a global wavefunction which is time- and space-independent and the measurement of a single and independent event. As a consequence, the measurement appears to transcend space and time in the *mathematical* formulation. The conventional model would have a superposition of photons that reach the same photodetector at separate times, and/or photons that reach separate photodetectors at the same time. Yet, the intrinsic optical field of photons as derived in Chapter 3 from quantum consideration cannot extend beyond a few wavelengths for one photon. Additionally, experimentally used optical sources cannot prevent amplification of spontaneously emitted photon, and processing dielectric devices – such as interferometric filters – distort the stream of single photons by multiple internal reflections of various durations, as explained in previous Chapters. Physically meaningful explanations for the experiments listed in the quotation have been presented in previous Chapters of this textbook.

The following statement has to do with the well-known Heisenberg principle of uncertainty:

> "In quantum mechanics, two physical quantities represented by noncommuting observables cannot be measured simultaneously with arbitrary precision. Whenever we measure one observable, we influence the state in such a way that the measurement outcomes for the other observable is disturbed." (Paneru *et al*. [30]).

Yet, an appropriate choice of quantum states to describe the physical reality of the interaction enables the vanishing of each of the two terms of the calculated commutator relation, as demonstrated in Section 7.2.2 above. An understanding of the transformation or transition brought about by measuring operators will enable the observer to identify the input quantum state and the causal effects involved in the measurement operation.

Additional statements read:

> "There is another fundamental issue of nonlocality pertaining to entangled states: the idea that measurements performed in spatially separated locations can affect each other." (Paneru *et al*. [30]).

> "Bell later showed that a local-realistic description of entangled states is inconsistent with quantum mechanics, effectively ruling out the local hidden variables description of entangled states." (Paneru *et al*. [30]).

> "In his seminal paper [24], John Bell proved that any theoretical prediction for measurement outcomes fulfilling the ideas of locality and realism is upper bounded for a given set of measurements (the so-called Bell inequality). He also showed that quantum mechanics allows for the possibility to exceed this bound proving that quantum correlations cannot be obtained from any local realistic hidden variable theories with the form described by Eq. (12). Since the time of his paper, numerous experiments have been performed that attest to the correctness of quantum mechanics and falsified the assumption of local hidden variables [29–33, 73], most recently even loophole-free [28, 74, 75]. Contrary to the EPR assumption, nature does seem to allow the measurement of one particle to affect the "reality" of the other." (Paneru *et al*. [30]).

These beliefs have already been disproved by clearly identified flaws in the interpretations of experimental outcomes as explained in references [18-21] and [24-27]. The quantum Rayleigh spontaneous emission that scatters entangled photons – as explained in this Chapter 7 – is totally absent from the review article of Paneru *et al*. [30].

Additional quotations from Paneru *et al*. [30]:

> "For a source that produces photons with perfectly correlated polarizations in any direction, the initial two-photon state is an entangled state which is written as,
>
> $$|\psi_i\rangle = (|H\rangle_A |H\rangle_B - |V\rangle_A |V\rangle_B)/\sqrt{2} \quad (14)$$
>
> where $|H\rangle$ and $|V\rangle$ refer to the horizontal and vertical polarization respectively." (Paneru *et al*. [30]).

These entangled photons are described by means of global functions which carry no space- and time- dependence. Therefore, *no* physical reality of the evolution of the two photons moving apart from each other to their respective remote photodetectors, is indicated by the wavefunction $|\psi_i\rangle$ suggested in the conventional model. These omissions are bound to lead to counter-intuitive physical pictures. The quantum Rayleigh scattering transforms the entangled states mentioned in the quotation into the polarisation states of eq. (7.6), as explained in eqs. (7.2) and (7.3).

Additionally, two local measurements carried out at a distance from each other, with identical optical sources generating the same states of polarization and with randomly rotated polarization filters, will result in the same correlation function as for "entangled" photons (see Section 7.2.1 above) which, while generated together, propagate separately to distant detectors. For a quantum interaction to take place, as required by a wavefunction "collapse", a Hamiltonian of interaction is needed, but no such Hamiltonian has been identified in the professional literature despite decades of experimental results. And since the Hilbert spaces describing the states of the two separated photons are carried away from each other and no longer overlap, any element of the transition matrix will vanish (Griffiths [24]).

The correlation function for two photons A and B of the state $|\psi\rangle = (|\mathrm{H}\rangle_A |\mathrm{H}\rangle_B + |\mathrm{V}\rangle_A |\mathrm{V}\rangle_B)/\sqrt{2}$ measured with two polarization filter operators $\hat{P}_A$ and $\hat{P}_B$ is expanded from eq. (7.7) as [24]:

$$\begin{aligned} E_c = \langle\psi | \hat{P}_A \otimes \hat{P}_B |\psi\rangle = {}& {}_A\langle \mathrm{H}| \hat{P}_A |\mathrm{H}\rangle_A \, {}_B\langle \mathrm{H}| \hat{P}_B |\mathrm{H}\rangle_B/2 + \\ & + {}_A\langle \mathrm{H}| \hat{P}_A |\mathrm{H}\rangle_A \, {}_B\langle \mathrm{V}| \hat{P}_B |\mathrm{V}\rangle_B/2 + \\ & + {}_A\langle \mathrm{V}| \hat{P}_A |\mathrm{V}\rangle_A \, {}_B\langle \mathrm{H}| \hat{P}_B |\mathrm{H}\rangle_B/2 + \\ & + {}_A\langle \mathrm{V}| \hat{P}_A |\mathrm{V}\rangle_A \, {}_B\langle \mathrm{V}| \hat{P}_B |\mathrm{V}\rangle_B/2 \end{aligned}$$

where $\hat{P}_j = \hat{P}(\theta_j)$, $j = A$ or B, and the rotation angle of polarization θ_j is set relative to a measurement basis of eigenstates in the Hilbert space of $\mathcal{H} = \mathcal{H}_A \otimes \mathcal{H}_B$. Each of the four terms of this correlation function is

measured simultaneously at the two spatially separated photodetectors, and no interaction between the two measurement locations is necessary or can be identified. It is at this stage of analysis that the projection by $\hat{P}_j$ of the incoming states onto the measurement Hilbert space for comparison purposes, is mistaken for a nonlocal interaction. The overall, or aggregate, statistical ensembles of the two sets of data are allocated to four distinct groups of possible combinations reminiscent of the statistical branches of the "multiverse" approach [18].

The use of a global wavefunction which is time- and space- independent is the root cause of confusion because it can be applied to any quantum events regardless of their time and space of their existence. After all, the Schrödinger wave equation is space and time-dependent.

The concept of non-contextuality is mentioned in (Paneru *et al*. [30]):

> "…non-contextuality, i.e. the notion that the measurement of a physical quantity is independent of the measurement of any other commuting physical quantities, or the "context" of the measurement, seemed like a valid assumption in quantum mechanics. However, Bell and Kochen-Specker (BKS) [84–86] separately proved that it is impossible for the commuting observables to have pre-existing values independent of the context of the measurement." (Paneru *et al*. [30]).

This interpretation has been disproved recently by R.B. Griffiths [24] who considered the sequence of operations performed in order to obtain a specific reading of the eigenvalues. Moreover, as already mentioned and explained in Section 7.2.2, the choice of a suitable quantum state that reflects the physical reality enables the Pauli operators to be measured together and for the input values to be assessed from the impact caused by the measuring operators and the measuring apparatus.

In relation to the beam splitter output, Paneru *et al*. [30] state:

> "The two photons are clearly entangled with each other after passing through the beamsplitter. Note that this is the famous Hong-Ou-Mandel (HOM) interference for two identical photons passing through a beamsplitter [50]. One crucial point to be made here is that the entangled state is created by the physical action of the beamsplitter on both of these photons." [30]

However, one photon per input radiation mode is, practically certain, to be scattered by the quantum Rayleigh spontaneous emission inside the dielectric medium of the beam splitter. The review of (Paneru *et al*. [30] fails to explain how the quantum Rayleigh scattering can be avoided. Alternative physical processes have been identified in this textbook leading

to individual photons coalescing into groups of monochromatic photons, and in so doing they manage to overcome the quantum Rayleigh scattering.

A final quotation reads (Paneru *et al*. [30]:

> "All contradictions to classical concepts and mind-boggling questions arose upon considering the particle nature of light, i.e. when using single photons. Hence, it is misleading to challenge fundamental concepts using states of light that are fully described by the electromagnetic wave picture and Maxwell's equations. Therefore, we suggest that the term entanglement should only be used in connection to quantum experiments with single or multiple particles, and in particular for the cases involving non-locality as it was originally suggested by Schrödinger". (Paneru *et al*. [30]

However, as already derived in Chapters 3 and 4, single photons spontaneously emitted will be amplified by the same medium and multi-photon states described by means of dynamic and coherent number states will carry the initial photon's features and properties without the need to invoke the "miracle" of entanglement.

We shall turn our attention now to a 2014 review by Shadbolt *et al*. [31] describing the testing of fundamentals of quantum mechanics with experimental outcomes involving photonic systems. The review emphasises that:

> "Experiments with light at the single-photon level have historically been at the forefront of fundamental tests of quantum theory and the current developments in photonic technologies enable the exploration of new directions." (Shadbolt *et al*. [31])

> "…single photons have played a pivotal role in tests of wave–particle duality" (Shadbolt *et al*. [31])

As already mentioned in foregoing comments on reference [30], this review article (Shadbolt *et al*. [31]) does not explain how a single photon overcomes the quantum Rayleigh spontaneous emission to propagate in a straight line across a dielectric component of the experimental configuration which contains several such elements. These are depicted in its Figure 3 (Shadbolt *et al*. [31]): crossed polarisers, polarising beam splitters, paired nonlinear BiBO crystals, half-wave plates, interference filters, and single-mode fibres. Nor does the review article (Shadbolt *et al*. [31]) explain how a single photon at any given time can be filtered by means of an interference which operates by creating a simultaneous superposition of many partial waves at its output. Additionally, the unavoidable parametric amplification of spontaneously emitted photons is completely ignored. Nevertheless, as already mentioned, the experimental results can be easily explained without

resorting to any quantum "miracles" arising from the global wavefunction of an ensemble of measurements of alleged single photon events.

Another quotation from Shadbolt *et al*. [31] reads:

> "The CHSH version of Bell's inequality sets an upper bound on the strength of correlations". (Shadbolt *et al*. [31])
>
> "The implications of rigorously violating this inequality have a profound effect on our intuition of how the Universe works, for it suggests that the two particles are instantaneously communicating with one another, even though they are far apart." (Shadbolt *et al*. [31])

Once again, the CHSH version of Bell's inequality can also be violated for classically linked variables [19-21]. The experimental outcomes can be easily explained [2], [18], [24-27] without invoking quantum nonlocality.

7.6 Conclusions

Quantum Rayleigh conversions of photons in dielectric media provide a physically meaningful explanation for experimental results of statistical and "nonlocal" quantum correlations supposedly associated with entangled states of photons. Single and independent qubits replace the annihilated entangled states and provide identical correlation functions between two sets of polarisation-related measurements carried out far apart from each other. This physically meaningful analysis rules out the existence of photonic-based quantum nonlocality processes and raises significant doubts about the concept of quantum nonlocality which has been repeatedly disproved by means of various and differing approaches.

The statistical character of the "quantum nonlocality" outcomes is actually reinforced by the 2018 worldwide series of simultaneous experiments presented in reference [32]. Those results indicate that the elimination of loopholes does not impact on the statistical correlations of the simultaneous and remote detections of separate photons which carry corelated values of their degrees of freedom as a consequence of their past involvement in a common interaction.

References

1. A. Aspect, "Closing the Door on Einstein and Bohr's Quantum Debate," Physics **8**, 123, (2015).

2. A. Vatarescu, “The Scattering and Disappearance of Entangled Photons in a Homogeneous Dielectric Medium,” Rochester Conference on Coherence and Quantum Optics (CQO-11), doi.org/10.1364/CQO.2019 .M5A.19.
3. M. Giustina *et al*. ‘‘Significant-Loophole-Free Test of Bell’s Theorem with Entangled Photons,’’ Phys. Rev. Lett., **115**, 250401 (2015).
4. L. K. Shalm *et al*., ‘‘Strong Loophole-Free Test of Local Realism,’’ Phys. Rev. Lett., **115**, 250402 (2015).
5. B. Hensen, *et al*., ‘‘Loophole-free Bell Inequality Violation Using Electron Spins Separated by 1.3 Kilometres,’’ Nature **526**, 682-686 (2015).
6. D. J. Griffiths, *Introduction to Quantum Mechanics*, Publisher: Pearson Prentice Hall (2005).
7. W. H. Louisell, *Quantum Statistical Properties of Radiation*, John Wiley & Sons (1973).
8. D. Marcuse, *Principles of Quantum Electronics,* Academic Press, (1980).
9. Z. Wang, H. Wu, X. Hu, N. Zhao, Qi Mo and & G. Li,” Rayleigh scattering in few-mode optical fibers”, *Sci. Rep*. **6**, 35844 (2016);
10. A. Vatarescu, “Photonic coupling between quadrature states of light in a homogeneous and optically linear dielectric medium,” J. Opt. Soc. Am. B, **31**, 1741–1745, (2014).
11. A. Vatarescu, “Phase-Sensitive Amplification with Low Pump Power for Integrated Photonics“, *OSA Advanced Photonics Congress*, paper ID: IM3A.6, 2016.
12. A. Vatarescu, “Photonic Quantum Noise Reduction with Low-Pump Parametric Amplifiers for Photonic Integrated Circuits”, *Photonics*, **3**, article 61, (2016).
13. F. Piacentini, A. Alessio Avella, F. Rebufello, R. Lussana, F. Villa, A. Tosi, M. Gramegna, G. Brida, E. Cohen, L. Vaidman, I.P. Degiovanni, and M. Genovese, “Determining the quantum expectation value by measuring a single photon”, Nat. Phys., **13**, 1191–1194, (2017).
14. K. Edamatsu, “Entangled Photons: Generation, Observation, and Characterization “, Jpn. J. Appl. Phys., **46**, 7175–7187, (2007).
15. J. C. Garrison and R. Y. Chiao, *Quantum Optics*, Oxford University Press, 2008.
16. J. F. Clauser, M. A. Horne, A. Shimony, R. A. Holt, “Proposed experiment to test local hidden-variable theories. Phys. Rev. Lett. 23, 880–884, (1969).
17. A. Zeilinger, “Experiment and the foundations of quantum physics“, Rev. Mod. Phys., **71**, S288 -297, Centenary 1999.

18. F. J. Tipler, "Quantum nonlocality does not exist", PNAS **111** (31), 11281-11286, (2014).
19. X.-F. Qian, B. Little, J. C. Howell, and J. H. Eberly, "Shifting the quantum-classical boundary: theory and experiment for statistically classical optical fields", Optica **2**, 611-615, (2015).
20. J. Gonzales, P. Sánchez, V. Avalos and F. De Zela, "Bell violations with entangled and non-entangled optical fields", J. Phys. B: At. Mol. Opt. Phys., **52**, 115403, (2019).
21. J. H. Eberly, X. F. Qian, A. Al Qasimi, H. Ali, M. A. Alonso, R. Gutiérrez-Cuevas, B. J. Little, J. C. Howell, T. Malhotra, and A. N. Vamivakas," Quantum and classical optics–emerging links", Phys. Scr. **91**, 063003 (2016)
22. R. J. Glauber, and M. Lewenstein, "Quantum optics of dielectric media", Phys. Rev. A, **43**, 467- 491, (1991.
23. N. Brunner, D. Cavalcanti, S. Pironio, V. Scarani, and S. Wehner, " Bell nonlocality", Rev. Mod. Phys. **86**, 419–478, (2014).
24. R. B. Griffiths, "Nonlocality claims are inconsistent with Hilbert-space quantum mechanics", Phys. Rev. A **101**, 022117, (2020).
25. S. Boughn, "Making Sense of Bell's Theorem and Quantum Nonlocality", Found. Phys., **47**, 640-657, (2017).
26. A. Khrennikov, "Get Rid of Nonlocality from Quantum Physics ", Entropy, **21**, 806, (2019).
27. M. Kupczynski, "Closing the Door on Quantum Nonlocality ", Entropy, **20**, 877, (2018).
28. M. Ringbauer, C. Giarmatzi, R. Chaves, F. Costa, A. G. White and A. Fedrizzi", Experimental test of nonlocal causality", Sci. Adv., **2**, e1600162**,** (2016).
29. R. Ursin *et al*., "Entanglement-based quantum communication over 144 km", Nat. Phys. **3**, 481–486, (2007).
30. D. Paneru, E. Cohen, R. Fickler, R. W. Boyd and E. Karimi, "Entanglement: quantum or classical? ", Rep. Prog. Phys., **83,** 064001, (2020).
31. P. Shadbolt, J. C. F. Mathews, A. Laing and J. L. O'Brien, "Testing foundations of quantum mechanics with photons", Nature Phys., **10**, 278-286, (2014).
32. The BIG Bell Test Collaboration, Challenging local realism with human choices, Nature **557**, 212-216, (2018).

CHAPTER EIGHT

THE PHYSICAL REALITY OF QUANTUM OPTICS

Over the past three decades, the research field of Quantum Optics has benefited greatly from the technological developments of various types of optical sources and processing devices. The predominant activities in Quantum Optics revolve around the generation and manipulation of one photon per radiation mode, otherwise known as single photon generation and processing of associated quantum information in the form of various degrees of freedom such as the optical frequency, state of polarisation, coherence length, etc. using devices for phase modulation, spectral filtering, etc.

It is common practice in Quantum Optics to adopt the same formalism for optical processing as for "classical "optics (Jacques *et al.* [1], p. 4).

> "As is well known from quantum optics [31], all optical phenomena like interference, diffraction and propagation, can be calculated using the classical theory of light even in the single-photon regime." (Jacques *et al.* [1], p. 4).

Even though this statement is apparently based on a widespread practice (Jacques *et al.* [2]; Gerry and Knight [3]) it has never been proved to be valid. This idea may have stemmed from the similarity between the statistical distributions of a global, mixed quantum state and that of an optical beam carrying a large number of photons which can be divided among a large number of pathways. If classical techniques were applicable in the quantum regime, then a group of photons would be involved as likely as a single photon. For example, in the case of interference filters, it was shown in Sections 5.4 and 5.5 that these filters introduce random time-delays through repeated reflections or bounces of photons inside a resonant cavity rather than being spectrum-shaping devices.

Moreover, the following approach espoused by Glauber [4] underpins the conventional, but problematic, model of Quantum Optics:

> "The things that interfere in quantum mechanics are not particles. They are probability amplitudes for certain events. It is the fact that probability

> amplitudes add up like complex numbers that is responsible for all quantum mechanical interferences. When the event in question represents the detection of one single photon, one can easily slide into the statement that the photon interferes with itself. When one deals, on the other hand, with two-photon states, one still encounters many species of interference effects, but it would generate intolerable confusion to interpret these as photons interfering with one another. It is not difficult, for example, by means based on nonlinear optics, to construct situations in which interference takes place between an amplitude for a state with a single blue photon and an amplitude for another state with two red photons. Quantum mechanics allows such interferences and a great many other varieties as well, but no one could sensibly speak of photon as interfering with themselves or any others in that sort of context." [3]

The nature of the descriptive states of photons is not specified, e.g., pure states for individual measurements which are time-dependent, or mixed states of the ensemble of measurements which describe a statistical distribution of measurements that is time-independent. Furthermore, the probability amplitudes can only be linked to ensemble distributions; yet, each and every single measurement is activated by the intrinsic field of photons interacting with electric dipoles of the detecting device. The probability amplitude is a consequence of a detection process preceding any mathematical description of the overall statistical distribution of measurements.

8.1 Processes for Physical Quantum Interference

Probability of events requires an ensemble of measurements in order to calculate a distribution of probabilities. The physical reality can only be identified at the level of individual events of the ensemble. The global wavefunction which is space- and time- independent is physically unrealistic, at least, in the context of propagating radiation modes which carry energy from one location to another.

A theory based on global quantum states discards spatial and temporal information, leading to counterintuitive interpretations. The flaws of this approach are compounded by the omission of quantum processes impacting on photons propagating through dielectric media. The location and time of a quantum even should be reflected in the wavefunction.

As already derived in Chapter 3, photons correspond to levels of energy of an electromagnetic field. A major property of photons is their intrinsic optical field which was derived in Chapter 3 to have longitudinal and transverse spatial field distributions – see eqs. (3.34) and (3.37). These field distributions of photons – obtained from the combination of the dynamic

and coherent number states and the Maxwell equations – specify the location and limited spread of the level of the optical field excitation. The photon may behave like a particle which carries an optical field but it is this field that will interfere with another photonic field.

For example, the quantum state of one photon having two optional pathways A and B from the source to a photodetector has the form

$$\Psi(\boldsymbol{r},t)\rangle = c_{\mathrm{A}}(\boldsymbol{r}_1, t_1)\,|1\rangle_{\mathrm{A}}\,|0\rangle_{\mathrm{B}} + c_{\mathrm{B}}(\boldsymbol{r}_2, t_2)\,|0\rangle_{\mathrm{A}}\,|1\rangle_{\mathrm{B}} \tag{8.1}$$

where the coefficients c_{A} and c_{B} identify the time t of the particular event at the location $\boldsymbol{r}$ of the photodetector. Bearing in mind that the zero-photon state $|0\rangle$ does not trigger an electronic signal, the measured events are:

$$c_{\mathrm{A}}(\boldsymbol{r},t) \neq 0 \quad for\ \boldsymbol{r} = \boldsymbol{r}_1\ and\ \ t = t_1 \tag{8.2a}$$

$$c_{\mathrm{B}}(\boldsymbol{r},t) \neq 0 \quad for\ \boldsymbol{r} = \boldsymbol{r}_2\ and\ \ t = t_2 \tag{8.2b}$$

Elsewhere the two coefficients, physically, vanish. This would correspond to a pure state for which the probability amplitudes of detection are:

$$\mathrm{A}(\boldsymbol{r}_1, t_1) = ({}_{\mathrm{B}}\langle 0 |\ {}_{\mathrm{A}}\langle 0 |)\,\hat{a}_{\mathrm{A}}\,|\,\Psi(\boldsymbol{r},t)\rangle = c_{\mathrm{A}}(\boldsymbol{r}_1, t_1) \tag{8.3a}$$

$$\mathrm{B}(\boldsymbol{r}_2, t_2) = ({}_{\mathrm{B}}\langle 0 |\ {}_{\mathrm{A}}\langle 0 |)\,\hat{a}_{\mathrm{B}}\,|\,\Psi(\boldsymbol{r},t)\rangle = c_{\mathrm{B}}(\boldsymbol{r}_2, t_2) \tag{8.3b}$$

The probability P of the two events occurring is:

$$\mathrm{P} = |\mathrm{A}(\boldsymbol{r}_1, t_1) + \mathrm{B}(\boldsymbol{r}_2, t_2)|^2 = |\,c_{\mathrm{A}}(\boldsymbol{r}_1, t_1)|^2 + |\,c_{\mathrm{B}}(\boldsymbol{r}_2, t_2)|^2 +$$

$$+ c_{\mathrm{A}}(\boldsymbol{r}_1, t_1)\,c_{\mathrm{B}}^{*}(\boldsymbol{r}_2, t_2) + c_{\mathrm{A}}^{*}(\boldsymbol{r}_1, t_1)\,c_{\mathrm{B}}(\boldsymbol{r}_2, t_2) \tag{8.4}$$

The interference term of eq. (8.4) will make a contribution only if the *two* events of one photon detection take place simultaneously at the same location, i. e., $\boldsymbol{r}_1 = \boldsymbol{r}_2$ and $t_1 = t_2$. Two photons overlapping in space and time are required for an interference pattern to appear. This is determined or created at the level of one single, individual event by its detection measurement. Each photon would follow a different pathway from the source to the photodetector, but reaching the same photodetector within their durations of the optical fields that the photons carry. The intrinsic optical fields of the two photons – as derived in Chapter 3 – will interfere with each other provided they overlap. The condition of "which way" is irrelevant in the physical context of pure quantum states describing one

single measurement because, as pointed out in eqs. (5.2), two photons are needed for interference processes to occur, even in the quantum regime.

Unless two photons are present simultaneously for an interference pattern to appear, the interference associated with the time-independent global state would create a quantum magic of transcending the temporal separation between the two events. One cannot distinguish optical pathways if there are at least two populated radiation modes, each carrying one photon, converging onto the same detection area. A zero-photon state is not measurable as it does not trigger a response; thus, an "interference" between quantum states is, in fact, an interference between their corresponding numbers of photons.

The absence of photons, such as the zero-photon state, does not create an interference pattern because the mathematical probability of detecting ono photon, assisted or hindered by the presence of another photon, arises from the physical processes of photon-dipole interactions. The cause of any interference pattern is the physical presence of photons at the detection area, in a simultaneous manner. This is, in fact, compatible with the need for both space and time overlaps of the respective Hilbert spaces describing the two photonic systems (Griffiths [5]).

A theory based on global quantum states discards spatial and temporal information, leading to counterintuitive interpretations. The flaws of this approach are compounded by the omission of quantum processes impacting on photons propagating through dielectric media. The location and time of a quantum even should be reflected in the wavefunction. So long as no experimental result can be demonstrated at the level of one single and individual measurement whereby one measurement – displaced in space and time from another measurement – affects the second measurement, the case for quantum nonlocality, whether spatial or temporal, cannot be substantiated.

8.2 The Question of Single Photon Sources

Quantum optically, the role of single photon sources is believed to be critical in the discovery of quantum features which are expected to open up new applications. One such source employs nonlinear crystals and its operation is based on the second-order spontaneous, parametric down-conversion of one pump photon being split into two photons, and the other source relies on quantum dots or single atoms embedded in a host material.

The parametric down-conversion of photons is modelled as the spontaneous emission of a pair of (signal and idler) photons which are believed to escape parametric amplification and remain entangled in their

properties. This model of generating single photons, for some reason, fails to take into account the presence of the parametric gain beyond the stage of spontaneous emission. As the parametric amplification of photons is driven by the same parameters as the spontaneous emission – see Chapter 4 – the amplification is unavoidable resulting in more than one photon per radiation mode exiting the crystal. Consequently, the claim that such devices can operate as one-photon sources is not justified. It may still be possible for only one photon to reach the photodetector because of the scattering induced by the quantum Rayleigh spontaneous emission in the intervening devices. The existence of the quantum Rayleigh spontaneous and stimulated emissions in a dielectric medium involving the photon-dipole interactions, as explained in Chapters 3, 4 and 5, can be overcome if the initial input contains a group of photons for the stimulated emission to recapture the absorbed photon.

Correlations of values of degrees of freedom established at the source of radiation when combined with post-selection of data after the measurements, are mistaken for a quantum collapse of the wavefunction or quantum state.

8.2.1 The spontaneous parametric down-conversion of photons

To exemplify the formalism presented in this textbook, let us consider the experimental results presented by Kolenderski *et al*. [6]. In this report, a type -II crystal is used for spontaneous parametric down conversion to generate signal and idler photons orthogonally polarised. Remote correlation measurements between heralding idler photons and polarisation-dependent laterally displaced signal photons give rise to Airy-like diffraction patterns brought about by the diffraction from the spot-like aperture of the collimated beams of polarised signal photons. For each polarisation state of the triggering idler photons, one diffraction pattern appears. The two laterally separate photonic beams emerging from locations s_H and s_V pass through the same polarisation filter, set at 45°, to reach an array of one-line photodetectors. Although sharing the same polarisation state, the two laterally displaced beams give rise to separate Airy-like diffraction patterns, so that the number of photons N counted at location x along the line of photodetectors is

$$N(x) = N_{tot}\,[cos^2(\theta_t)\,|\,A_H(x, s_H)|^2 + \, sin^2(\theta_t)|A_V(x, s_V)|^2] \qquad (8.5)$$

where the diffraction pattern at location x of the array is described by the function $A_{H\ or\ V}(x, s_{H\ or\ V})$, and the absence of an interference term is due

to the lack of a temporal overlap between two consecutive photons reaching the detectors. The coefficients $cos\ \theta_t$ and $sin\ \theta_t$ are determined by the θ_t – rotated polarisation of the triggering photons, relative to the V eigen-polarisation of the beam splitter of the triggering branch. The idler photons, in the first stage of $\theta_t = 0$, activate triggering detectors D1 and D2 with polarisation V and H, respectively. In the second stage of the experiment, the polarisation of the idler photons is rotated and some H-polarised photons may trigger D1 and some V-polarised photons may trigger D2. The two signal patterns may overlap horizontally if a polarising filter is placed in the path of the idler photons before the polarisation beam splitter, so that, for a group of photons exiting the nonlinear crystal, both polarisation states can trigger the correlated measurement of signal diffractions. As the linear polarisation filter is rotated, the ratio of the photons coupled into the orthogonal polarisations of the triggering detectors varies. As a result, the weighted superposition of the two diffraction patterns which may overlap on their common side will change giving rise to a common peak which was interpreted as follows:

> "By post-selecting on a particular point in the interference pattern, it is possible to prepare the idler photon in a specific polarization state. Such a flexible remote state preparation could be very helpful in photonic quantum information processing." (Kolenderski *et al*. [6])

However, as that state is selected – rather than created – as a result of the measurement at the signal's detection, the properties of the idler photons along with those of the signal photons were determined at the original source of the nonlinear crystal. Consequently, entangled photons are not needed to explain the correlated results.

Another typical application of spontaneous parametric down-conversion of photons is the interference of temporally distinguishable photons. The Hong-Ou-Mandel dip would result from the destructive interference of two pairs of photons represented by a global, mixed quantum state and detected at different times by two sperate photodetectors. As an alternative, the case of time-resolved two-photon quantum interference would also have the field operators of photon annihilation and creation split into two by a beam splitter, leading to each photon of a pair being detected twice by the same operator which is now located at both detecting stations. (Legero *et al*. [7]). These assumptions are physically unsubstantiated, prompting counterintuitive conclusions.

The interpretation of time-resolved quantum interference experiments (Orre *et al*. [8]) ignores the quantum Rayleigh spontaneous emission which prevents a single photon from propagating in a straight line in a dielectric

medium. This interpretation also disregards the random phase of the parametrically generated spontaneous photons and their unavoidable parametric amplification resulting in, at least, several photons per spectral radiation mode, and the related parametric phase-pulling effect (see Chapters 3, 5, and 6). Each coincidence measurement by the two separate photodetectors (Orre *et al*. [8]) involves the same photonic intrinsic fields exiting the optical fibre leading the photons from the fibre chirped Bragg grating to the Y-junction directing the photons to the two detectors. The time-resolved interference patterns shared by the photodetectors arises from the intrinsic optical field carried by each photon. The role of the chirped Bragg grating is to spread out, in time, each group of monochromatic photons as a photon can be scattered by any electric dipole and reflected from any location in the grating filter, randomly in any direction.

The fourth-order numerical or electronic interference patterns arising from the product of the two intensities-induced photocurrents (Orre *et al*. [8]) involve the conventionally known signal-idler (*s i*) pairs of photons of the first delayed group with the corresponding pairs of photons from the secondary delayed groups emerging from the Bragg grating. The relative phase for the second-order interference are:

$$\theta_{si,j} = (\omega_s - \omega_i)\, t + (\omega_s - \omega_i)\, \tau_j + \varphi_s(t) - \varphi_i(t)$$

where j =1 or 2 identifies the time-delay stage τ_j, and the random phases of the spontaneous emissions are denoted by $\varphi_{s;i}(t)$. The phase difference of the intensities' correlation function (see Section 5.3.1) is given by

$$\theta_{si,1} - \theta_{si,2} = (\omega_s - \omega_i)\,(\tau_1 - \tau_2)$$

in line with the treatment of the Hong-Ou-Mandel interference patterns for nondegenerate frequencies. The case for the sum of frequencies is treated similarly to the analysis of Section 5.3.1 for the output of the Mach-Zehnder configuration sketched in Fig.5.3.

By ignoring well established physical processes, one may be led to believe in the "magic" of quantum optics to transcend time and space in having two photons influencing each other despite reaching the same detector at different time, or arriving at two separate photodetectors at the same time.

As a matter of physical understanding, quantum effects and processes are best described by pure quantum states representing one single measurement. The aggregate of these measured values will build up a statistical distribution for the expansion of the mixed quantum state which

by its definition disregards properties and phenomena associated with instantaneous events.

8.2.2 The quantum dot sources of photons

Another type of device that can serve as single-photon sources is based on the quantum dots or single atoms, but their location in a high finesse resonator cavity has the potential to retain the emitted photons inside the cavity for a large number of excitation periods leading, as a consequence, to an amplification of the first photon which turns into a group of monochromatic photons whose optical filed is described by the longitudinal and lateral spatial distributions found in Chapter 3. Once again, the claim that only single photons emerge from these devices is not substantiated as explained in Sections 5.4 and 5.5 of this textbook.

Additionally, if single photons reach an interference filter or a beam splitter such as in references [1] and [2], the photons may not exit after their first transition across the device and may be reflected. In this way, any two photons – from different radiation modes – reaching the same dipole simultaneously may transfer energy to each other depending on their relative phase, as explained in Chapter 3 for the quantum Rayleigh coupling of photons between two radiation modes described by means of the dynamic and coherent number states. As a result, the two photons will appear in the same radiation mode, which explain, without any quantum mystery, the original result of the Hong-Ou-Mandel interference dip or the polarisation-dependent interference patterns of [2].

As an example, consider the experimental setup of Loredo *et al*. [9]. Groups of photons are formed inside the micro-cavity, as well as inside the cubic polarisation beam splitters. Equally, the input phase-difference to the fibre directional coupler operating as a beam splitter, will determine the direction of photon coupling and the levels of output numbers of photons in the two radiation modes as the gain coefficient of the quantum Rayleigh stimulated emission is phase-sensitive as well as dependent on the ratio of photons in the two interacting modes – see Chapter 3. The more photons there are in each radiation mode, the lower the degree of coupling at the output will be – see Chapter 3.

Another shortcoming of the global quantum mixed states which are independent of time and space can be found in the article by Loredo *et al*. [9]. Therein it is claimed that the visibility of the ensemble interference is determined by the probability of the zero-photon number state. This is physically questionable because the zero-photon number state does not deliver an intrinsic optical field that would interact with the detector. The

zero-photon state is needed to generate an annihilation transition from the one-photon state, but the expectation value should be evaluated with the same quantum state as explained in Chapter 3 for the dynamic and coherent number states.

The global wavefunction is interpreted as producing aggregate or cumulative outcomes which are, in fact, descriptive of "classical" circumstances where the statistical outcome is obtained in one measuring step. The interpretation by Loredo *et al*. [9] relies on the following assumptions:

> "The pure states of photon-number superpositions… are in the form $|\Psi_a\rangle = \sqrt{p_0}\,|\,0_a\,\rangle + e^{i\phi}\sqrt{p_1}\,|\,1_a\,\rangle$ and form $|\Psi_b\rangle = \sqrt{p_0}\,|\,0_b\,\rangle + e^{i\phi}\sqrt{p_1}\,|\,1_a\,\rangle$ … where $p_0 + p_1 = 1$, $p_{0,1}$ are the vacuum and one-photon populations and ϕ is the relative phase between the states." (Loredo *et al*. [9], p.804)

However, at the level of one single measurement, there is supposed to be only one photon present throughout the experimental setup, or none at all. The absence of any time dependence of the input states would be at odds with the time-synchronisation for the overlapping of photonic wavepackets. Therefore, the coefficients of expansion should be:

$$|\Psi\rangle = c_0\,|\,0\,\rangle + e^{i\phi}c_1\,|\,1\,\rangle \tag{8.6}$$

with $c = 1$ or 0. The role of the zero-photon sate $|\,0\,\rangle$ is to deliver a non-zero value for the absorption-induced transition. A physically meaningful explanation for the experimental results of Loredo *et al*. [9] is provided by the formalism developed in Chapters 3, 5 and 6 involving the intrinsic optical fields of photons in the context of one single event described by the pure quantum state of the dynamic and coherent number states.

It is the intrinsic fields of photons that interact with the detector to create an interference pattern, and probability amplitudes are evaluated mathematically afterwards. An additional quotation from Loredo *et al*. [9] reads:

> "That is, if states are pure in the photon-number basis, their interference leads to oscillations measured at the output of the interferometer device, with a visibility amplitude equal to the vacuum population p_0.
>
> The previous example describes the idealized case of pure states – instances non-existing in the physical world. To account for impurity in the photon-number basis, we consider that each light wavepacket impinging on the beamsplitter is described by a density matrix." (Loredo *et al*. [9], p.804)

This interpretation is rather questionable because the physical reality is determined at the level of each individual measurement. Physical interactions require time and space overlaps between the quantum states and operators (Griffiths [5]).

The equivalence between a global, mixed quantum state and a classical optical beam is hidden in the Dirac notation. The mixed state

$$|\Psi\rangle_{mix} = \Sigma_j \, \Phi(\omega_j) \, |1\rangle_j \tag{8.7}$$

describes a superposition of modes j, each carrying one photon with a spectral distribution $\Phi(\omega_j)$, but with only one mode populated at any given time. Mathematically, this mixed state delivers upon absorption a time-independent spectral distribution

$$\langle 0 \mid \hat{a} \, |\Psi\rangle_{mix} = \Sigma_j \, \Phi\left(\omega_j\right) = \Sigma_j \, E\left(\omega_j\right) \tag{8.8}$$

which can be treated like the spectral distribution $E\left(\omega_j\right)$ of a classical optical beam, in which case all radiation modes carry photons at the same time.

8.3 The Case for a Paradigm Shift

The conventional interpretation of quantum optic experiments is predicated on one photon per radiation mode, the unimpeded propagation of this photon through a dielectric medium, and the use of global and entangled quantum states to create interference patterns between two photons separated in time and space.

The multitude of omissions and unphysical assumptions associated with the theory of Quantum Optics raise justifiable doubts about its validity. A major omission is the absence of the quantum Rayleigh spontaneous and stimulated emissions which involves photons propagating across dielectric devices. The quantum Rayleigh scattering replaces entangled photons with independent ones, and the stimulated emission requires the local values of the number of photons and related phase to be described locally by a pure quantum state. Similarly, the unavoidable parametric amplification of spontaneously emitted photons is disregarded, as is the time delay caused by multiple reflections of photons inside a high finesse (micro-) cavity. Overall, these well documented physical processes distort substantially any initial stream of periodic single photons.

By contrast, a smooth transition from the quantum regime of one or a few photons to the classical one of a large number of photons is possible

due to the adequate choice of a wavefunction in the form of the pure, dynamic and coherent states – see eq. (3.14) – derived in Chapter 3. These states deliver the correct number of photons carried by a radiation mode as well as its field amplitude and phase quadratures. The rate equations for the evolution of these variables were derived in Chapter 3 and applied in the following Chapters for any level of mode excitation and photon-dipole interactions, both optically linear and nonlinear.

Measurements of instantaneous wave fronts are described by pure, dynamic and coherent number states which erase any quantum-classical boundary. While the intrinsic optical field of photons is very critical for time-correlation at the level of one or few photons, its importance could still be significant at high levels of photon numbers for a monochromatic group of photons as the optical field does not have a Fourier spectrum but is represented by a mixed time-frequency structure (Cohen [10]) of the form $S(\omega, t)$. That is, the monochromatic spectral component exhibits a time-varying amplitude – corresponding to a time-varying number of monochromatic photons – which is not related to a time-independent optical Fourier spectrum.

Entangled photons are scattered by the quantum Rayleigh spontaneous emission but the same remote correlation of measured states of polarisations are still reproduced by single and independent photons.

The quantum Rayleigh photon-dipole interaction may involve two photons colliding at a dipole, with a possible outcome being the transfer of the excitation from one radiation mode to the other, providing a physically meaningful explanation for the "miracle" of the HOM dip. This process may take place inside the dielectric medium of an interference filter or beam splitter, thereby creating groups of monochromatic photons from initially independent photons bouncing back and forth inside a resonant cavity.

Equally, a remote wavefunction state preparation through a detection of one of the entangled photons is practically impossible because the photodetector's excitation is triggered by an energy level of its structure rather than a quadrature state of a quantum harmonic oscillator.

Consequently, a paradigm shift in the interpretation of experimental outcomes of Quantum Optics is highly necessary, being based on the following physical processes and elements:

1. The quantum Rayleigh spontaneous and stimulated emissions;
2. The unavoidable parametric amplification of spontaneous emission, and the formation of groups of monochromatic photons in a high finesse cavity incorporating a quantum dot;
3. Self-contained quantisation of the optical field without any harmonic oscillators leading to the dynamic and coherent number states;

4. The intrinsic optical field of photons and their localised spatial distributions;
5. The description of instantaneous and localised photon-dipole interactions by means of pure, dynamic and coherent number states;
6. The quantum evolution and predictions being described by the Ehrenfest theorem, for any level of optical field excitation, to evaluate the expectation value of an operator in the context of a given set of pure wavefunctions.
7. Identifying quantum phenomena at the level of single events and measurements with a space- and time-dependence, leading to quantum locality and realism.

Overall, there are no quantum optic "miracles" once the physically present effects are correctly identified.

8.4 Conclusions

Over the past few decades the modelling used in Quantum Optics was based on global quantum states which possess no time- or space-dependence leading to the belief of quantum miracles of interactions between photons separated by large intervals of time and space. These "miracles" seemed to be supported by single-photon sources which are placed inside experimental configurations containing resonant cavities and dielectric devices. The operations of these components result in a variety of methods for increasing the number of photons through parametric amplification and/or quantum Rayleigh coupling of photons.

Therefore, the physical reality of Quantum Optics rules out single-photon interference operations and is characterised by a smooth transition from the quantum regime to the classical one.

References

1. V. Jacques, N. D. Lai, A. Dréau, D. Zheng, D. Chauvat, F. Treussart, P. Grangier and J-F. Roch, "Illustration of quantum complementarity using single photons interfering on a grating", New J. Phys., **10,** 123009, (2008).
2. V. Jacques, E. Wu, F. Grosshans, F. Treussart, P. Grangier, A. Aspect and J-F Roch, "Experimental realization of Wheeler's delayed-choice gedanken experiment" Science, **315**, 966–968, (2007).

3. C. Gerry and P. Knight, *Introductory Quantum Optics* (Cambridge University Press) 2004.
4. R. J. Glauber, "Dirac's famous dictum on interference: One photon or two?", Am. J. Phys. **63**, 12, (1995).
5. R. B. Griffiths, "Nonlocality claims are inconsistent with Hilbert-space quantum mechanics", Phys. Rev. A **101**, 022117, (2020).
6. P. Kolenderski, C. Scarcella, K. D. Johnsen, D. R. Hamel, C. Holloway, L. K. Shalm, S. Tisa, A. Tosi, K. J. Resch and T. Jennewein, "Time-resolved double-slit interference pattern measurement with entangled photons ", Sci. Rep. **4**, 4685, (2014).
7. T. Legero, T. Wilk, A. Kuhn, and G. Rempe,"Time-Resolved Two-Photon Quantum Interference", Appl. Phys. B, **77**, 797, (2003).
8. V. V. Orre, E. A. Goldschmidt, A. Deshpande, A. V. Gorshkov, V. Tamma, M. Hafezi and S. Mittal, "Interference of Temporally Distinguishable Photons Using Frequency-Resolved Detection", Phys. Rev. Lett., **123**, 123603, (2019).
9. J. C. Loredo, C. Antón, B. Reznychenko, P. Hilaire, A. Harouri, C. Millet, H. Ollivier, N. Somaschi, L. De Santis, A. Lemaître, I. Sagnes, L. Lanco, A. Auffèves, O. Krebs & P. Senellart," Generation of non-classical light in a photon-number superposition", Nat. Photonics **13,** 803–808, (2019).
10. L. Cohen, *Time-Frequency Analysis*, Prentice Hall, 1995.

INDEX

amplification 6, 7, 15, 23, 24, 36, 59, 64, 65, 68, 76, 86, 95, 108, 113, 119, 124, 132, 145, 153, 156, 160.
see parametric gain

beam splitter 2, 3, 6, 14, 80, 82, 83, 86, 88, 91, 99
- glass plate 91, 94
- cubic prism 95
- fibre optic coupler 96

coincidences 103, 104
- photon counting 108, 111, 125
- interference pattern 5, 93, 103, 110, 113, 116, 123, 151

correlations 2, 10, 90, 103, 110, 115,
- balanced homodyne detection 117
- functions 134, 138
- nonlocal 153
- optical field 120, 125
- quantum 127

dynamic and coherent number states 9, 36, 37, 48, 55, 122
- applications 52, 89, 108, 145, 151, 157, 160
- properties 41, 43, 51,

Ehrenfest theorem 40, 46, 159

ensemble average 112, 116, 117

electro-optic 59
- coupling photons 66, 68, 69
- modulation 74

field quantisation 40
- self -contained 40

filter, optical 66, 69, 83, 98, 116, 125
- interference 96, 114, 158
- resonant cavity 11, 96, 98, 116, 148
- Bragg reflector 98, 100, 155

gain, parametric 17, 20, 62, 124, 132, 153
- phase dependent or sensitive 9, 62, 64
- first order 47
- second order 63

equations of motion
- first order parametric 47
- second order parametric 63
- microwave modulation 74

expectation value 37, 39, 44, 46, 48, 54, 55, 62

Hamiltonian
- Rayleigh coupling 46, 105, 131
- second- order nonlinear 62

Heisenberg uncertainty 51, 52, 135

Hilbert space 34, 40, 115, 132, 134, 138, 142, 152

Hong-Ou-Mandel 6, 80, 83, 85, 91, 94, 117, 159
see interference patterns

interference patterns 89, 93, 111, 113, 116, 155
- second-order interference 110
- fourth-order interference 112

measurements
- Hanbury Brown and Twiss 4, 80, 83, 105
- Hong-Ou-Mandel 6, 11, 80, 83, 85, 94, 105, 155
- pure state 34, 38, 87, 97, 134, 135, 150, 151
- mixed state 3, 34, 36, 38, 40, 53, 84, 87, 88, 97, 133, 136, 156, 158

optical field 3, 8, 9, 20, 36, 41, 43, 46, 49, 50, 51, 75, 94, 96, 104,
- detection 41, 114, 141, 157

parametric
- amplification 6, 59, 62, 65, 69, 72, 108, 113, 124, 153, 160
- phase pulling effect 62, 64, 87

phase
- conjugate 65

photons
- entangled 82, 86, 94, 106, 124, 136, 137
- intrinsic field profile 3, 9, 34, 37, 88
  - longitudinal 48, 93, 96
  - lateral 50, 96
- number fluctuations 66
- phase fluctuations 65, 68
- scattering 2, 22, 29, 114, 116, 122, 127, 131, 141, 144
- simultaneous measurements 51, 130, 136, 139

physical quantum interference 6, 80, 84, 116, 150, 154

polarisation, state of, 132

probability amplitude 151
- and intrinsic optical filed of photons 151

propagation
- single photon 131, 145, 155

quadrature 45
- operator 44
- state 45

quantum
- imaging 122
- local realism 138

quantum noise 58,
- reduction 58, 66
- Sub-Poissonian distribution 66

quantum nonlocality
- non-existence 138
- deficiencies of, 140, 146

quantum operators
- annihilation and creation 41
- photon number, two-term definition 42
- quadrature 44, 45
- phase quadrature 45

quantum states
- global 2, 80, 88 ,104, 119, 133, 144, 146, 150
- mixed – *see* measurements of
- pure – *see* measurements of

quantum Rayleigh 7, 10, 14, 29, 106, 108, 114, 127, 141, 142
- coupling of photons 6, 14, 20, 25, 86
- emissions 21, 80
  - spontaneous 3, 29, 90, 109, 124, 144, 159
  - stimulated 25, 99, 109

Rayleigh applications
- phase-sensitive amplification 124, 59, 69

Schrödinger wave equation 38, 55, 106, 139, 144

single photon sources 152
- distorted output 98, 127

spontaneous emissions
- amplification 15, 23, 29, 66, 74, 76, 90, 104, 145, 160
- parametric down-conversion 90, 97, 120, 152, 154
- Rayleigh, *see* quantum Rayleigh